EERING
RARY

RR

SEP 13 1949

THE AERONAUTICAL QUARTERLY

Volume I MAY 1949 Part I

CONTENTS

Foreword

Control Reversal Effects on Swept-Back Wings — *H. Templeton*

Calculation of Downwash behind a Supersonic wing — *G. N. Ward*

Estimation of the Effect of a Parameter Change on the Roots of Stability Equations — *K. Mitchell*

Flutter of Systems with Many Freedoms — *W. J. Duncan*

Note on Propeller-Turbine Reduction Methods — *E. C. Pike*

Determination of the Drag of Jet-Propelled Aircraft in Flight — *G. W. Trevelyan* and *D. R. Blundell*

Notes on the Linear Theory of Incompressible Flow round Symmetrical Swept-Back Wings at Zero Lift — *F. Ursell*

LONDON
ROYAL AERONAUTICAL SOCIETY
4 HAMILTON PLACE W1

10/-

Engin
TA
501
.A2509
Q9

THE AERONAUTICAL QUARTERLY

Editorial Board

W. G. A. PERRING, F.R.Ae.S. (*Chairman*)

Dr. H. ROXBEE COX, D.I.C., F.R.Ae.S., F.I.Ae.S.

Professor S. GOLDSTEIN, F.R.S., F.R.Ae.S.

Sir RICHARD SOUTHWELL, M.A., LL.D., F.R.S., F.R.Ae.S.

G. H. DOWTY, F.R.Ae.S. (Chairman of the JOURNAL Committee of the Royal Aeronautical Society)

J. SMITH, C.B.E., F.R.Ae.S., A.M.I.Mech.E. (Chairman of the Technical Board and Executive Committee of the Society of British Aircraft Constructors)

Editorial Executives

Capt. J. Laurence Pritchard, Hon.F.R.Ae.S., Hon.F.I.Ae.S.

Joan Bradbrooke, A.R.Ae.S. Dr. D. M. A. Leggett, A.F.R.Ae.S.

The Aeronautical Quarterly is published at the Offices of The Royal Aeronautical Society, 4 Hamilton Place, Piccadilly, London, W.1, at 10s. 0d. net for a single number to non-members and 7s. 6d. net for a single number to members of The Royal Aeronautical Society. Instructions for Contributors are given on page 4 of the cover. None of the papers must be taken as expressing the opinion of the Council of The Royal Aeronautical Society unless such is definitely stated to be the case. All communications for publication or advertisements in the Quarterly should be addressed to—The Secretary, J. Laurence Pritchard, 4 Hamilton Place, W.1.

Telephone: Grosvenor 3515 (5 lines). Telegraphic Address: Didaskalos, Audley, London.

Engineering
Southeast
8-18-49
67647
vol. no 1-

FOREWORD

The growth of aeronautical engineering and science, particularly during recent years, has been more rapid than the means for disseminating the experimental and analytical knowledge acquired during that growth, or of presenting the results of much of the original work done by the Industry, Universities, and Research Establishments.

Progress in aeronautics is dependent on the results of these researches and on the development of new and improved methods of analysis or experimental techniques, and the publication of such original work will not only stimulate and encourage the workers engaged in these activities, but should ensure that their work is more widely known and applied.

Under the terms of its Charter, the Royal Aeronautical Society is charged with the duty of advancing Aeronautical Art, Science and Engineering and, among other things

"to facilitate the exchange of information and ideas amongst the members of the Society and others."

In carrying out this task, it is the primary object of the Editorial Board of *The Aeronautical Quarterly* to encourage workers to submit papers describing new and original work, or papers reviewing the progress in some specialised field of activity and, through the medium of this new publication, to make the results of these researches available to all workers or design groups concerned with aviation.

To ensure that the high standard set by the Council of the Society shall be reached and maintained, the Editorial Board has been fortunate in having the willing co-operation of the leading authorities in various branches of aeronautical engineering and science to act as referees on all papers submitted for publication.

The Council of the Society was greatly encouraged to sponsor this new venture by the response it received from members of the Society to its enquiry as to the need of such a publication. The future of *The Aeronautical Quarterly* is dependent on the support it receives; it is hoped, therefore, that this support will be forthcoming from all sections of the Society, so that the success of the new venture is assured.

CONTROL REVERSAL EFFECTS ON SWEPT-BACK WINGS

by

HAYDN TEMPLETON, B.Sc., A.F.R.Ae.S.*

(Structures Department, Royal Aircraft Establishment)

SUMMARY

Aileron reversal effects on swept-back wings in general and elevon reversal effects on tailless swept-back wings in particular are discussed on a non-mathematical basis, attention being confined to the orthodox flap type of control. The main purpose of the paper is to convey in the simplest terms possible a clear physical picture of the conditions producing loss of control power, emphasis being naturally laid upon the part played by structural wing distortion. Certain qualitative features relating to the two phenomena are also discussed. As a general introduction to the discussion on aileron reversal effects, the definition of "aileron power" in relation to the actual dynamic condition of rolling is described at some length. For elevon reversal effects on tailless aircraft the effect of wing flexibility on both "elevon power" and on trim in steady symmetric flight is considered.

With the descriptive treatment adopted the analysis is of necessity broad and general but is designed to appeal to those not too familiar with the subject. The results of certain calculations on a hypothetical wing, which may be of interest, are included. A mathematical analysis for the quantitative estimation of both aileron and elevon reversal effects is given in the Appendix.

1. WING DISTORTION

Implicit in the study of control reversal effects is the consideration of how a wing distorts under the action of applied loads. The phenomenon of control reversal effects may in general terms be described as follows. A particular control is deflected in order to produce a certain aerodynamic effect, but the aerodynamic

---

Paper received November 1947.

* This paper is based on work done while the author was with Sir W. G. Armstrong-Whitworth Aircraft Ltd.

[The Aeronautical Quarterly, Vol. 1, May 1949]

loads resulting from the control deflection distort the flexible wing and the aerodynamic effect of the wing distortion modifies the effect that would have been obtained from the control on a rigid wing. The loads which produce the wing distortion are finally the net result of the loads due to the control and the loads due to the wing distortion itself. In the calculation of aeroelastic effects two problems therefore present themselves: the determination of the elastic deformation of the wing structure under an applied loading system, and the determination of the aerodynamic loads for a given wing configuration. Both these are major problems in themselves, one structural and the other aerodynamic, but when combined as they are in aeroelastic phenomena, where wing distortion and aerodynamic loads mutually affect each other, then some simplification is inevitable if a practicable solution is to be obtained.

Methods used so far fall into two main categories. Either the semi-rigid principle is employed in which arbitrary modes of distortion are used and the solution based on the determination of the absolute displacements at some reference section; or the mode is correctly determined from the elastic characteristics, in which case an iterative process must be used. A combination of these two methods is described later in this paper. Whatever method is used, however, it seems that for a reasonably workable solution simplifying assumptions must be applied to both the structural and aerodynamic sides of the problem.

On the structural side it is a question of how the wing distorts under typical loading actions and of how the distortion should be represented in terms of its aerodynamic significance. As a preliminary it is convenient to establish certain useful definitions with regard to direction. The chord is measured parallel to the longitudinal axis of the aeroplane and a chordwise direction is therefore one parallel to this axis. Normal direction is that at right angles to the wing, or more specifically to the wing flexural axis (*see* Figs. 2 and 3). These are the definitions adopted here and are not of course necessarily universal.

If the aerodynamic loads are expressed in terms of lift and pitching moment on the chordwise section, then it follows that any distortion which involves a change in incidence or shape of the chordwise section is significant aerodynamically. A plain change in incidence produces a change in lift at the aerodynamic centre: a change in shape is more complicated but can be represented as an effective change of camber, producing changes in both lift and moment at the aerodynamic centre. It should, incidentally, be stated here that as discussion is confined to steady or effectively steady states, only the displacements due to distortion, and not velocities or accelerations, are to be considered. Pure translation of the chordwise section in a direction normal to the air stream, for instance, has in the steady state no aerodynamic effect, whereas velocity of translation in this direction has of course a direct aerodynamic effect resulting from the effective change of incidence due to the superimposed velocity.

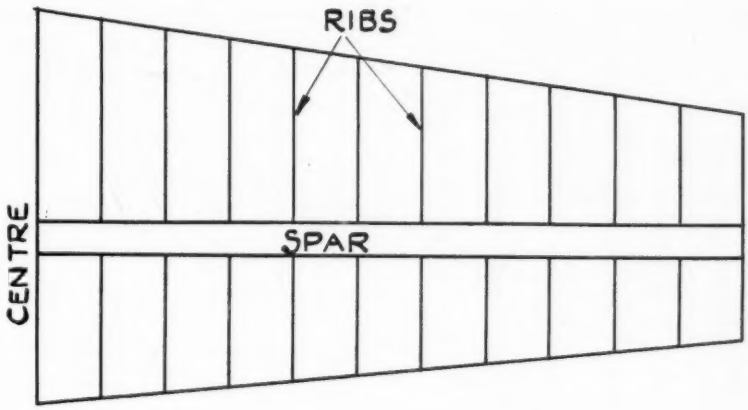

Fig. 1.
Unswept wing with chordwise ribs.

Considering first of all the case of an unswept wing with the usual arrangement of ribs running chordwise from the spar (Fig. 1), it is evident that as far as the spar itself is concerned only torsional deformation is significant, resulting in rotation of the chordwise section. Flexural deformation produces only a translation of the chordwise section and has therefore no effect. Deformation of the ribs may, in addition, produce both rotation and distortion (change of shape) of the chordwise section, and deformation of the skin between the ribs could have a similar effect. To take account of all these possible sources of distortion would be a formidable task and in the estimation of aileron reversal effects on unswept wings it has been the practice to consider only the torsional deformation of the spar, excluding the more local deformations of ribs and skin by what amounts in effect to an assumption of rigid closely-spaced ribs.

Coming now to the swept-back wing, there are two different arrangements to be considered. In the first (Fig. 2) the ribs again run chordwise. If the assumption of rigid closely-spaced ribs is maintained there can be no distortion of the chordwise section, but as a purely geometrical consequence of the sweepback both torsional and flexural deformations of the spar produce rotation of the chordwise section. Relative to the centre say, torsional deformation results directly in a rotation θ' of the normal section which produces a rotation $\theta' \cos\gamma$ of the chordwise section, γ being the angle of sweepback. Flexural deformation, on the other hand, results directly in a change of slope ψ along the flexural axis which produces a rotation $\psi \sin\gamma$ of the chordwise section. Increasing the sweepback therefore respectively

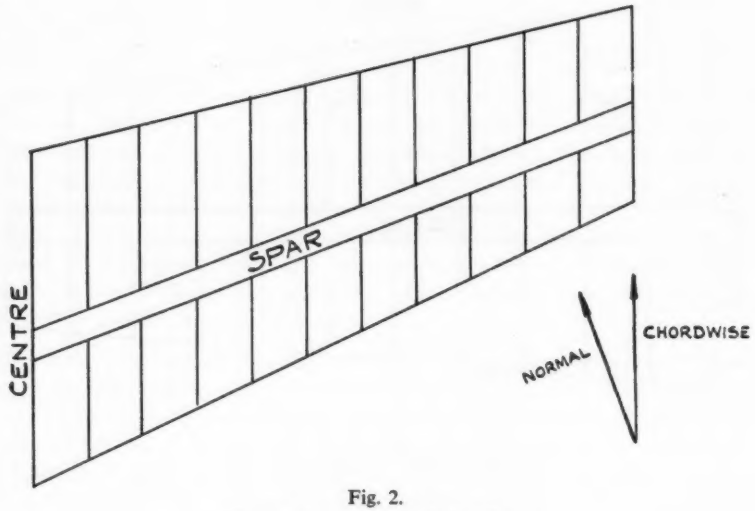

Fig. 2.
Swept wing with chordwise ribs.

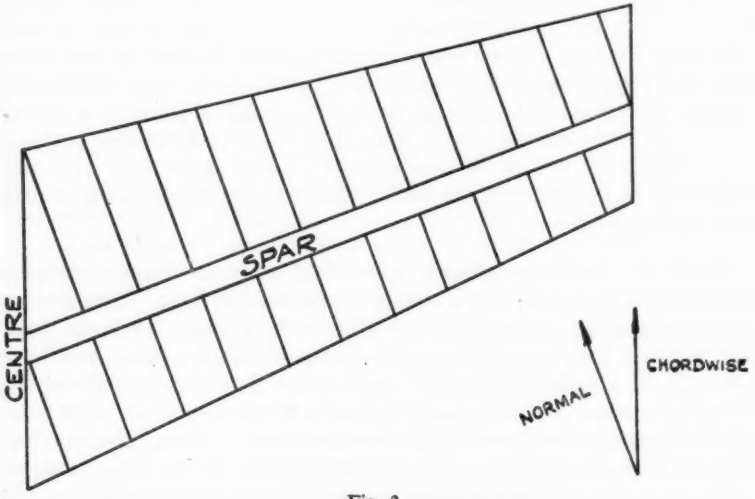

Fig. 3.
Swept wing with normal ribs.

reduces and increases the contributions due to torsional and flexural deformation of the spar. These rotations of the chordwise section relative to the centre constitute an aerodynamic wash-in or wash-out depending upon the sign of the basic deformation. They may be summarised as follows:—

Basic deformation (relative to centre)	*Aerodynamic effect*
1. Nose-down twisting 2. Upward flexing	Wash-out
3. Nose-up twisting 4. Downward flexing	Wash-in

In the second arrangement to be considered (Fig. 3) the ribs run in the normal direction and with the same assumption of rigid ribs there is therefore no distortion of the normal section, from which it must be concluded that there is distortion of the chordwise section. This distortion is probably not important in the case of torsional deformation of the spar, but with flexural deformation it appears as a direct change of camber. The effect is illustrated in Fig. 4, which really does no

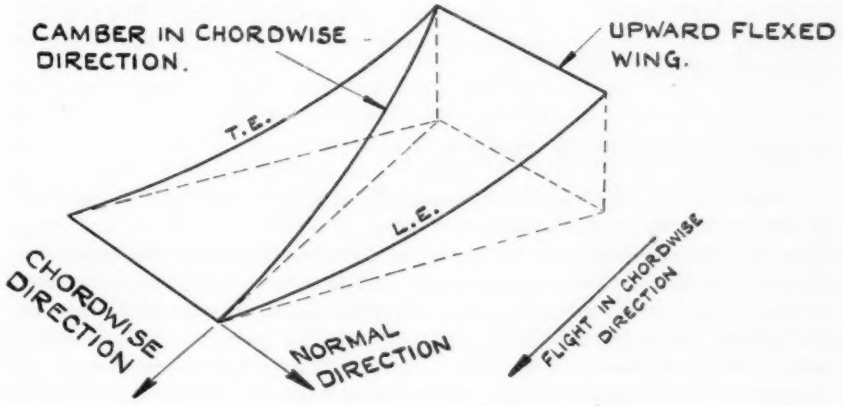

Fig. 4.
Camber change on swept wing.

more than point the well-known fact that in a curved surface there can be only one direction in which there is no curvature. The amount of the camber change is a function of the angle of sweepback and of the curvature of the flexural axis in the mode of flexural deformation: its sign is directly related to that of the flexural mode, as follows:—

Upward flexing — negative camber change

Downward flexing — positive camber change

In addition to distortion, the chordwise section also suffers a rotation which to a first approximation is the same as that in the preceding case with ribs running chordwise.

For swept-back wings, then, it appears that relative to the centre there is a rotation of the chordwise section caused by both torsional and flexural deformations of the spar irrespective of whether the ribs run in the chordwise or in the normal direction. In the latter case there is an additional camber change in respect of the flexural deformation of the spar. In a discussion of control reversal effects on a swept-back wing it therefore seems that some differentiation should be made according to the particular rib arrangement adopted.

What evidence there is suggests that quantitatively the effect of the camber change is relatively small in the case of the normal rib arrangement. Also, it is probably true to say that of the two the chordwise arrangement is the more usual. In what follows distortion effects are therefore confined in the first place to rotation of the chordwise section and the general effect of the camber change is discussed later, as a separate item. The analysis presented in the Appendix, upon which the calculated results quoted are based, also excludes the camber effect, being originally developed with the chordwise arrangement in mind. The camber effect could of course be included.

2. AILERON REVERSAL EFFECTS

When aileron is applied the aeroplane rolls as a direct result of the differential lift load increments produced on the two halves of the wing by the up- and down-going ailerons. Rolling performance, by which is meant the general response in roll, is a function of the wing-aileron system, the inertia of the aeroplane about the rolling axis, and the forward speed. It is convenient to separate inertia from the other effects, which together then constitute the rolling power: a study of rolling performance then resolves itself into a study of rolling power, regarded as the criterion for aileron action. In other words, rolling power is the effect obtained from control deflection in this particular case, the effect that is modified by aeroelastic distortion of the wing. Before considering the effects of wing distortion it is necessary to establish what shall be taken as a measure of rolling power.

Starting from the steady flight condition the application of aileron generates a rolling moment and the aeroplane commences to roll, the acceleration in the roll being governed by the inertia of the aeroplane. As rolling velocity increases an opposing rolling moment proportional to the rate of roll is set up, this being the damping in roll associated with the standard stability derivative l_p. Eventually a steady state is reached when the applied rolling moment is exactly balanced by the damping moment: the aeroplane then continues to roll with constant velocity, this being the maximum velocity achieved in the roll. The whole process can therefore be split up into three stages: the initial stage during which aileron is applied, the unsteady stage in which aileron angle is constant but rolling velocity is increasing and finally, the steady stage where rolling velocity is constant.

To make an exact analysis of conditions in the initial stage would be a complicated matter as the rate of application of aileron, the rate of generation of wing distortion, and the rate of generation of rolling velocity would all have to be considered simultaneously. A considerable simplification is effected if it is assumed that the aileron angle and the accompanying wing distortion are achieved instantaneously before the aeroplane begins to roll appreciably. The initial stage is then in effect compressed into a single instant where the applied rolling moment is the result of aileron deflection and wing distortion and is balanced by an inertia moment appropriate to the acceleration in roll. Any additional accelerations due to the variation of wing distortion with time are assumed negligible in comparison: the condition is then effectively a steady state as far as distortion is concerned. Rolling velocity being zero, there is no damping moment. Wing distortion is in turn the result of the applied aerodynamic loads (due to both aileron and wing distortion) and the inertia loads.

Even with the assumption of instantaneous application of aileron this initial condition is probably fairly representative of actual conditions at the beginning of the roll. It was, in fact, the practice until fairly recently to simplify the condition still further by postulating a static case in which the aeroplane is imagined fixed at the centre to prevent rolling, thus deleting the inertia loads. Conditions are otherwise the same as in the initial condition described above.

Recently it has been realised that the static case is perhaps a little too unrepresentative of the actual conditions of rolling and emphasis has therefore been laid more upon the final steady rolling condition, which has the advantage that it can be analysed as an exact dynamic condition without any simplifying assumptions and is at the same time much less complicated than the initial or unsteady stage. In the steady rolling condition there are no inertia effects, the applied rolling moment due to aileron deflection and wing distortion being balanced by the damping moment. Wing distortion is in this case the result of the aerodynamic loads due to aileron, wing distortion, and damping in roll.

One may therefore take as a measure of rolling power either the rolling moment in the initial condition (hypothetical but fairly representative), the rolling moment in the static condition (hypothetical and less representative), or finally, either the rolling moment or rolling velocity in the steady rolling condition (completely representative). These three conditions are for convenience summarised in Table I.

For the avoidance of undue loss of rolling power due to distortion effects it has been the practice to ensure that the speed at which reversal occurs, when rolling power becomes zero, is well above the maximum design speed of the aeroplane. By such means it is guaranteed that over the full speed range there is at least positive rolling power. At reversal the three conditions postulated above become one and the same. If there is no rolling moment in the initial condition there is no acceleration and there are consequently no inertia effects; and similarly in the steady rolling condition if the rolling velocity is zero there is no damping. Both these conditions are then identical with the static condition with zero rolling moment, in which both inertia and damping effects are absent. Rolling moment due to aileron deflection is exactly balanced by the rolling moment due to wing distortion, and the wing distortion itself is the result of the combined aerodynamic loads due to aileron deflection and wing distortion. The reversal conditions may, on the same lines as the others, be summarised as in Table II on page 11.

TABLE I

	Initial condition	*Static condition*	*Steady rolling condition*
Rolling motion	Zero velocity	Zero velocity and acceleration	Zero acceleration
Applied rolling moment due to aileron and wing distortion balanced by	Inertia moment	Restraint at centre	Damping moment
Wing distortion due to loads from	Aileron deflection, wing distortion, and inertia	Aileron deflection and wing distortion	Aileron deflection, wing distortion and damping
Criterion for rolling power	Rolling moment	Rolling moment	Rolling moment or rolling velocity

CONTROL REVERSAL EFFECTS ON SWEPT-BACK WINGS

Having established what is to be taken as a measure of rolling power, the effect of wing distortion on the rolling power of a swept-back wing may now be considered. Sweepback of course not only introduces additional distortion effects but also alters the aerodynamic characteristics of wing and aileron, all of which influence the rolling power. The purpose of this paper is not to assess the overall effect of sweep on rolling power but merely to provide a clear physical picture of the effects produced by distortion on a swept-back wing and of the conditions promoting control reversal. The purely aerodynamic aspect of sweep does not therefore enter specifically into the discussion.

TABLE II

	Reversal condition
Rolling motion	Zero velocity and acceleration
Applied rolling moment due to aileron and wing distortion	Zero
Wing distortion due to loads from	Aileron deflection and wing distortion

Starting with the simplest case of all, that of a swept-back wing in the static condition, aileron deflection produces aerodynamic loads which for, say, the port half of the wing with down aileron, are as shown in Fig. 5. These "aileron" loads, which are distributed over the length of the aileron, are

A—upward lift loads applied at the aerodynamic centre,

B—nose-down moment loads applied in the chordwise plane.

Attention is confined to the port wing, effects on the starboard wing with up aileron being simply reversed.

Assuming for the moment the flexural and aerodynamic axes coincident, these aileron loads produce a nose-down twisting and an upward flexing of the wing, both of which involve an aerodynamic wash-out. This introduces the distortion loads C pictured in Fig. 6, downward or negative lift loads distributed over the whole wing and increasing outwards from the centre. In the equilibrium condition the wing distortion is then the result of both aileron and distortion loads, as follows:—

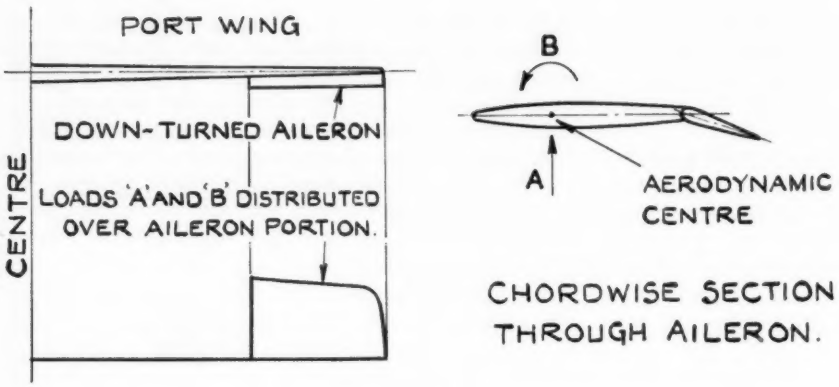

Fig. 5.
"Aileron" loads.

Torsional distortion = nose-down twisting due to component of loads B in normal direction.

Upward flexing = flexing due to component of loads B along spar + flexing due to loads A − flexing due to loads C.

The distortion loads C at the same time apply a rolling moment opposed to that produced by the aileron loads A, and in the equilibrium condition

Net rolling moment = rolling moment due to loads A
− rolling moment due to loads C.

Since the aileron loads increase with speed, so also does the wing distortion. Loads C, which increase with distortion and speed, therefore increase relative to loads A until reversal is reached, when the net rolling moment becomes zero.

It is interesting to note that the relative amounts of torsional and flexural distortion change with speed. At low speeds the distortion loads C are small compared with the aileron loads A, whereas at reversal they are equivalent in so far as they produce a numerically equal rolling moment. To a rough approximation one may therefore say that

Upward flexing at low speeds = flexing due to component of loads B along spar
+ flexing due to loads A.

Upward flexing at reversal = flexing due to component of loads B along spar.

Torsional distortion, on the other hand, is directly proportional to the aileron loads B over the whole speed range.

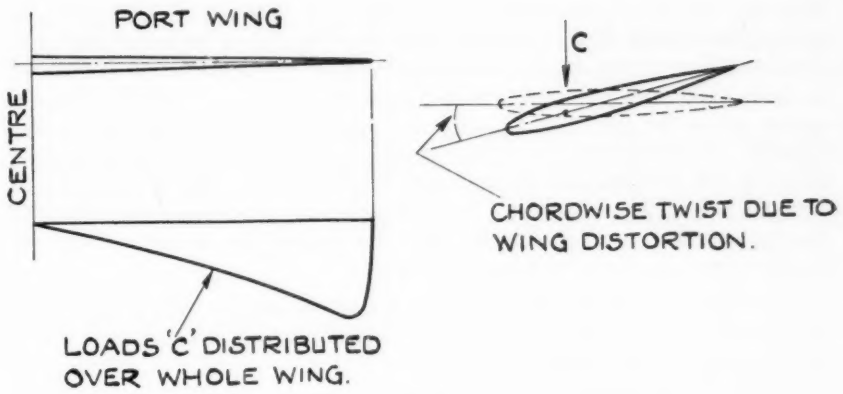

Fig. 6.
Distortion loads—aileron.

It is apparent, therefore, that the ratio of flexural to torsional distortion decreases with speed, this being particularly so in the case of moderate sweepback where the flexing effect of the component of loads B along the spar is small compared with that of loads A. In such a case the upward flexing at low speeds is almost entirely due to loads A while the flexing at reversal is practically nil. It is, of course, not quite true that at reversal there is no flexural distortion due to lift loads, because although loads A and C give equal and opposite rolling moments about the centre, the fact that they are not distributed in the same way along the wing means that they may still provide some flexural moment at intermediate points. This, however, is a secondary effect and would not alter the general conclusions already reached.

If the flexural and aerodynamic axes are not coincident then in the equilibrium condition there will be some torsion about the flexural axis, due to the net upward lift loads (A—C) acting at the aerodynamic centre. With a flexural axis in front of the aerodynamic axis this torsion results in a further nose-down twisting of the wing, thus increasing the distortion effects already present. A rearward flexural axis would of course have the opposite effect. In any case, the effect of the position of the flexural axis, since it depends upon the net lift loads (A—C), must progressively decrease with speed and will be small at reversal. One would expect, therefore, that at speeds below reversal a forward flexural axis should reduce and a rearward flexural axis increase the net rolling power, but that neither should greatly affect the reversal speed.

Finally, there are the additional effects introduced when considering cases other than the static condition: namely, rolling inertia loads in the initial condition and damping loads in the steady rolling condition. As far as flexural distortion is

concerned, the effect is much the same in either case; addition of either inertia or damping load results in zero net moment about the longitudinal axis at the centre, and flexural moment on the wing is consequently reduced, as in the reversal condition of the static case. One may expect to find, therefore, that flexural distortion plays a smaller part in the more realistic initial and steady rolling conditions than it does in the static condition. Since the damping and inertia loads act downwards, torsional distortion will be increased with a flexural axis behind the aerodynamic or inertia axis and reduced if it is in front. These departures from the static condition will be most apparent at low speeds; as reversal is approached the three conditions, as already argued, become one and the same.

If there is any camber change due to flexural distortion it will, if the wing is flexing upwards, be a negative change, involving additional negative lift loads at the aerodynamic centre together with nose-up pitching moment loads in the chordwise plane. These additional loads are directly opposed to the aileron loads A and B and, in fact, the effect of the negative camber change is mostly simply seen as a plain reduction in the positive camber induced by the down-turned aileron: except, of course, that the camber change due to flexural distortion occurs over the whole wing instead of over the aileron portion alone. The net effect can be represented as an effective scaling down of the aileron loads, resulting in a corresponding reduction of both distortion effects and rolling power. As the camber change is proportional to the flexural distortion its effect will decrease with speed and should therefore be small at reversal.

Aileron reversal effects, that is rolling power and the associated reversal speed, can be estimated for a swept-back wing by methods similar to those used for unswept wings, the analysis being merely extended along the lines already suggested to cover the effects of flexural distortion. Broadly speaking, a choice of two methods is offered; either the semi-rigid method in which arbitrary modes of distortion are assumed and the absolute displacements at some reference section obtained by a direct single-stage solution, or the more exact method in which the modes of distortion appropriate to the actual loading are deduced from the elastic characteristics as the result of an iterative process.

An alternative method representing a compromise between these two was developed by the author, originally for the estimation of elevon reversal effects, but later applied to aileron reversal effects. The method is presented in the Appendix to this paper, and a general description of its nature will suffice here. Chordwise rotation (relative to the centre) due to both torsional and flexural distortion is represented as a series function of the spanwise co-ordinate, the series consisting of a linear term plus a Fourier series. Using the Schrenk approximation suitably modified to cater approximately for the effect of sweepback, the aerodynamic loads are then obtainable as functions of the series coefficients; hence the distortion itself is obtained (still as a function of the series coefficients) by an "exact" treatment

using the applied loads in combination with the elastic characteristics of the spar. The chordwise rotation due to this distortion is then equated to the original series function to give an equation (called for convenience the "twist" equation) in the series coefficients.

By applying the "twist" equation at as many stations as there are coefficients a direct solution is provided for the coefficients and hence the distortion and corresponding reversal effects. The method is in fact analogous to the standard Glauert method for determining aerodynamic loading by lifting-line theory. With an infinite number of coefficients the method is a true elastic one and with some justification may be therefore termed an "elastic wing series solution"; but in practice the value of the method obviously depends upon a good approximation being obtained with relatively few coefficients.

This principle is demonstrated by the results of calculations made upon a hypothetical V wing. Calculated reversal speeds were obtained using one to five terms in the series function and the results are given in Table III.

The calculations were performed only to slide-rule accuracy, but it is evident that in this particular case the two-term solution is sufficiently accurate, while even the one-term solution gives quite a fair result, underestimating the reversal speed by only 4 per cent. The one-term solution, which involves only the linear term in the series function, corresponds to an assumption of linear distribution of the chordwise rotation due to distortion: the extent to which the one-term solution is in error therefore represents the degree to which this assumption is fallacious.

In Fig. 7 the calculated values of rolling moment coefficient by the one-term solution for the same wing in the static condition are plotted against speed and compared with the values given by a semi-rigid method. Aerodynamic characteristics were the same for both and the results are therefore directly comparable. In the semi-rigid method a linear mode was assumed for the net chordwise rotation due to both torsional and flexural distortion; torsion due to lift loads about the flexural axis was ignored.

It is interesting to note that over the first two-thirds of the speed range the semi-rigid method provides a good approximation, but the reversal speed is underestimated by 14 per cent. compared with the one-term solution and by 17 per cent. compared with the four-term solution.

TABLE III

Number of terms	1	2	3	4	5
Reversal speed, m.p.h.	299	314	314	312	312

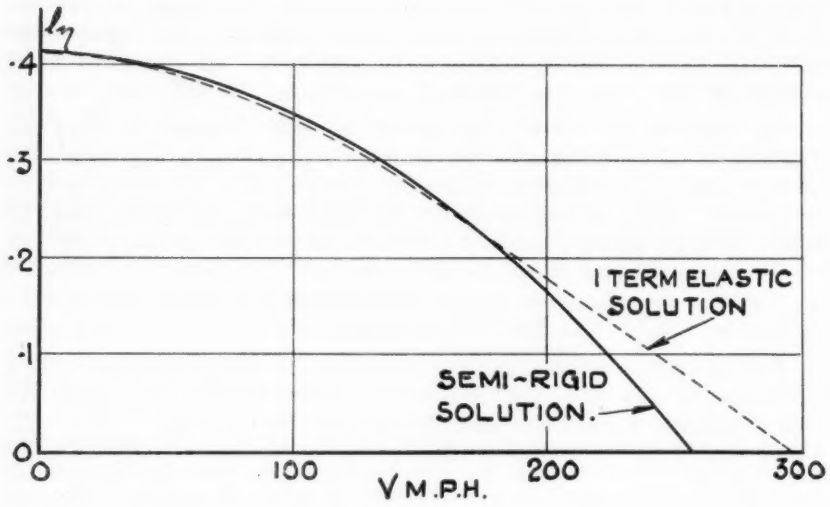

Fig. 7.
Static rolling moment for V wing.

3. ELEVON REVERSAL EFFECTS

Elevon reversal effects are applicable only to a tailless aeroplane and refer to the control reversal effects associated with the use of the elevon as an elevator. Because of the fairly recent development that has taken place in tailless aircraft the subject is relatively new compared with aileron reversal effects, although the essential principles underlying the two phenomena are the same. There are, however, certain interesting differences, not the least of which is the relative importance of the two effects. Although aileron reversal would be a highly undesirable feature, particularly on a military aeroplane, elevon reversal would be completely disastrous on any type, involving in its extreme form inability to pull out of a dive.

When flying at high speed it may not always be absolutely necessary to execute lateral manœuvres, but it must invariably be essential to be able to trim the aeroplane without danger of structural failure due to large wing distortion consequent upon use of the elevon; it is equally important that elevon effectiveness should not be reduced to the extent that the available elevon movement is insufficient for trim. In short, because of the natural juxtaposition of earth and sky symmetric manœuvres in the vertical plane must attain in the limit greater significance than lateral manœuvres in the horizontal plane and, apart from manœuvres, the aeroplane must

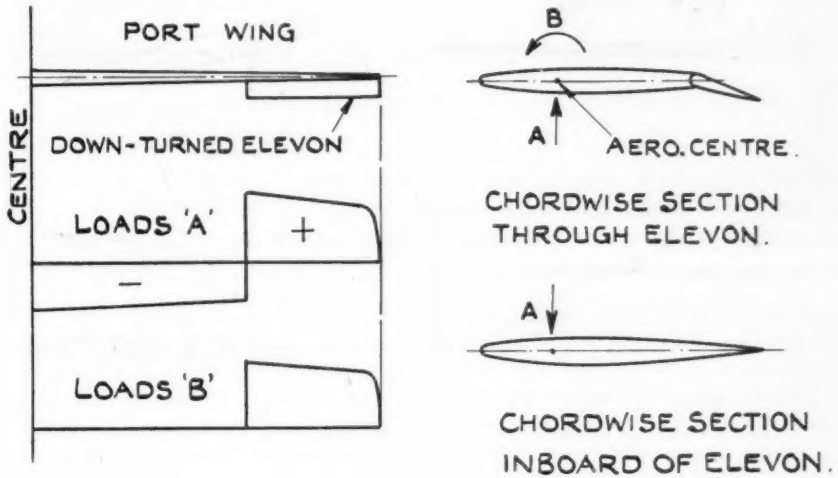

Fig. 8.
"Elevon" loads (no-lift condition).

be capable of being maintained in the steady flight condition. It is fortunate that from the nature of things, as will be seen later, a greater margin is automatically guaranteed for reversal of the elevon used as an elevator, than for reversal when used as an aileron.

As rolling power is a measure of aileron effectiveness, so there is an analogous elevon power representing the effectiveness of the elevon used as an elevator in symmetric manœuvres. Again, as with the aileron, a complete representation of elevon power would be based on a dynamic condition, as for instance rate of pitch or number of "g" achieved in a steady pull-out. These effects depend ultimately upon the power of the elevon as a pitching moment or C_{mo} producer, and this can be represented conveniently by a static condition analogous to that used for the rolling power of the aileron.

Static elevon power is thus defined as the additional C_{mo} per unit elevon angle in the static condition and is represented directly by the total pitching moment produced on the wing with deflected elevon when the wing is held at the centre with the mean no-lift line of the wing-elevon combination parallel to the air stream. Any extraneous symmetric effects due to initial camber or twist of the undistorted wing are excluded, only the symmetric effects arising from the elevon deflection being considered.

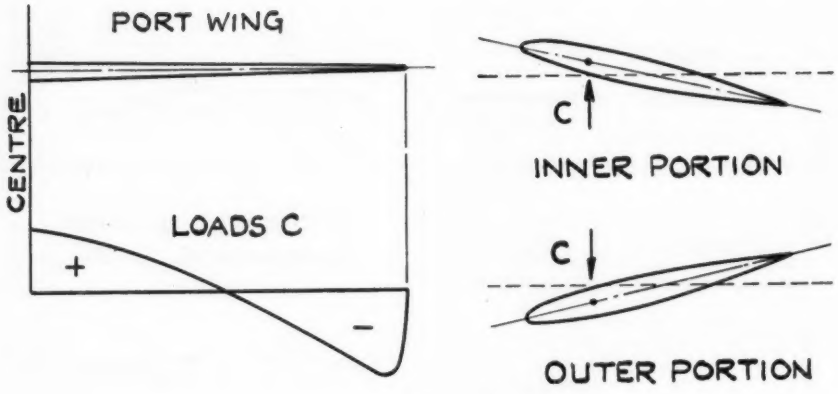

Fig. 9.
Distortion loads—elevon (no-lift condition).

For this condition the same qualitative analysis of loads and distortions can be made as was done for the aileron. The "elevon" loads due to downward elevon deflection are shown in Fig. 8 for the no-lift condition, and consist of

A—lift loads symmetrically distributed on the two halves of the wing, up over the elevon portion, down over the inner portion.

B—nose-down moment loads confined to the elevon portion, applied in the chordwise plane.

Assuming for the moment, as before, that flexural and aerodynamic axes coincide, these elevon loads produce nose-down twisting and upward flexing as on the port wing in the aileron case. The resulting symmetric aerodynamic wash-out provided by both these effects gives rise to the distortion loads C which for the no-lift condition are as pictured in Fig. 9: upward lift loads over the inner portion, downward lift loads over the outer portion. In the equilibrium condition the wing distortion, as before, is finally composed of

Torsional distortion = nose-down twisting due to component of loads B in normal direction.

Upward flexing = flexing due to component of loads B along spar + flexing due to loads A − flexing due to loads C.

The C_{mo} produced by the elevon deflection alone is represented by the pitching moment due to the elevon lift loads A and moment loads B of Fig. 8. These are

additive and give a nose-down or negative C_{mo}. Distortion loads C of Fig. 9, give a positive C_{mo}, and the net C_{mo} is therefore reduced numerically from what it would be for the rigid wing. In the equilibrium condition

Net C_{mo} = (C_{mo} due to moment loads B) + (C_{mo} due to lift loads A) − (C_{mo} due to lift loads C).

This reduction in power is progressive with speed, as in the case of the aileron, and a reversal condition is therefore possible in which the net elevon power becomes zero. In the reversal condition interesting differences arise between aileron and elevon.

For the aileron the lift loads C due to distortion balance in effect the lift loads A due to control deflection to produce zero rolling moment. To produce zero pitching moment in the elevon reversal condition, the lift loads C due to distortion must balance both lift and moment loads (A and B) due to control deflection: therefore distortion must be greater, involving a higher speed. From qualitative considerations alone, therefore, it can be deduced that the elevon reversal speed on a given tailless aeroplane must be greater than the aileron reversal speed.

The second important difference lies in the qualitative effect of flexural distortion. Since at reversal the distortion loads C provide a pitching moment numerically equal to that given by the elevon lift and moment loads together, then loads C must be appreciably greater than loads A. It is therefore quite possible for the net downward lift loads (C—A) to be greater in their effect than the component of loads B along the spar, with the result that the wing flexes *downwards*. In the case of the aileron the wing was judged to flex upwards, although to a relatively decreasing extent, over the whole speed range up to reversal: with the elevon, however, the extension of the speed range consequent upon the higher reversal speed results in an increasingly downward flexed wing over the upper end of the speed range. As the upward flexed wing reduces elevon power, so the downward flexed wing augments it and the effect of flexural distortion, therefore, is to delay reversal, opposing in fact the effect of torsional distortion. At the low speed end, where the wing is flexing upwards, flexural distortion acts in the same sense as torsional distortion to reduce elevon power. Since flexural distortion delays reversal, it is conceivable that if the flexural stiffness is low enough, compared with the torsional stiffness, reversal might be delayed indefinitely.

The additional effects of flexural axis position and of any camber change due to flexing will be similar to what they were in the case of aileron reversal. Except, that in so far as they depend upon the net lift loads the effect will be reversed at the high speed end. A forward flexural axis position, for example, will be bad as it was for the aileron at the low speed end, but will change to a good effect at, or near, reversal.

Any dynamic conditions involving the addition of "*g*" effects on the wing, that is inertia loads and associated wing lift, if the weights, as is usual, are concentrated more towards the centre than the lift, will result in upward flexing of the wing and a corresponding wash-out. In the pull-out this will assist the upward-turned elevon. On the other hand, curvature of the flight path induces a wash-in which opposes the elevon.

In addition to the question of elevon power there is the problem of trim in the steady symmetric flight condition. The two are related in the sense that the lower the elevon power, the more elevon angle would be required for trim and, proceeding to the limit, an infinite elevon angle would, theoretically, be required at the reversal speed. It is advisable, therefore, to ensure that at the maximum speed of the aeroplane there is sufficient angle available for trim, with a comfortable margin, even though the maximum speed may be well below the reversal speed.

In the steady symmetric flight condition there are, as in the static condition envisaged in the consideration of elevon power, loads due to elevon deflection and wing distortion; but in addition there are also loads due to basic (or initial) camber and twist of the wing and loads due to gravity and the associated wing lift. Wing distortion is the net result of all these loads. For a constant attitude of flight, say level flight, loads due to gravity and the associated wing lift remain constant with speed and have only a small effect at high speed. Loads due to initial wing camber and twist, however, increase with speed and in consequence may have a major effect. A wing, for instance, may be given considerable initial positive camber for design reasons and in order to cancel the negative pitching moment due to this camber an initial wash-out may also be applied, so that at high speed the elevon angle required for trim should be small.

The initial wash-out, in fact, corresponds to tail setting on a tailed aircraft. At high speed the lift loads due to this initial wash-out can easily exceed the effect of gravity and wing lift and produce a downward flexing of the wing, as opposed to the upward flexing which would normally result if there were no initial camber and twist. Wash-in induced by the downward flexing of the wing requires a corresponding negative or upward increment of elevon angle for balance. The sign of the increment of elevon angle required to trim due to wing flexibility, therefore, may be acutely dependent upon the degree of initial wing camber and twist present. Particular attention is drawn to this feature because in the author's experience the possibility of downward flexing of a tailless wing at high speed seems not always to be realised.

The elastic wing series solution described in the preceding section is equally applicable to the estimation of elevon reversal effects, for which, as already stated, it was originally developed. In the presentation of the method given in the Appendix to this paper the two applications are given jointly. The only differences that arise

are concerned with the symmetric and asymmetric nature of the two phenomena. In the case of elevon reversal effects, for instance, allowance must be made for the change in mean wing no-lift line due to the symmetric distribution of wing distortion and elevon angle. In the consideration of elevon power attention is confined to the static condition. The method is also easily extended to include the effect of loads due to initial wing camber and twist, gravity, and wing lift in the steady symmetric flight condition. This is also included in the Appendix. In this case the elevon angle required for trim enters as a further unknown but is provided for by the introduction of an additional equation representing the general pitching moment equilibrium of the complete aeroplane.

Calculations have been made by this method for the same hypothetical wing as was used for aileron reversal effects. In the first place convergence tests were made, as before, to examine the effect of the number of terms taken in the series function. In this case, however, the tests were made by calculating not reversal speed, but the increment in elevon angle $\Delta\eta$ required to trim due to wing flexibility in the level flight condition at 500 m.p.h. E.A.S. The results, given in Table IV, indicate that at least three and preferably four terms should be used, although a fair result is given by the two-term solution. The error involved in the one-term solution is a direct indication of the lack of linearity in the distribution of the chordwise rotation due to distortion in this case.

By systematic variations of certain of the design parameters, the effect of these parameters on the elevon reversal characteristics of the hypothetical wing was also investigated. The parameters concerned were flexural axis position, aspect ratio, angle of sweepback, wing loading, and the torsional and flexural stiffnesses. In the case of aspect ratio the wing span was altered in order to keep wing area constant. Also, for both aspect ratio and sweepback the elevon percentage chord was varied in order to maintain a consistent representative design. For each set of variations the elevon reversal speed V_R and the increment in elevon angle $\Delta\eta$ due to wing flexibility for trim in level flight at 500 m.p.h. were calculated for a range of values of the appropriate parameter, using the one-term solution. Although the convergence tests showed the unreliability of the one-term solution for absolute values,

TABLE IV

Number of terms	1	2	3	4	5
$\Delta\eta$ radians	– .0406	– .0213	– .0223	– .0232	– .0236

it is still reasonable to suppose that it should predict tendencies fairly well. Figs. 10 to 16 give the results of these calculations as plots of V_R and $\Delta\eta$ against the value of the relevant parameter, whose basic value appropriate to the hypothetical wing is indicated in each case.

It will be noted, incidentally, that the elevon reversal speed of the basic wing is 600 m.p.h. by the one-term solution. Although this may be considerably in error it is evident from the convergence test results that since the higher term solutions show the wing capable of being trimmed at 500 m.p.h., the true reversal speed must therefore be at least greater than 500 m.p.h. This is much higher than the aileron reversal speed of 312 m.p.h. for the same wing, thus confirming the qualitative conclusions already reached.

The effects of the design parameters as given in Figs. 10 to 16 are summarised in Table V by designating them broadly as either "good" or "bad." In most cases the changes in V_R and $\Delta\eta$ are consistent, one increasing while the other decreases, but where they conflict precedence is given to the change in $\Delta\eta$ on the principle that more practical significance is attached to the trim condition than to the actual reversal condition.

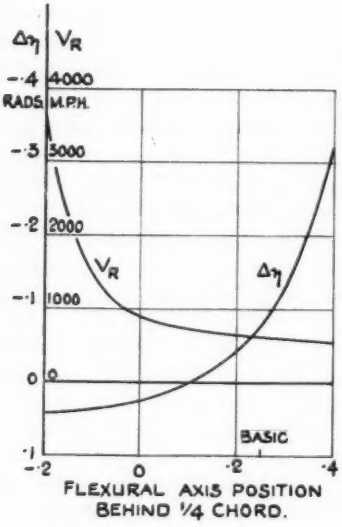

Fig. 10.
Effect of flexural axis position.

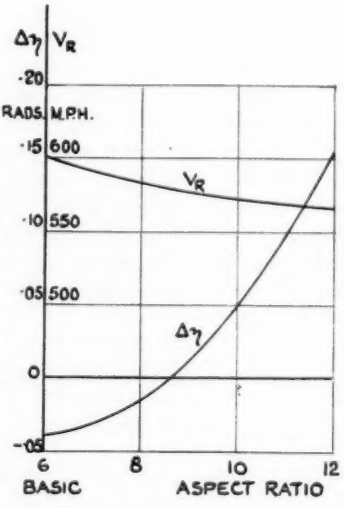

Fig. 11.
Effect of aspect ratio.

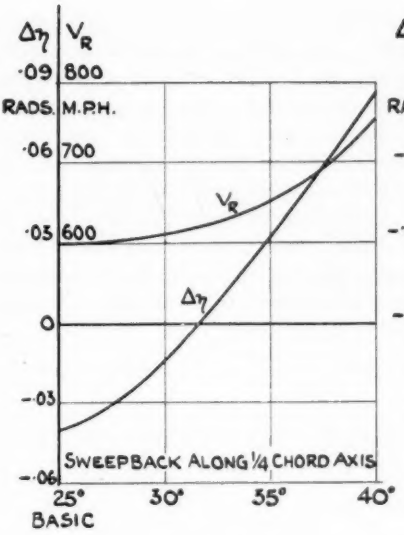

Fig. 12.
Effect of sweepback.

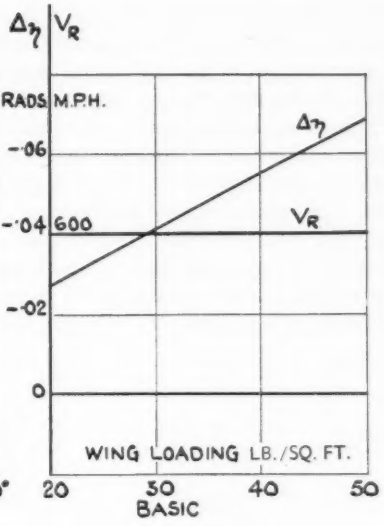

Fig. 13.
Effect of wing loading.

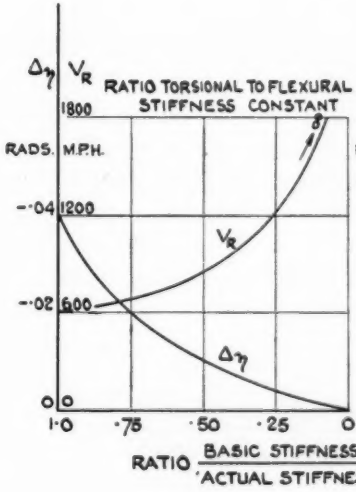

Fig. 14.
Effect of overall stiffness.

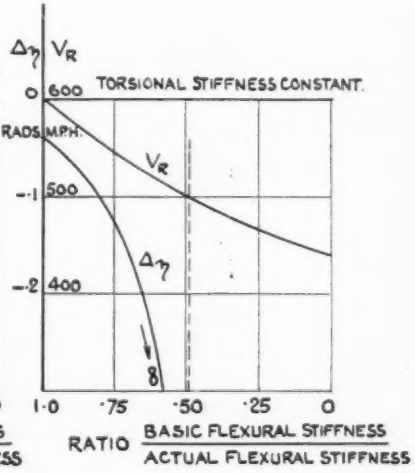

Fig. 15.
Effect of flexural stiffness.

It is interesting to note that the effect of flexural axis position is as predicted qualitatively. For a given flight condition V_R is independent of, and $\Delta\eta$ is directly proportional to, wing loading. Three diagrams are devoted to the effect of varying stiffness. In the first, Fig. 14, both torsional and flexural stiffnesses are increased, their ratio being kept constant. Reversal speed is proportional to the square root of either stiffness and therefore becomes infinite for infinite stiffness and $\Delta\eta$ correspondingly zero. In Fig. 15 the flexural stiffness is increased while the torsional stiffness is maintained at the basic value. As the reversal speed falls to 500 m.p.h. so the value of $\Delta\eta$ becomes theoretically infinite. In Fig. 16 the torsional stiffness is increased while the flexural stiffness is maintained at the basic value. Here it is demonstrated that, as was anticipated, there is a critical value of the ratio of flexural to torsional stiffness below which reversal is completely inhibited.

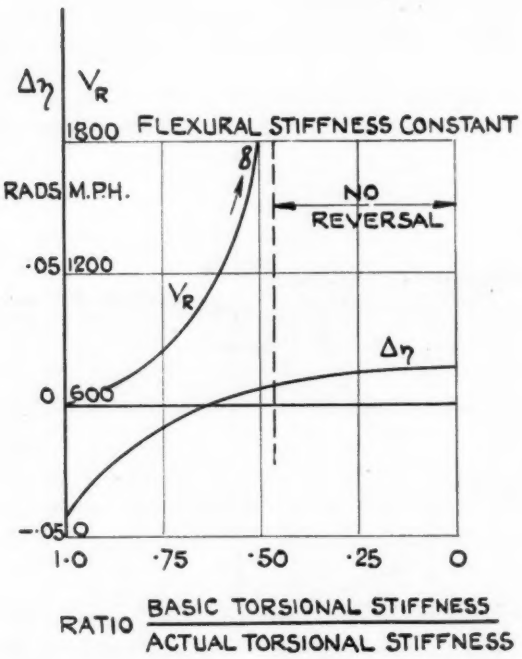

Fig. 16.
Effect of torsional stiffness.

TABLE V

Parameter	*Effect of increasing the parameter*		
	V_R	$\Delta\eta$	*General*
Rearward position of flexural axis	Decreases	Increases	Bad
Aspect ratio	Decreases	Increases	Bad
Sweepback	Increases	Increases	Bad
Wing loading	Unaffected	Increases	Bad
Values of both stiffnesses	Increases	Decreases	Good
Ratio of torsional to flexural stiffness	Increases	Decreases	Good

APPENDIX

ELASTIC WING SERIES SOLUTION FOR CONTROL REVERSAL EFFECTS

1. *Notation*

a_m effective local dC_L/dz for twist-without-lift loading (*see* equation (8)).

A moment of inertia of aeroplane about the longitudinal axis.

c wing section chord.

$\bar{c}$ wing mean chord.

$\bar{C}_L$ mean wing lift coefficient.

C_{La} section C_L due to lift-without-twist (proportional to $\bar{C}_L$)

by Schrenk, $C_{La}/\bar{C}_L = 0.5 + \left(\frac{2}{\pi}\right)\left(\frac{\bar{c}}{c}\right)(1-z^2)^{\frac{1}{2}}$.

C_{Le} twist-without-lift section C_L due to unit elevon or aileron angle.

for symmetric elevon application:

$C_{Le} = a_m(\delta_e - \bar{\delta})$ over elevon portion and $= -a_m\bar{\delta}$ elsewhere.

for asymmetric aileron application:

$C_{Le} = a_m\delta_e$ over aileron portion and $= 0$ elsewhere } port wing.

C_{Lp}	additional section C_L due to rolling, per unit ps/V.
C_{mo}	pitching moment coefficient at zero lift.
$\overline{C}_{mo}$	mean pitching moment coefficient at zero lift.
C_{mow}	additional section C_{mo} due to initial wing camber.
C_{moc}	additional section C_{mo} due to unit elevon or aileron angle.
$\overline{C}_{mow}$	$\overline{C}_{mo}$ of plain undistorted wing, due to initial camber and initial twist.
E.A.S.	equivalent air speed.
EI	flexural rigidity of normal section.
GJ	torsional rigidity of normal section.
g	acceleration due to gravity.
L_η	total applied rolling moment (whole wing) per unit aileron angle.
l_p	rolling moment derivative due to rolling.
l_η	rolling moment coefficient $= L_\eta/qSs$.
$l_{\eta R}$	value of l_η for the static rigid wing, that is due to aileron deflection only.
m_η	net elevon power in the static condition, that is additional wing $\overline{C}_{mo}$ per unit elevon angle.
$m_{\eta R}$	value of m_η for the static rigid wing, that is due to elevon deflection only.
M	moment about a chordwise axis through the flexural centre.
M'	moment about a normal axis.
p	rolling velocity, radians per sec.
q	dynamic pressure $\frac{1}{2}\rho V^2$.
s	wing semi-span.
S	total wing area.
T	moment about a lateral axis through the flexural centre.
T'	moment about the flexural axis.
V	aeroplane forward speed (ft./sec.).
V_R	elevon reversal speed.
w_c	concentrated weight.

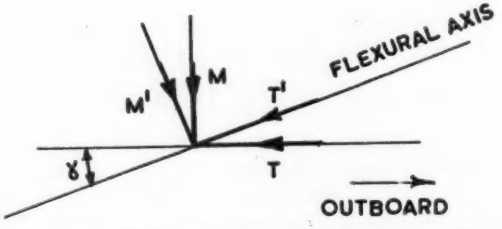

Moments are positive as shown, with the usual convention of the right-hand screw in the direction of the arrow.

w_d distributed weight per unit span.

$\bar{w}$ mean span loading $= W/2s$.

W total aeroplane weight.

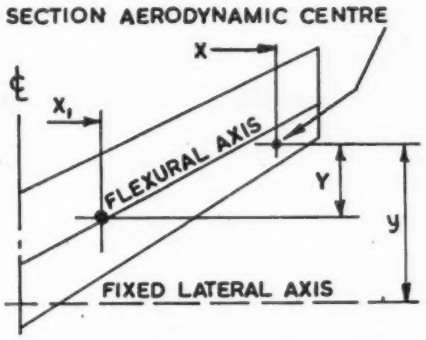

x spanwise distance from the centre, measured laterally.

x_1 distance outboard along the flexural axis.

K_n stick fixed static margin.

y distance of section aerodynamic centre behind a fixed lateral axis.

Y distance of section aerodynamic centre at x behind a lateral axis through the flexural centre at x_1, inboard of x. For weights, Y similarly defines the c.g. position.

z spanwise co-ordinate x/s.

α angle of incidence, in definition of a_m.

γ local angle of sweepback of the flexural axis.

$\Delta\eta$ increment in elevon angle required to trim due to wing flexibility.

δ_c increase in section no-lift angle due to unit elevon or aileron angle.

$\bar{\delta}$ increase in wing no-lift angle due to unit elevon angle.

η elevon or aileron angle relative to wing in chordwise plane, positive downward, assumed the same at all sections.

θ' torsional twist of the normal section, positive nose-up.

θ chordwise rotation due to wing distortion relative to section at centre, positive nose-up.

$\bar{\theta}$ increase in wing no-lift angle due to wing distortion.

θ_o initial chordwise rotation of the undistorted wing relative to section at centre, positive nose-up.

$\bar{\theta}_o$ wing no-lift angle relative to section at centre, positive nose-up, for the undistorted wing.

ρ air density.

ψ change of slope due to flexure, measured along the flexural axis.

2. *Chordwise rotation due to wing distortion*

Equilibrium conditions at any section give

$$M' = M\cos\gamma - T\sin\gamma$$
$$T' = T\cos\gamma + M\sin\gamma.$$

The net increment in chordwise rotation due to torsional and flexural distortion is

$$d\theta = d\theta'\cos\gamma - d\psi\sin\gamma.$$

Also, $d\theta' = \left(\frac{T'}{GJ}\right)dx'$

and $d\psi = \left(\frac{M'}{EI}\right)dx'$.

Substituting for $d\theta'$ and $d\psi$, and for M' and T', and writing $dx' = dx/\cos\gamma$ gives finally

$$\frac{d\theta}{dx} = K_t T + K_m M, \quad . \quad . \quad . \quad . \quad . \quad (1)$$

where $K_t = \left(\frac{1}{GJ} + \frac{\tan^2\gamma}{EI}\right)\cos\gamma$

$$K_m = \left(\frac{1}{GJ} - \frac{1}{EI}\right)\sin\gamma.$$

Equation (1) is the general equation for chordwise rotation due to wing distortion and is applicable to all reversal effects. The effective flexibilities K_t and K_m will vary in general from section to section.

3. *Elevon reversal effects on a tailless aeroplane*

The effects considered are symmetric and account must be taken of the position of the mean wing no-lift line.

Chordwise rotation due to wing distortion is represented by the series function

$$\theta = \Sigma\, a_n . \sin n\pi z, \quad . \quad . \quad . \quad . \quad . \quad (2)$$

$$(n = 0, 1, 2, 3, \text{etc.})$$

where, in the case of $n = 0$, $\sin n\pi z$ is replaced by z.

The net incidence of the wing relative to the mean no-lift line is $(\theta_o - \bar{\theta}_o)$ due to initial twist and $(\theta - \bar{\theta})$ due to distortion. By the Schrenk approximation

$$\bar{\theta}_o = \int_0^1 \theta_o (c/\bar{c})\, dz$$

$$\bar{\theta} = \int_0^1 \theta (c/\bar{c})\, dz = \Sigma\, a_n \cdot {}_n\zeta_{S1} \quad . \quad . \quad . \quad . \quad . \quad (3)$$

$$\text{and } {}_n\zeta_{S1} = \int_0^1 \sin n\pi z\, (c/\bar{c})\, dz.$$

The contribution to wing $\bar{C}_{mo}$ provided by the distortion is

$$\bar{C}_{mo} = -\int_0^1 a_m (\theta - \bar{\theta})(c/\bar{c})(y/\bar{c})\, dz$$

$$= \Sigma\, a_n \cdot {}_n\zeta_{S2}$$

$$\text{where } {}_n\zeta_{S2} = \int_0^1 a_m ({}_n\zeta_{S1} - \sin n\pi z)(c/\bar{c})(y/\bar{c})\, dz.$$

Adding $\bar{C}_{mow}$ for the plain wing (including the effect of the initial twist θ_o) and $m_{\eta R}\eta$ for elevon deflection then gives the total wing $\bar{C}_{mo}$. The condition for pitching moment equilibrium is therefore

$$\Sigma\, a_n \cdot {}_n\zeta_{S2} + \bar{C}_{mow} + m_{\eta R}\eta - K_n \bar{C}_L = 0, \quad . \quad . \quad . \quad . \quad (4)$$

referred to generally as the "trim" equation.

Wing distortion effects are represented by applying equation (1) with the appropriate conditions. The net component torque and bending moment due to aerodynamic loads and weights are, at station x_1,

$$T = \int_{x_1}^{s} C_{mo} qc^2 dx - \int_{x_1}^{s} C_L qcY dx + \int_{x_1}^{s} w_d Y dx + \sum_{x_1}^{s} w_c Y \quad . \quad . \quad (5)$$

$$M = \int_{x_1}^{s} C_L qc\,(x - x_1)\, dx - \int_{x_1}^{s} w_d (x - x_1)\, dx - \sum_{x_1}^{s} w_c (x - x_1). \quad . \quad (6)$$

The total section C_{mo} and section C_L due to all the various effects, including wing distortion, are

$$C_{mo} = C_{mow} + \eta C_{moe} \quad . \quad . \quad . \quad . \quad . \quad (7)$$

$$C_L = C_{La} + a_m (\theta_o - \bar{\theta}_o) + a_m (\theta - \bar{\theta}) + \eta C_{Le}. \quad . \quad . \quad . \quad (8)$$

Substituting (5), (6), (7) and (8) in equation (1) gives finally

$$\frac{d\theta}{dx} = qs\bar{c}^2 (A_1 + B_1\bar{C}_L + C_1\eta + \Sigma a_n \cdot {}_n\zeta_3), \quad . \quad . \quad . \quad (9)$$

where, for station $x_1 = z_1 s$,

$$A_1 = K_t \int_{z_1}^{1} \{ C_{mow} (c/\bar{c})^2 - a_m (\theta_o - \bar{\theta}_o) (c/\bar{c}) (Y/\bar{c}) \} dz +$$

$$+ K_m \int_{z_1}^{1} a_m (\theta_o - \bar{\theta}_o) (c/\bar{c}) \left(\frac{x - x_1}{\bar{c}}\right) dz$$

$$B_1 = K_t \int_{z_1}^{1} \left\{ -\left(\frac{C_{La}}{\bar{C}_L}\right)(c/\bar{c}) (Y/\bar{c}) + \left(\frac{w_d}{\bar{w}}\right) (Y/\bar{c}) \right\} dz + K_t \sum_{z_1}^{1} \left(\frac{2w_c}{W}\right) (Y/\bar{c}) +$$

$$+ K_m \int_{z_1}^{1} \left\{ \left(\frac{C_{La}}{\bar{C}_L} (c/\bar{c})\right)\left(\frac{x - x_1}{\bar{c}}\right) - \left(\frac{w_d}{\bar{w}}\right)\left(\frac{x - x_1}{\bar{c}}\right) \right\} dz - K_m \sum_{z_1}^{1} \left(\frac{2w_c}{W}\right)\left(\frac{x - x_1}{\bar{c}}\right)$$

$$C_1 = K_t \int_{z_1}^{1} \left\{ C_{moc} (c/\bar{c})^2 - C_{Lc} (c/\bar{c}) (Y/\bar{c}) \right\} dz + K_m \int_{z_1}^{1} C_{Lc} (c/\bar{c}) \left(\frac{x - x_1}{\bar{c}}\right) dz$$

$${}_n\zeta_3 = K_t \int_{z_1}^{1} a_m ({}_n\zeta_1 - \sin n\pi z) (c/\bar{c}) (Y/\bar{c}) dz -$$

$$- K_m \int_{z_1}^{1} a_m ({}_n\zeta_1 - \sin n\pi z) (c/\bar{c}) \left(\frac{x - x_1}{\bar{c}}\right) dz.$$

K_t and K_m are the effective flexibilities at station x_1.

Integrating equation (9) gives the chordwise rotation due to wing distortion as

$$\theta = qs^2\bar{c}^2 (A_2 + B_2\bar{C}_L + C_2\eta + \Sigma a_n \cdot {}_n\zeta_4), \quad . \quad . \quad (10)$$

where $A_2 = \int_0^z A_1 dz$, etc.

and ${}_n\zeta_4 = \int_0^z {}_n\zeta_3 dz$

This must agree with equation (2), and equating the two gives finally the "twist" equation as

$$\Sigma a_n \left\{ {}_n\zeta_4 - \left(\frac{4}{qS^2}\right) \sin n\pi z \right\} + A_2 + B_2 \bar{C}_L + C_2 \eta = 0. \quad . \quad . \quad (11)$$

For a given speed, q and $\bar{C}_L$ are known. The "twist" equation (11) is applied at as many stations as there are coefficients a_n. With the "trim" equation (4) this provides a set of simultaneous linear equations for the solution of the coefficients a_n and elevon angle η.

Net elevon power in static condition

The net elevon power ($\bar{C}_{mo}$ per unit elevon angle) due to elevon deflection and wing distortion is

$$m_\eta = m_{\eta R} + \Sigma a_n \cdot {}_n\zeta_2, \quad . \quad . \quad . \quad . \quad . \quad (12)$$

where the coefficients a_n give the chordwise rotation due to distortion arising from application of unit elevon angle in the static condition.

The "twist" equation is equation (11) with the A and B functions omitted to exclude all effects other than those due to elevon deflection and wing distortion. With $\eta = 1$, the "twist" equation then becomes

$$\Sigma a_n \left\{ {}_n\zeta_4 - \left(\frac{4}{qS^2}\right) \sin n\pi z \right\} + C_2 = 0. \quad . \quad . \quad . \quad (13)$$

For a given speed the "twist" equation (13) provides a set of simultaneous linear equations for the solution of the coefficients a_n, which when substituted in equation (12) give the net elevon power m_η.

The elevon reversal condition is given by putting m_η in equation (12) equal to zero. With the "twist" equation (13) this provides a solution for the coefficients a_n and the speed $V = \sqrt{(2q/\rho)}$ (see later under *Aileron reversal condition*).

4. *Aileron reversal effects*

These effects are asymmetric and there is therefore no change in the mean wing no-lift line. Consider, for example, the port wing with unit down aileron angle.

Static condition

The only loads which arise are those due to aileron deflection and wing distortion.

The total rolling moment for the whole wing due to aileron deflection alone is

$$2\int_0^s C_{Lc}qcxdx = l_{\eta R}qSs,$$

where $$l_{\eta R} = \int_0^1 C_{Lc}\,(c/\bar{c})\,zdz.$$

The total rolling moment due to chordwise rotation is similarly

$$2\int_0^s a_m\theta qcxdx = qSs\,\Sigma\, a_n \cdot {}_n\zeta_{S2},$$

where now $${}_n\zeta_{S2} = \int_0^1 a_m \sin n\pi z\,(c/\bar{c})\,zdz.$$

The net applied rolling moment is then $L_\eta = l_\eta qSs,$

where $$l_\eta = l_{\eta R} + \Sigma\, a_n \cdot {}_n\zeta_{S2}. \quad . \quad . \quad . \quad . \quad . \quad (14)$$

The "twist" equation is exactly the same as equation (13) for elevon power, except that the functions are for asymmetric aileron effects instead of symmetric elevon effects. $\bar{\theta}$ being now zero, ${}_n\zeta_{S3}$ is derived with ${}_n\zeta_{S1} = 0$ and C_1 is also derived using the appropriate values for C_{Lc}.

For a given speed the "twist" equation provides a set of simultaneous linear equations for the solution of the coefficients a_n, which when substituted in equation (14) gives the net rolling moment coefficient l_η.

Initial condition

Additional downward loads arise due to inertia appropriate to the rolling acceleration dp/dt, the inertia load on a weight w being $(w/g)\,xdp/dt$. Also, since $dp/dt = L_\eta g/A = qSsl_\eta g/A$, the inertia loads can be expressed in terms of the net rolling moment coefficient l_η.

By a process similar to that followed for the other effects, the effect of the inertia loads on the wing distortion is given by an additional term in the "twist" equation, which becomes

$$\Sigma a_n \left\{ {}_n\zeta_{S4} - \left(\frac{4}{qS^2}\right)\sin n\pi z \right\} + C_2 + E_2 l_\eta = 0, \quad . \quad . \quad . \quad (15)$$

where $$E_2 = \int_0^z E_1 dz,$$

and $$E_1 = K_t\left(\frac{Ss}{A}\right)\int_{z_1}^1 w_d\,(x/\bar{c})\,(Y/\bar{c})\,dz + K_t\left(\frac{S}{A}\right)\sum_{z_1}^1 w_c\,(x/\bar{c})\,(Y/\bar{c}) -$$

$$- K_m\left(\frac{Ss}{A}\right)\int_{z_1}^1 w_d\,(x/\bar{c})\left(\frac{x-x_1}{\bar{c}}\right)dz - K_m\left(\frac{S}{A}\right)\sum_{z_1}^1 w_c\,(x/\bar{c})\left(\frac{x-x_1}{\bar{c}}\right).$$

For a given speed the rolling moment equation (14) and "twist" equation (15) provide a set of simultaneous linear equations for the solution of the coefficients a_n and the net rolling moment coefficient l_η.

Steady rolling condition

In addition to the loads due to aileron deflection and wing distortion there are also aerodynamic loads due to damping in roll. These loads are proportional to the rolling velocity p and can be represented by an additional section C_L given by

$$C_L = C_{Lp} \cdot \frac{ps}{V} .$$

The "twist" equation now becomes

$$\Sigma a_n \left\{ {}_n\zeta_4 - \left(\frac{4}{qS^2}\right) \sin n\pi z \right\} + C_2 + D_2 \frac{ps}{V} = 0, \quad . \quad . \quad (16)$$

where $D_2 = \int_0^z D_1 \, dz$,

and $$D_1 = -K_t \int_{z_1}^1 C_{Lp} (c/\bar{c}) (Y/\bar{c}) \, dz + K_m \int_{z_1}^1 C_{Lp} (c/\bar{c}) \left(\frac{x - x_1}{\bar{c}}\right) dz.$$

Rolling moment due to damping is given by the standard stability derivative l_p as equal to $qS \cdot 2s \cdot l_p \cdot ps/V$. For equilibrium of rolling moments the rolling moment equation then becomes

$$l_{\eta R} + \Sigma a_n \cdot {}_n\zeta_2 + 2l_p \frac{ps}{V} = 0 \quad . \quad . \quad . \quad . \quad . \quad (17)$$

For a given speed the rolling moment equation (17) and "twist" equation (16) provide a set of simultaneous linear equations for the solution of the coefficients a_n and the rolling velocity p.

Aileron reversal condition

At reversal the static, initial and steady rolling conditions become identical. Putting $l_\eta = 0$ in equation (14) or $p = 0$ in equation (17) gives the same rolling moment equation,

$$l_{\eta R} + \Sigma a_n \cdot {}_n\zeta_2 = 0. \quad . \quad . \quad . \quad . \quad . \quad (18)$$

Similarly, putting $l_\eta = 0$ in equation (15) or $p = 0$ in equation (16) gives the same "twist" equation as for the static condition, namely

$$\Sigma a_n \left\{ {}_n\zeta_4 - \left(\frac{4}{qS^2}\right) \sin n\pi z \right\} + C_2 = 0. \quad . \quad . \quad . \quad (19)$$

The rolling moment and "twist" equations provide a solution for the coefficients a_n and the speed $V = \sqrt{(2q/\rho)}$. As in the case of elevon reversal the equations are non-linear in a_n and q, but the coefficients a_n can be eliminated to give a direct solution for q. For aileron reversal, for instance, the solution is given by

$$\begin{vmatrix} {}_0\zeta_2 & {}_1\zeta_2 & — & {}_m\zeta_2 & l_{\eta R} \\ {}_1\alpha_0 & {}_1\alpha_1 & — & {}_1\alpha_m & {}_1C_2 \\ — & — & — & — & — \\ {}_{m+1}\alpha_0 & {}_{m+1}\alpha_1 & — & {}_{m+1}\alpha_m & {}_{m+1}C_2 \end{vmatrix} = 0, \quad (20)$$

where, in general,

$${}_r\alpha_s = {}_s\zeta_4 - \left(\frac{4}{qS^2}\right) \sin s\pi z \text{ at station } z = z_r,$$

and ${}_rC_2$ is the value of C_2 at station $z = z_r$. (m, r and s denote here any integer).

If this direct form of solution proves too cumbersome it may be simpler to calculate the net power for the static condition over a range of speeds and hence find by graphical interpolation at what speed the power is zero.

CALCULATION OF DOWNWASH BEHIND A SUPERSONIC WING

by

G. N. WARD

(Department of Mathematics, The University, Manchester)

Once the linearised lift problem for a supersonic wing has been solved and the disturbance velocity potential or the pressure is known at every point on the surface, the complete flow round the wing and the downwash behind the wing may be found by the following procedure.

Let x, y, z be a right-handed system of Cartesian co-ordinates such that x is measured in the direction of the undisturbed stream (velocity U) upstream from the wing. Then the disturbance velocity potential ϕ, such that the disturbance velocity $\mathbf{u}$ is given by

$$\mathbf{u}=\nabla\phi, \qquad . \quad . \quad . \quad . \quad . \quad . \quad (1)$$

satisfies the well-known equation

$$B^2\frac{\partial^2\phi}{\partial x^2}-\frac{\partial^2\phi}{\partial y^2}-\frac{\partial^2\phi}{\partial z^2}=0, \qquad . \quad . \quad (2)$$

where $B^2=M^2-1$

and M is the Mach number of the undisturbed stream.

Consider now a wing of infinitesimal thickness at a small finite incidence to the stream and lying very nearly in the plane $z=0$, then it follows from the antisymmetry of the system that the potential and its x and y derivatives will be odd functions of z, and $\partial\phi/\partial z$ will be an even function of z. Since $\partial\phi/\partial x$ (the pressure) must be continuous except through the wing, it follows that $(\partial\phi/\partial x)_{z=0}=0$ except over the wing. There will be a vortex sheet extending downstream from the trailing edge of the wing and lying approximately in the plane $z=0$, for which the vorticity must be

Paper received August 1948.

[The Aeronautical Quarterly, Vol. 1, May 1949]

constant along streamlines, which in this case are approximately straight lines parallel to the x-axis. Hence the difference of potential between the two sides of the vortex sheet must be a function of y only. Also the potential must be continuous everywhere except through the wing and the vortex sheet, so that the potential on, say, the upper side of the vortex sheet must be equal to the potential at the trailing edge of the wing on its upper side (which is assumed to be known) on any line $y=$constant. In the plane $z=0$, at points not on the wing or the vortex sheet, we must have $\phi=0$ since the potential is continuous at these points. Thus the potential is known everywhere on both sides of the plane $z=0$.

From the anti-symmetry of the problem we can confine our attention to the half-space $z>0$. The potential $\phi(x, y, z)$ satisfying equation (2) and having the value $\phi(x, y, +0)$ on $z=+0$ is given by the known expression due to Hadamard,[1]

$$\phi(x, y, z)=-\frac{1}{\pi}{}^{*}\iint \phi(x', y', +0)\frac{\partial}{\partial z}\left(\frac{1}{\{(x-x')^2-B^2(y-y')^2-B^2z^2\}^{\frac{1}{2}}}\right)dx'dy' \quad (3)$$

the integration being taken over the area of the plane $z=0$ for which

$$x' \leqslant x-B\{(y-y')^2+z^2\}^{\frac{1}{2}} \quad . \quad . \quad . \quad . \quad . \quad (4)$$

and where * denotes that the "finite part" of the integral must be taken.

In the case under consideration $\phi(x, y, +0)=0$ except on the wing and the vortex sheet, so that the integral is taken over those parts of the areas of the wing and the vortex sheet for which equation (4) holds.

By integrating equation (3) by parts with respect to x' and remembering that the potential ϕ is continuous and is zero on the leading edge of the wing, we have

$$\phi(x, y, z)=\frac{1}{\pi}\iint \frac{\partial\phi(x', y', +0)}{\partial x'}\frac{z(x-x')}{[(y-y')^2+z^2][(x-x')^2-B^2(y-y')^2-B^2z^2]^{\frac{1}{2}}}dx'dy'$$
$$. \quad . \quad . \quad . \quad . \quad . \quad . \quad . \quad (5)$$

the integration now being taken over that part of the wing alone for which equation (4) holds, since $\partial\phi/\partial x=0$ on the vortex sheet. This gives ϕ everywhere in $z>0$ and the velocities may be found by differentiation. The quantity usually required will be $(\partial\phi/\partial z)_{z=0}$, giving the downwash in the plane of the wing.

In order to illustrate the method it will be applied to calculate the downwash far behind a symmetrical flat delta wing at incidence, whose leading edges lie inside the Mach cone from its vertex. The result for this case has been given previously by Robinson and Hunter-Tod[2, 3] following some rather complicated analysis. To facilitate comparison of the results their notation is used.

Let γ = semi-vertex angle of the wing, $\eta = \tan\gamma$, $\lambda = B\eta$,
c = maximum chord of the wing,
d = distance behind the trailing edge of the wing,
α = incidence of the wing.

Take the origin of co-ordinates at the vertex of the wing.

For this delta wing it is known[4] that

$$\left(\frac{\partial\phi}{\partial x}\right)_{z=0} = \frac{\alpha U\eta^2}{E'(\lambda)} \cdot \frac{x}{(\eta^2x^2 - y^2)^{\frac{1}{2}}} \quad . \quad . \quad . \quad . \quad (6)$$

When $x > c(1+\lambda) + B\,|\,z\,|$, *i.e.* $d > \lambda c + B\,|\,z\,|$, equations (5) and (6) give

$$\begin{aligned}\phi(x, y, z) &= \frac{\alpha U\eta^2}{\pi E'(\lambda)} \int_0^c z(x-x')x'dz' \times \\ &\qquad \times \int_{-\eta x'}^{\eta x'} \frac{dy'}{[(y-y')^2 + z^2]\,[(x-x')^2 - B^2(y-y')^2 - B^2z^2]^{\frac{1}{2}}[\eta^2x'^2 - y'^2]^{\frac{1}{2}}} \\ &= \frac{\alpha U\eta^2}{\pi E'(\lambda)} \int_0^c z(x-x')x'dx' \times \\ &\qquad \times \int_{-\pi/2}^{\pi/2} \frac{d\theta}{[(y-\eta x'\sin\theta)^2 + z^2]\,[(x-x')^2 - B^2(y-\eta x'\sin\theta)^2 - B^2z^2]^{\frac{1}{2}}} \quad (7)\end{aligned}$$

The evaluation of $(\partial\phi/\partial z)_{z=0}$ from this integral is a little tedious in the general case, but for $y = z = 0$ the integral assumes a simple form; in this case, the integral with respect to θ becomes

$$2\int_0^{\pi/2} \frac{d\theta}{[\eta^2x'^2\sin^2\theta + z^2]\,[(x-x')^2 - B^2z^2 - \lambda^2x'^2\sin^2\theta]^{\frac{1}{2}}} \quad . \quad . \quad (8)$$

As $z \to 0$, this integral is of the form

$$A_{-1}/z + A_0 + A_1z + \ldots\ldots \quad . \quad . \quad . \quad . \quad (9)$$

and in order to calculate $(\partial\phi/\partial z)_{z=0}$ we require only the term A_0, because of the factor z in (7). Now

$$A_{-1} = \lim_{z\to 0} \frac{2z}{x-x'} \int_0^{\pi/2} \frac{d\theta}{\eta^2x'^2\sin^2\theta + z^2} \cdot \quad . \quad . \quad . \quad . \quad (10)$$

Therefore, if $k = \lambda x'/(x-x')$,

$$\begin{aligned}\frac{1}{2}\eta^2x'^2(x-x')A_0 &= \int_0^{\pi/2} \left(\frac{1}{\sin^2\theta\,(1-k^2\sin^2\theta)^{\frac{1}{2}}} - \frac{1}{\sin^2\theta}\right)d\theta \\ &= \int_0^{\pi/2} \frac{k^2\sin^2\theta\,d\theta}{(1-k^2\sin^2\theta)^{\frac{1}{2}}} + [\cot\theta - \cot\theta(1-k^2\sin^2\theta)^{\frac{1}{2}}]_0^{\pi/2} \\ &= K(k) - E(k). \quad . \quad . \quad . \quad (11)\end{aligned}$$

Hence

$$\frac{\partial\phi(x,0,0)}{\partial z} = \frac{2\pi U\eta^2}{\pi E'(\lambda)}\int_0^c \frac{K(k)-E(k)}{\eta^2 x'}\,dx'$$

$$= \frac{2\pi U}{\pi E'(\lambda)}\int_0^{\frac{\lambda c}{d}} \frac{\lambda\,[K(k)-E(k)]}{k(k+\lambda)}\,dk \quad . \quad . \quad . \quad (12)$$

$$= -\frac{2\pi U}{\pi E'(\lambda)}\left\{E\left(\frac{\lambda c}{d}\right) + \int_0^{\lambda c} \frac{K(k)-E(k)}{k+\lambda}\,dk\right\} \quad (13)$$

which is the result given in Ref. 3 for $d > \lambda c$. The corresponding value for $0 < d < \lambda c$ is easily obtained by this method and is given in Ref. 3.

REFERENCES

1. HADAMARD, J. (1923). *Lectures on Cauchy's Problem.* Yale, 1923.
2. ROBINSON, A. (1948). On Source and Vortex Distributions in the Linearised Theory of Steady Supersonic Flow. College of Aeronautics Report No. 9. A.R.C. 11132. Also *Quarterly Journal of Mechanics and Applied Mathematics*, 1, 4, 408, 1948.
3. ROBINSON, A. and HUNTER-TOD, J. H. (1947). Bound and Trailing Vortices in the Linearised Theory of Supersonic Flow and the Downwash in the Wake of a Delta Wing. College of Aeronautics Report No. 10. A.R.C. 11296, October 1947.
4. ROBINSON, A. (1946). Aerofoil Theory of a Flat Delta Wing at Supersonic Speeds. A.R.C. 10222, September 1946.

ESTIMATION OF THE EFFECT OF A PARAMETER CHANGE ON THE ROOTS OF STABILITY EQUATIONS

by

K. MITCHELL, Ph.D., A.F.R.Ae.S.

(*Lecturer in Mathematics at King's College, Newcastle upon Tyne*)

SUMMARY

A method is given for calculating approximately the changes in the roots of a stability secular equation caused by a change in any of the parameters involved. General formulæ are given applicable to any quartic equation, and special formulæ are also given applicable to the stability of an aeroplane: lateral stability in the text, and longitudinal stability in an appendix.

The method of using the formulæ is illustrated by applying them to a particular calculation of the lateral stability of an aeroplane, and a check of the results is made by comparing the predicted approximate changes with those calculated by solution of the modified period equations. It is shown that the formulæ are reliable, for this typical case, for any reasonable changes in any parameter other than n_v.

If the changes in the derivatives are made equal to the probable error with which they can be measured, the formulæ enable us to evaluate the probable errors of the roots. These are found to be considerable, and to arise mainly from uncertainties in y_v, n_v, and n_r: if these could be reduced to 0.03 in y_v and 0.006 in the others, the uncertainties in the roots would be reduced to some ten per cent. of their values, except for a larger uncertainty in the root corresponding to the slow spiral motion.

1. INTRODUCTION

There can be few people who have completed any calculation in the field of aeroplane lateral stability without feeling some doubt as to the physical meaning

Paper received November 1947.

[The Aeronautical Quarterly, Vol. 1, May 1949]

to be attached to the results. The difficulty resides in our imperfect knowledge of the values of the derivatives and other parameters entering the lateral stability equations. Some of these are commonly measured in wind tunnels, and may be taken as known within the accuracy permitted by experimental technique, and by scale effect from tunnel to full scale. For others we use theoretical estimates, based on a theory sketchily confirmed by a handful of experimental results. Of other derivatives we know little, and assume less: we take them to be zero! What credence, then, are we to give to the results of our calculations?

Our doubts could be resolved by better knowledge of the lateral stability derivatives, but this is likely to come only slowly, in view of the difficulty of the subject, both theoretically and practically. There is, however, another way. We can carry out a numerical examination of lateral stability, to see how great in fact are the uncertainties in the roots corresponding to the uncertainties of the derivatives. Such a survey, carried out by exact solution of the secular equations for lateral stability, would be an overwhelming task. Approximate methods must be used, but not approximate formulæ for the roots, such as those given by Bryant and Hopwood[1], Gandy[2], and Mitchell, Thorpe, and Frayn[3]. These formulæ represent compromises which attempt to give the values of the roots over a wide range of conditions, and sacrifice accuracy to range of applicability. What we need for the proposed survey is a method of estimating the rates of change of the roots with respect to the parameters concerned. One possible method* is found by generalising an idea due to Cowley and Skan[4].

Cowley and Skan examined the rates of change of the roots of a polynomial equation with respect to its constant term, and went on to develop a method of solution of polynomial equations depending upon the integration of the formulæ obtained. The author has never been able to regard this transformation of a polynomial equation into a differential equation otherwise than as a retrograde step, as a method of solution. We may use it, however, to estimate the approximate changes in stability due to a small, but not infinitesimal, change in the constant term. In this form, and generalised to include effects due to variations of any coefficient, and by a further extension to include those due to variations of any parameter upon which the coefficients depend, it is exactly what is desired.

This method of calculating the rates of change of the stability roots with respect to the stability derivatives enables us to solve our original problem, and some others of rather greater practical importance. The designer of aeroplanes is often faced with the problem of estimating the effect upon stability of some proposed design

* A similar method is applicable to many types of stability problems, and the flutter problem has already been studied in this way by Buxton and Minhinnick[9]; the author was unaware of this paper when the above introduction was written.

change, or with the converse problem of amending a proposed design so as to bring about a desired change in stability. The methods to be developed in this paper enable him to solve both problems in a rapid approximate manner and, if it is desired to go further and evaluate the changes accurately, the modified coefficients in the modified secular equation can be obtained exactly from formulæ to be given later.

It is thought that this problem is of sufficient importance to the designer to justify the preparation of a paper mainly devoted to it. Our original problem, the investigation of the probable errors of stability roots, will involve much numerical computation: to await the completion of this would delay publication, and we return to it only briefly in Section 6. It will be necessary to evaluate the rates of change of the stability roots with the derivatives over a large range of possible cases, and it is to be hoped that, while answering the somewhat theoretical question proposed, the survey of lateral stability that is involved will yield results of more direct practical value. Some of the particular formulæ for the rates of change may be too complicated to be of other than numerical use: others, it is to be hoped, may lend themselves to simplification and approximation, so contributing to our general knowledge of the subject.

It may be added that it is a necessary condition for the validity of the formulæ to be developed below, that they are not to be applied in cases where the stability equation has nearly equal roots. It is precisely this condition which has led us to confine our attention to lateral stability in the text of this paper, though some of the corresponding formulæ for longitudinal stability are given in an Appendix. In lateral stability* equal roots appear only for negative values of the parameter n_v, or for very small n_v coupled with positive l_v: both are conditions which should be, and usually are, avoided in practice. Our formulæ are therefore of general usefulness in the lateral stability field. In longitudinal stability, on the other hand, the region of the stability field in which equal roots occur can hardly be avoided in practice, though its stability characteristics are far from perfect. In this case an approximate theory already exists†, which, in the circumstances, is probably of more use than the methods of this paper. The appendix on longitudinal stability, therefore, contains merely the basic formulæ for the changes in the coefficients due to changes in the derivatives. These, although of little theoretical interest, will be of assistance in the setting up of the modified stability equation corresponding to any proposed change in design.

---

* The only published calculation of the "locus of equal roots," the curve in the $l_v - n_v$ diagram along which the roots are equal, was given by Mitchell, Thorpe and Frayn[5]. A few other calculations have been made by the same authors (unpublished), and the statement in the text is true as far as present knowledge goes.

† *See* Neumark[6], especially Appendix II.

2. VARIATIONAL FORMULÆ FOR A QUARTIC

2.1. *General*

We now consider the rates of change of the roots of a polynomial equation with respect to a parameter upon which its coefficients depend. We take the quartic equation

$$f(p) \equiv Ap^4 + Bp^3 + Cp^2 + Dp + E = 0, \quad . \quad . \quad . \quad . \quad (2.1.1)$$

whose coefficients A, B, C, D, E, are functions of a parameter κ, and take standard values A_0, B_0, C_0, D_0, E_0, when this parameter takes a standard value κ_0. If p_0 denotes the value of a root of (2.1.1) when κ has its standard value κ_0, and if $p_0 + dp$ is the value of the corresponding root when $\kappa = \kappa_0 + d\kappa$, we have, to the first order of small quantities,

$$\{ A_0 + (\partial A/\partial\kappa)d\kappa \}(p_0^4 + 4p_0^3 dp) + \{ B_0 + (\partial B/\partial\kappa)\, d\kappa \}(p_0^3 + 3p_0^2 dp) +$$
$$+ \{ C_0 + (\partial C/\partial\kappa)\, d\kappa \}(p_0^2 + 2p_0 dp) + \{ D_0 + (\partial D/\partial\kappa)\, d\kappa \}(p_0 + dp) +$$
$$+ E_0 + (\partial E/\partial\kappa)\, d\kappa = 0.$$

Subtracting the terms of zero order, which vanish separately, we obtain a relation between dp and $d\kappa$. In the case of a real root, $p_0 = -q$, this takes the form

$$dq = -d\kappa \frac{\frac{\partial A}{\partial\kappa} q^4 - \frac{\partial B}{\partial\kappa} q^3 + \frac{\partial C}{\partial\kappa} q^2 - \frac{\partial D}{\partial\kappa} q + \frac{\partial E}{\partial\kappa}}{4A_0 q^3 - 3B_0 q^2 + 2C_0 q - D_0}. \quad . \quad . \quad . \quad (2.1.2)$$

For a complex pair, $p_0 = -r \pm is$, we obtain

$$dr - ids = -d\kappa \frac{\frac{\partial A}{\partial\kappa}(r-is)^4 - \frac{\partial B}{\partial\kappa}(r-is)^3 + \frac{\partial C}{\partial\kappa}(r-is)^2 - \frac{\partial D}{\partial\kappa}(r-is) + \frac{\partial E}{\partial\kappa}}{4A_0(r-is)^3 - 3B_0(r-is)^2 + 2C_0(r-is) - D_0}, \quad (2.1.3)$$

which can be split into its real and imaginary parts to give formulæ for dr and ds separately.

These formulæ express the rates of change of the roots as linear functions of the quantities $(1/A_0)\,\partial A/\partial\kappa$, etc., the coefficients being functions of the roots alone.*

---

* For, if $-q_1$ be any root of (2.1.1.), and $-q_2$, $-q_3$, $-q_4$, the remaining roots, for the standard case, then

$$4A_0 q_1^3 - 3B_0 q_1^2 + 2C_0 q_1 - D_0 = A_0(q_1 - q_2)(q_1 - q_3)(q_1 - q_4).$$

The formulæ are conveniently written in the forms

$$\frac{dq}{d\kappa} = \frac{1}{A_o}\left(K_{qA}\frac{\partial A}{\partial \kappa} + K_{qB}\frac{\partial B}{\partial \kappa} + K_{qC}\frac{\partial C}{\partial \kappa} + K_{qD}\frac{\partial D}{\partial \kappa} + K_{qE}\frac{\partial E}{\partial \kappa}\right), \quad . \quad (2.1.4)$$

for a real root $-q$, with coefficients K_{qA}, etc., and for the real and complex parts of the complex root $-r+is$, with coefficients K_{rA}, etc., and K_{sA}, etc.

The values of the twenty coefficients K depend upon the values of the roots, and upon whether they are real or complex. The cases of four real, two real and two complex, and four complex, roots therefore require separate consideration.

2.2. *All roots real*

The roots may be denoted by $p=-q_i$; $i=1, 2, 3, 4$. We then have

$$K_{q1E} = -1/\{(q_1-q_2)(q_1-q_3)(q_1-q_4)\}, \quad . \quad . \quad . \quad (2.2.1)$$

with similar expressions for the other coefficients K_{qiE}. Also, in general,

$$K_{qiD} = -q_iK_{qiE}, \quad K_{qiC} = -q_iK_{qiD}, \quad K_{qiB} = -q_iK_{qiC}, \quad K_{qiA} = -q_iK_{qiB} \quad . \quad (2.2.2)$$

Calculated values may be checked by the relations

$$\left.\begin{aligned} &\sum_{i=1}^{4} K_{qiE} = \sum_{i=1}^{4} K_{qiD} = \sum_{i=1}^{4} K_{qiC} = 0 \\ &\sum_{i=1}^{4} K_{qiB} = 1 \\ &\sum_{i=1}^{4} K_{qiA} = -B_o/A_o \end{aligned}\right\} \quad . \quad . \quad . \quad (2.2.3)$$

2.3. *Two roots real and two roots complex*

The roots will be denoted by $-q_1$, $-q_2$, real, and $-r\pm is$, the complex pair. We then have

$$\left.\begin{aligned} K_{q1E} &= -1/[(q_1-q_2)\{(q_1-r)^2+s^2\}] \\ K_{q2E} &= -1/[(q_2-q_1)\{(q_2-r)^2+s^2\}] \end{aligned}\right\}, \quad . \quad . \quad . \quad (2.3.1)$$

the remaining coefficients for the real roots being obtained from (2.2.2) as above. For the complex pair, we have

$$\left.\begin{aligned} K_{rE} &= (2r-q_1-q_2)/[2\{(r-q_1)^2+s^2\}\{(r-q_2)^2+s^2\}] \\ K_{sE} &= \{(r-q_1)(r-q_2)-s^2\}/[2s\{(r-q_1)^2+s^2\}\{(r-q_2)^2+s^2\}] \end{aligned}\right\}, \quad (2.3.2)$$

and the remaining coefficients may be calculated from the relations

$$\left.\begin{aligned} K_{rD} &= -rK_{rE}+sK_{sE} \\ K_{sD} &= -rK_{sE}-sK_{rE} \end{aligned}\right\}, \quad . \quad . \quad . \quad . \quad . \quad (2.3.3)$$

etc. Checking relations are

$$\left.\begin{aligned} &K_{q1E}+K_{q2E}+2K_{rE}=K_{q1D}+K_{q2D}+2K_{rD}=K_{q1C}+K_{q2C}+2K_{rC}=0 \\ &K_{q1B}+K_{q2B}+2K_{rB}=1 \\ &K_{q1A}+K_{q2A}+2K_{rA}=-B_0/A_0 \end{aligned}\right\} . \quad (2.3.4)$$

These check by implication all K_s up to K_{sB}: to check K_{sA} we use the additional identity

$$q_1K_{q1A}+q_2K_{q2A}+2rK_{rA}-2sK_{sA}=(A_0C_0-B_0^2)/A_0^2 . \quad . \quad (2.3.5)$$

2.4. *All roots complex*

The roots are $-r_1 \pm is_1$, $-r_2 \pm is_2$. Then we have

$$\left.\begin{aligned} K_{r1E} &= (r_1-r_2)/[\{(r_1-r_2)^2+(s_1-s_2)^2\}\{(r_1-r_2)^2+(s_1+s_2)^2\}] \\ K_{s1E} &= \{(r_1-r_2)^2+s_2^2-s_1^2\}/[2s_1\{(r_1-r_2)^2+(s_1-s_2)^2\}\{(r_1-r_2)^2+(s_1+s_2)^2\}] \end{aligned}\right\} , \quad (2.4.1)$$

with similar expressions for K_{r2E} and K_{s2E}. The remaining coefficients K_{r1D} etc. are calculated by formulæ of type (2.3.3), and the checking relations become

$$\left.\begin{aligned} &K_{r1E}+K_{r2E}=K_{r1D}+K_{r2D}=K_{r1C}+K_{r2C}=0 \\ &K_{r1B}+K_{r2B}=\tfrac{1}{2} \\ &K_{r1A}+K_{r2A}=-\tfrac{1}{2}B_0/A_0 \end{aligned}\right\} , \quad . \quad . \quad (2.4.2)$$

checking all save K_{sA}. To check these, we add the identity

$$r_1K_{r1A}+r_2K_{r2A}-s_1K_{s1A}-s_2K_{s2A}=\tfrac{1}{2}(A_0C_0-B_0^2)/A_0^2 . \quad . \quad . \quad (2.4.3)$$

2.5. *Derivation of checking relations*

Using $-q_i$; $i=1, 2, 3, 4$; to denote the roots of (2.1.1), we have the partial fraction expansion

$$\frac{A_0}{f(p)} = -\Sigma \frac{1}{(q_1-q_2)(q_1-q_3)(q_1-q_4)} \frac{1}{p+q_1} .$$

Expanding both sides in ascending powers of $1/p$, and equating coefficients, we conclude that

$$\sigma_n = \Sigma \frac{{q_1}^n}{(q_1-q_2)(q_1-q_3)(q_1-q_4)}$$

is equal to the coefficient of $(-1/p)^{n+1}$ in the expansion of $A_0/f(p)$. Thus

$$\left.\begin{aligned} &\sigma_0=\sigma_1=\sigma_2=0,\ \sigma_3=1 \\ &\sigma_4=B_0/A_0,\ \sigma_5=(B_0^2-A_0C_0)/A_0^2 \end{aligned}\right\}.$$

These lead immediately to the previous checking relations.

3. APPLICATION TO LATERAL STABILITY

3.1. Notation

For the lateral stability period equation we have

$$\left.\begin{aligned}
A &= 1-\frac{(i_E)^2}{i_A i_C} \\
B &= -\left(\frac{l_p}{i_A}+\frac{n_r}{i_C}+\frac{i_E}{i_A}\frac{n_p}{i_C}+\frac{i_E}{i_C}\frac{l_r}{i_A}\right)-y_v\left(1-\frac{(i_E)^2}{i_A i_C}\right) \\
C &= \left(\frac{l_p}{i_A}\frac{n_r}{i_C}-\frac{l_r}{i_A}\frac{n_p}{i_C}\right)+y_v\left(\frac{l_p}{i_A}+\frac{n_r}{i_C}+\frac{i_E}{i_A}\frac{n_p}{i_C}+\frac{i_E}{i_C}\frac{l_r}{i_A}\right)+ \\
&\quad+\left(1-\frac{y_r}{\mu_2}\right)\left(\frac{\mu_2 n_v}{i_C}+\frac{i_E}{i_C}\frac{\mu_2 l_v}{i_A}\right)-\frac{y_p}{\mu_2}\left(\frac{\mu_2 l_v}{i_A}+\frac{i_E}{i_A}\frac{\mu_2 n_v}{i_C}\right) \\
D &= -y_v\left(\frac{l_p}{i_A}\frac{n_r}{i_C}-\frac{l_r}{i_A}\frac{n_p}{i_C}\right)+ \\
&\quad+\left(1-\frac{y_r}{\mu_2}\right)\left(\frac{\mu_2 l_v}{i_A}\frac{n_p}{i_C}-\frac{\mu_2 n_v}{i_C}\frac{l_p}{i_A}\right)+\frac{y_p}{\mu_2}\left(\frac{\mu_2 l_v}{i_A}\frac{n_r}{i_C}-\frac{\mu_2 n_v}{i_C}\frac{l_r}{i_A}\right)- \\
&\quad-k\left(\frac{\mu_2 l_v}{i_A}+\frac{i_E}{i_A}\frac{\mu_2 n_v}{i_C}\right)-k\tan\gamma_0\left(\frac{\mu_2 n_v}{i_C}+\frac{i_E}{i_C}\frac{\mu_2 l_v}{i_A}\right) \\
E &= k\left(\frac{\mu_2 l_v}{i_A}\frac{n_r}{i_C}-\frac{\mu_2 n_v}{i_C}\frac{l_r}{i_A}\right)-k\tan\gamma_0\left(\frac{\mu_2 l_v}{i_A}\frac{n_p}{i_C}-\frac{\mu_2 n_v}{i_C}\frac{l_p}{i_A}\right)
\end{aligned}\right\}. \qquad (3.1.1)$$

The notation used is that of Bryant and Gates[7], with the replacement of their θ_0 by γ_0, and with the addition of the dimensionless product of inertia coefficient

$$i_E = 4E/(mb^2), \quad . \quad . \quad . \quad . \quad . \quad . \quad (3.1.2)$$

and of extra dimensionless derivatives y_p and y_r, defined in terms of their natural counterparts Y_p and Y_r by the equations

$$\frac{y_p}{Y_p} = \frac{y_r}{Y_r} = \frac{2}{S\rho U_e b} \quad . \quad . \quad . \quad . \quad . \quad (3.1.3)$$

Here S is wing area (ft.^{2}), b is span (ft.), U_e is forward speed (ft./sec.), ρ is air density (slugs/ft.^{3}), m is mass (slugs) and E the xz-product of inertia (slugs. ft.^{2}).

Care should be taken not to confuse E of (3.1.2) with the coefficient E of (3.1.1).

We shall also use the supplementary notation developed by the author[6], with minor modifications—the replacement of 2 by 3 in l_2 and n_2, now l_3 and n_3, and of $\overline{y_r}$ by y_2. The symbolism found useful here is as follows:

$$\left.\begin{aligned} l_1 &= -l_p/i_A, & l_3 &= l_r/i_A \\ n_1 &= -n_p/i_C, & n_3 &= -n_r/i_C \\ y_2 &= -y_r \\ \mathscr{L} &= -\mu_2 l_r/i_A, & \mathscr{N} &= \mu_2 n_r/i_C \\ \epsilon_A &= -i_E/i_A, & \epsilon_C &= -i_E/i_C \end{aligned}\right\}, \quad . \quad . \quad (3.1.4)$$

and

$$\left.\begin{aligned} \Gamma_1 &= \frac{l_1 + n_3 - \epsilon_A n_1 + \epsilon_C l_3}{1 - \epsilon_A \epsilon_C} \\ \Gamma_2 &= \frac{l_1 n_3 + l_3 n_1}{1 - \epsilon_A \epsilon_C} \\ \Pi_1 &= \frac{\mathscr{N} + \epsilon_C \mathscr{L}}{1 - \epsilon_A \epsilon_C}, & \Pi_2 &= \frac{\mathscr{L} + \epsilon_A \mathscr{N}}{1 - \epsilon_A \epsilon_C} \\ \Pi_3 &= \frac{l_1 \mathscr{N} + n_1 \mathscr{L}}{1 - \epsilon_A \epsilon_C}, & \Pi_4 &= \frac{n_3 \mathscr{L} - l_3 \mathscr{N}}{1 - \epsilon_A \epsilon_C} \end{aligned}\right\} \quad . \quad . \quad . \quad (3.1.5)$$

These symbols allow us to express the coefficients of the period equation in the simple and convenient forms

$$\left.\begin{aligned} B/A &= \Gamma_1 + y_2 \\ C/A &= \Gamma_2 + \Gamma_1 y_2 + \Pi_1 (1 - y_r/\mu_2) + \Pi_2 y_p/\mu_2 \\ D/A &= \Gamma_2 y_2 + \Pi_3 (1 - y_r/\mu_2) + \Pi_4 y_p/\mu_2 + k (\Pi_2 - \Pi_1 \tan \gamma_e) \\ E/A &= k (\Pi_4 - \Pi_3 \tan \gamma_e) \end{aligned}\right\} \quad . \quad (3.1.6)$$

3.2. *Formulæ for variations of coefficients*

In calculating changes of coefficients, or the resulting changes in roots, it is found convenient to introduce an intermediate parameter κ' and to regard the quantities $(1/A_0)\,\partial A/\partial\kappa$, etc., as the products of the quantities $(1/A_0)\,d\kappa'/d\kappa$ and $\partial A/\partial\kappa'$. Formulæ for these quantities are given in Table I. The parameters taken are y_v, y_p, y_r ; l_v, l_p, l_r ; n_v, n_p, n_r ; μ_2, $\tan\gamma_e$; $1/i_A$, $1/i_C$; i_E : the coefficients A, B, C, D, E, are linear functions of each of these, except i_E, and the table can therefore be used to calculate exactly the changes in the coefficients due to any changes, small or large, in these parameters. If κ is changed by $\Delta\kappa$, we deduce that the coefficients become $A_0+\Delta A$, etc., where

$$\Delta A = A_0\left(\frac{1}{A_0}\frac{d\kappa'}{d\kappa}\right)\left(\frac{\partial A}{\partial\kappa'}\right)\Delta\kappa. \qquad . \quad . \quad . \quad (3.2.1)$$

To render possible the same accurate calculation of changes in coefficients due to changes in i_E, we have added two extra rows to the table, giving the rates of change with respect to i_E and $(i_E)^2$, regarded as independent. The changes are then calculated by means of

$$\Delta A = A_0\left(\frac{1}{A_0}\frac{d\kappa'}{d\kappa}\right)_{i_E}\left(\frac{\partial A}{\partial\kappa'}\right)_{i_E}\Delta i_E + A_0\left(\frac{1}{A_0}\frac{d\kappa'}{d\kappa}\right)_{(i_E)^2}\left(\frac{\partial A}{\partial\kappa'}\right)_{(i_E)^2}\Delta\,(i_E)^2, \quad (3.2.2)$$

and similar relations.

4. NUMERICAL EXAMPLE OF THE USE OF TABLE I

4.1. *Data*

We proceed now to give a numerical example showing the use that may be made of Table I. We shall suppose that an investigation is being made into the lateral stability of a lightly loaded aeroplane of large wing span flying level at a speed near its maximum. Values of the derivatives and other parameters are taken to be

$$\left.\begin{aligned} &y_v=-0.2,\ \ y_p=y_r=0\\ &l_v=-0.06,\ l_p=-0.42,\ \ l_r=0.06\\ &n_v=0.024,\ \ n_p=-0.03,\ n_r=-0.048\\ &i_A=0.10,\quad i_C=0.15,\quad i_E=0\\ &\mu_2=10,\quad C_L=0.2,\ \tan\gamma_e=0,\ k=0.1 \end{aligned}\right\} \quad . \quad . \quad . \quad (4.1.1)$$

From this the roots of the period equation are evaluated; there are two real roots and two complex roots, $-q_s$, $-q_r$, $-r \pm is$, where

$$\left.\begin{aligned} q_s &= 0.010\ 946, \quad q_r = 4.272\ 817 \\ r &= 0.218\ 118, \quad s = 1.415\ 952 \end{aligned}\right\} \quad . \quad . \quad . \quad . \quad (4.1.2)$$

In the process of setting up and solving the lateral stability period equation certain other quantities are evaluated: these are

$$\left.\begin{aligned} &l_1 = 4.2, \quad l_3 = 0.6, \quad n_1 = 0.2, \quad n_3 = 0.32 \\ &y_2 = 0.2, \quad \mathscr{L} = 6, \quad \mathscr{N} = 1.6, \quad \epsilon_A = \epsilon_C = 0 \\ &\Gamma_1 = 4.52, \quad \Gamma_2 = 1.464 \\ &\Pi_1 = 1.60, \quad \Pi_2 = 6, \quad \Pi_3 = 7.92, \quad \Pi_4 = 0.96 \\ &A_0 = 1, \quad B_0 = 4.72, \quad C_0 = 3.968, \quad D_0 = 8.8128 \\ &E_0 = 0.096 \end{aligned}\right\} \quad . \quad . \quad (4.1.3)$$

4.2. *Calculation of variations of roots*

The suggested application of the formulæ of this paper is to the estimation of the stability change due to a design change, which may affect only a single parameter. To make any such calculation, it is necessary to evaluate $4(n+1)$ of the 20 constants K of Section 2.1, where n is the degree of the term of highest degree in the period equation in which the parameter to be varied occurs. Here, for completeness, we evaluate the complete set at once. Using (2.3.1) and (2.2.2) for the real roots, and (2.3.2) and (2.3.3) for the complex roots, we find the values given in Table II.

TABLE II

Values of the quantities K_{qE}, etc.

	$K_{.A}$	$K_{.B}$	$K_{.C}$	$K_{.D}$	$K_{.E}$
K_{qs}	0	0	0.000 014	−0.001 254	0.114 579
K_{qr}	−4.240 006	0.992 321	−0.232 240	0.054 353	−0.012 721
K_r	−0.239 999	0.003 841	0.116 114	−0.026 550	−0.050 929
K_s	0.031 403	−0.168 905	0.020 599	0.077 914	−0.026 596

TABLE I

Values of quantities $(1/A_0)\,d\kappa'/d\kappa$, $\partial A/\partial\kappa'$, etc., needed in calculating chan

(*a*) Parameters entering linearly. Coefficient change (exact) $\Delta A = A_0\left(\frac{1}{A_0}\frac{d\kappa'}{d\kappa}\right)\frac{\partial A}{\partial\kappa'}\Delta\kappa$, etc. Ro

κ	$\frac{1}{A_0}\frac{d\kappa'}{d\kappa}$	$\partial A/\partial\kappa'$	$\partial B/\partial\kappa'$	$\partial C/\partial\kappa'$	
y_v	-1	0	1	Γ_1	
y_p	$+1/\mu_2$	0	0	Π_2	
y_r	$-1/\mu_2$	0	0	Π_1	
l_v	$-\frac{\mu_2}{i_A(1-\epsilon_A\epsilon_C)}$	0	0	$\frac{y_p}{\mu_2}+\epsilon_C\left(1-\frac{y_r}{\mu_2}\right)$	(1
l_p	$-\frac{1}{i_A(1-\epsilon_A\epsilon_C)}$	0	1	n_3+y_2	
l_r	$+\frac{1}{i_A(1-\epsilon_A\epsilon_C)}$	0	ϵ_C	$\epsilon_C y_2+n_1$	
n_v	$+\frac{\mu_2}{i_C(1-\epsilon_A\epsilon_C)}$	0	0	$1-\frac{y_r}{\mu_2}+\epsilon_A\frac{y_p}{\mu_2}$	(
n_p	$-\frac{1}{i_C(1-\epsilon_A\epsilon_C)}$	0	$-\epsilon_A$	$l_3-\epsilon_A y_2$	
n_r	$-\frac{1}{i_C(1-\epsilon_A\epsilon_C)}$	0	1	l_1+y_2	
μ_2	$+1/\mu_2$	0	0	Π_1	
$\tan\gamma_0$	$-k$	0	0	0	
$1/i_A$	$\frac{i_A}{1-\epsilon_A\epsilon_C}$	$-\epsilon_A\epsilon_C$	$B_0-n_3-y_2$	$C_0-n_3y_2-\left(1-\frac{y_r}{\mu_2}\right)\mathcal{N}$	
$1/i_C$	$\frac{i_C}{1-\epsilon_A\epsilon_C}$	$-\epsilon_A\epsilon_C$	$B_0-l_1-y_2$	$C_0-l_1y_2-\frac{y_p}{\mu_2}\mathcal{L}$	

(*b*) Parameters entering other than linearly. Coefficient change (exact), $\Delta A = A_0\left(\frac{1}{A_0}\frac{\partial\kappa'}{\partial\kappa}\right)_{i_E}$

i_E	$-\frac{1}{i_A i_C(1-\epsilon_A\epsilon_C)}$	0	l_r+n_p	$y_2(l_r+n_p)-l_v(\mu_2-y_r)+n_v y_p$	
$(i_E)^2$	$-\frac{1}{i_A i_C(1-\epsilon_A\epsilon_C)}$	1	y_2	0	

(*c*) As (*b*). Approximate root change, or approximate coefficient change, as (*a*) above.

i_E	$-\frac{1}{i_A i_C(1-\epsilon_A\epsilon_C)}$	$2i_E$	$l_r+n_p+2y_2 i_E$	$y_2(l_r+n_p)-l_v(\mu_2-y_r)+n_v y_p$	

ating changes in coefficients and stability roots.

κ, etc. Root change (approximate) $\Delta q = \frac{1}{A_0}\frac{d\kappa'}{d\kappa}\left(K_{q\Delta}\frac{\partial A}{\partial \kappa'} + \ldots\right)\Delta\kappa.$

	$\partial D/\partial\kappa'$	$\partial E/\partial\kappa'$
	Γ_2	0
	Π_4	0
	Π_3	0
	$\left(1-\frac{y_r}{\mu_2}\right)n_1+\frac{y_p}{\mu_2}n_3+k\,(1-\epsilon_C\tan\gamma_e)$	$k\,(n_3-n_1\tan\gamma_e)$
	$n_2y_2+\mathscr{N}\left(1-\frac{y_r}{\mu_2}\right)$	$-k\mathscr{N}\tan\gamma_e$
	$n_1y_2-\frac{y_p}{\mu_2}\mathscr{N}$	$-k\mathscr{N}$
	$\left(1-\frac{y_r}{\mu_2}\right)l_1-\frac{y_p}{\mu_2}l_3+k\,(\epsilon_A-\tan\gamma_e)$	$-k\,(l_3+l_1\tan\gamma_e)$
	$l_2y_2+\left(1-\frac{y_r}{\mu_2}\right)\mathscr{L}$	$-k\mathscr{L}\tan\gamma_e$
	$l_1y_2+\frac{y_p}{\mu_2}\mathscr{L}$	$k\mathscr{L}$
	$\Pi_3+k\,(\Pi_2-\Pi_1\tan\gamma_e)$	$k\,(\Pi_4-\Pi_2\tan\gamma_e)$
	Π_1	Π_3
$\mathscr{N}$	$D_0+k\mathscr{N}\tan\gamma_e$	E_0
	$D_0-k\mathscr{L}$	E_0

$\left(\frac{1}{A_0}\frac{\partial\kappa'}{\partial\kappa}\right)_{i_E}\left(\frac{\partial A}{\partial\kappa'}\right)_{i_E}\Delta i_E+A_0\left(\frac{1}{A_0}\frac{\partial\kappa'}{\partial\kappa}\right)_{(i_E)^2}\left(\frac{\partial A}{\partial\kappa'}\right)_{(i_E)^2}\Delta\,(i_E)^2.$

n_ry_p	$\mu_2k\,(n_r+l_r\tan\gamma_e)$	0
	0	0

above.

n_ry_p	$\mu_2k\,(n_r+l_r\tan\gamma_e)$	0

These satisfy the checking relations (2.3.4) and (2.3.5), the residuals, starting with $K_{.A}$ and ending with (2.3.5), being 0, −1, +2, +3, −4, +5, in units of the sixth decimal place.

The next step in examining the effect of a single design change would be to evaluate the appropriate quantities $(1/A_o)\,\partial A/\partial\kappa'$, etc., from a single row of Table I, and by multiplying these by the appropriate sets of constants K from Table II, to form the rates of change of the roots with respect to the varied parameter. We shall multiply the labour involved in so doing 14-fold, by carrying out this calculation for variations of each of the parameters. We therefore proceed to construct a numerical version of Table I, which we give as Table III. Making only a single parameter change, of course, we should need only a single row of this table.

TABLE III

Typical numerical version of Table I

κ	$\frac{1}{A_o}\frac{\partial\kappa'}{\partial\kappa}$	$\frac{\partial A}{\partial\kappa'}$	$\frac{\partial B}{\partial\kappa'}$	$\frac{\partial C}{\partial\kappa'}$	$\frac{\partial D}{\partial\kappa'}$	$\frac{\partial E}{\partial\kappa'}$
y_v	−1	0	1	4.52	1.464	0
y_p	+0.1	0	0	6	0.96	0
y_r	−0.1	0	0	1.6	7.92	0
l_v	−100	0	0	0	0.3	0.032
l_p	−10	0	1	0.52	1.664	0
l_r	+10	0	0	0.2	0.04	−0.16
n_v	+200/3	0	0	1	4.2	−0.06
n_p	−20/3	0	0	0.6	6.12	0
n_r	−20/3	0	1	4.4	0.84	0.6
μ_2	+0.1	0	0	1.6	8.52	0.096
$\tan\gamma_e$	−0.1	0	0	0	1.6	7.92
$1/i_A$	+0.1	0	4.2	2.304	8.8128	0.096
$1/i_C$	+0.15	0	0.32	3.128	8.2128	0.096
i_E	−200/3	0	0.03	0.606	0.024	0

From this we construct the gradients of the roots with respect to the parameters, obtained by forming the sums by rows of products of quantities in corresponding columns of Tables II and III, and multiplying the final result by the appropriate quantity $(1/A_o)\,\partial\kappa'/\partial\kappa$. For example, taking the top rows of both tables, we find

$$\partial q_s/\partial y_v = (-1)\{0\times 0+1\times 0+4.52\times 0.000\ 014+1.464\times(-0.001\ 254)+$$
$$+0\times 0.114\ 579\} = 0.001\ 773.$$

The quantities so obtained are given in Table IV, which contains also the residuals, in units of the sixth decimal place, calculated from the checking formulæ

$$\frac{\partial q_s}{\partial \kappa}+\frac{\partial q_r}{\partial \kappa}+2\frac{\partial r}{\partial \kappa}-\frac{1}{A_0}\frac{\partial B}{\partial \kappa}+\frac{B_0}{A_0^2}\frac{\partial A}{\partial \kappa}=0, \quad . \quad . \quad . \quad . \quad (4.2.1)$$

$$q_s\frac{\partial q_s}{\partial \kappa}+q_r\frac{\partial q_r}{\partial \kappa}+2r\frac{\partial r}{\partial \kappa}-2s\frac{\partial s}{\partial \kappa}+\frac{1}{A_0}\frac{\partial C}{\partial \kappa}-\frac{B_0}{A_0^2}\frac{\partial B}{\partial \kappa}-\frac{A_0C_0-B_0^2}{A_0^3}\frac{\partial A}{\partial \kappa}=0. \quad (4.2.2)$$

TABLE IV

Table of rates of change of roots with respect to parameters

κ	$\partial q_s/\partial\kappa$	$\partial q_r/\partial\kappa$	$\partial r/\partial\kappa$	$\partial s/\partial\kappa$	Residuals (4.2.1)	Residuals (4.2.2)
y_v	0.001 773	−0.022 169	−0.489 807	−0.038 269	−10	+8
y_p	−0.000 112	−0.134 126	0.067 120	0.019 839	+2	+1
y_r	0.000 991	−0.005 889	0.002 449	−0.065 004	0	0
l_v	−0.329 033	−1.589 883	0.959 473	−2.252 313	+30	+9
l_p	0.020 794	−9.619 996	−0.200 411	0.285 446	−24	+163
l_r	−0.183 800	−0.422 385	0.303 094	0.114 917	+3	−3
n_v	−0.808 503	−0.212 943	0.510 649	23.295 571	−148	−107
n_p	0.051 107	−1.288 643	0.618 784	−3.261 287	+32	+11
n_r	−0.451 704	−0.056 593	−3.079 221	0.191 861	−72	−21
μ_2	0.000 034	0.009 028	−0.004 531	0.069 423	0	0
$\tan\gamma_0$	−0.090 546	0.001 379	0.044 584	0.008 598	+1	+1
$1/i_A$	−0.000 002	0.411 045	0.004 479	0.002 215	+1	+14
$1/i_C$	0.000 112	0.005 440	0.021 225	0.097 258	+2	+2
i_E	0.001 441	7.310 889	−4.656 207	−0.619 052	−84	−3

5. TEST OF THE FORMULÆ BY CALCULATION OF EXACT AND APPROXIMATE CHANGES IN ROOTS

The entries in Table IV are the rates of change of the roots with respect to the various parameters, and to check the validity of the method, we must calculate the exact changes in the roots of the secular equation caused by various hypothetical

changes in the parameters. These changes can then be compared with the approximate changes obtained by multiplying the entries in Table IV by the appropriate changes in the parameters.

To take a typical example in detail, let us suppose that y_v is decreased by 0.1, so that $\Delta y_v = -0.1$. From Table IV and the root values (4.1.2) we infer that approximate values for the changed roots will be given by

$$\left.\begin{aligned} q_s &= 0.010\,946 - 0.1 \times \ 0.001\,773 \ = 0.010\,769 \\ q_r &= 4.272\,817 - 0.1 \times (-0.022\,169) = 4.274\,986 \\ r &= 0.218\,118 - 0.1 \times (-0.489\,807) = 0.267\,098 \\ s &= 1.415\,952 - 0.1 \times (-0.038\,269) = 1.419\,779 \end{aligned}\right\} \quad . \quad . \quad (5.1)$$

Again, using Table III, we calculate the new coefficients of the stability equation as

$$\left.\begin{aligned} A &= 1 \quad\quad + (-0.1) \times (-1) \times 0 \quad\ = 1 \\ B &= 4.72 \quad + (-0.1) \times (-1) \times 1 \quad\ = 4.82 \\ C &= 3.968 \ + (-0.1) \times (-1) \times 4.52 \ = 4.420 \\ D &= 8.8128 + (-0.1) \times (-1) \times 1.464 = 8.9592 \\ E &= 0.096 \ + (-0.1) \times (-1) \times 0 \quad\ = 0.096 \end{aligned}\right\} \ .$$

and solution of this modified equation gives us the roots

$$\left.\begin{aligned} q_s &= 0.010\,772, \quad q_r = 4.275\,081 \\ r &= 0.267\,074, \quad s = 1.418\,924 \end{aligned}\right\} \quad . \quad . \quad . \quad (5.2)$$

Comparison of (5.1) and (5.2) shows no significant error in any of the dampings; in the case of the frequency factor s a larger, but still unimportant, discrepancy is noticeable.

The same process has been carried out for each of the parameters involved in the equations, with the results shown in Table V. The procedure is identical, except for change of i_E, and here we have solved exactly both the exact stability equation, obtained by proceeding as in (*b*) of Table I, and the approximate stability equation, obtained from (*c*), Table I. These equations may be put on record: Taking $\Delta i_E = -0.005$, they are

$$\left.\begin{aligned} 0 &= p^4 + 4.737\,563 p^3 + 4.176\,962 p^2 + 8.835\,526 p + 0.096\,160 : \text{ exact} \\ 0 &= p^4 + 4.73 p^3 \quad\quad + 4.17 p^2 \quad\quad + 8.8248 p \quad + 0.096 : \text{ approximate} \end{aligned}\right\} . \quad (5.3)$$

Table V shows only the exact and approximate root changes due to the changes in the parameters specified in the first column.

TABLE V

Comparison of exact and approximate changes in stability roots

Change in parameter	Change in Spiral Damping (0.010 946)		Change in Rolling Damping (4.272 817)		Change in Oscillation Damping (0.218 118)		Change in Oscillation frequency (1.415 952)	
	Exact	Approx.	Exact	Approx.	Exact	Approx.	Exact	Approx.
$\Delta y_v = -0.1$	−0.000 174	−0.000 177	0.002 264	0.002 217	0.048 956	0.048 981	0.002 972	0.003 827
$\Delta y_p = 0.1$	−0.000 011	−0.000 011	−0.013 448	−0.013 413	0.006 730	0.006 712	0.001 979	0.001 984
$\Delta y_r = 0.1$	0.000 101	0.000 099	−0.000 590	−0.000 589	0.000 245	0.000 245	−0.006 518	−0.006 500
$\Delta l_v = -0.02$	0.006 173	0.006 581	0.031 369	0.031 798	−0.018 770	−0.019 199	0.044 080	0.045 046
$\Delta l_p = -0.06$	−0.001 119	−0.001 248	0.581 006	0.577 200	0.010 058	0.012 247	−0.015 698	−0.017 127
$\Delta l_r = 0.02$	−0.003 666	−0.003 676	−0.008 460	−0.008 448	0.006 064	0.006 062	0.002 305	0.002 298
$\Delta n_v = 0.024$	−0.010 946	−0.019 404	−0.004 710	−0.005 111	0.007 828	0.012 256	0.478 308	0.559 094
$\Delta n_p = 0.015$	0.000 825	0.000 767	−0.019 561	−0.019 330	0.009 368	0.009 282	−0.050 041	−0.048 919
$\Delta n_r = 0.024$	−0.010 946	−0.010 841	−0.001 311	−0.001 358	−0.073 846	−0.073 901	0.002 104	0.004 605
$\Delta \mu_2 = 2$	0.000 057	0.000 068	0.017 614	0.018 056	−0.008 835	−0.009 062	0.132 130	0.138 846
$\Delta \tan \gamma_e = 0.1$	−0.009 035	−0.009 055	0.000 138	0.000 138	0.004 449	0.004 458	0.000 879	0.000 860
$\Delta (1/i_A) = 2$	−0.000 003	−0.000 004	0.824 480	0.822 090	0.007 762	0.008 958	0.003 309	0.004 430
$\Delta (1/i_C) = -5/3$	−0.000 241	−0.000 187	−0.009 151	−0.009 067	−0.035 304	−0.035 075	−0.173 333	**−0.161 930**
$\Delta i_E = -0.005$	−0.000 007	−0.000 007	−0.030 170	−0.036 554	0.022 870	0.023 281	0.002 976	0.003 095
	−0.000 012*		−0.036 694*		0.023 354*		0.003 304*	

* From approximate stability equation, ignoring $(i_g)^2$.

Agreement between the exact and approximate values in Table V is in general very good. The damping is given more accurately than the frequency factor, in general, and the accuracy of the former is clearly more than sufficient for practical purposes, for derivative changes of the orders of magnitude considered, with the exception of changes in n_v, for which the approximate formulæ are wildly in error. Clearly the method of estimating stability changes suggested here can give excellent results. Whether the formulæ will behave with comparable accuracy for variations from another standard set of conditions is open to doubt, but we may mention that the case considered was deliberately chosen from the start as one likely to be unfavourable. Further comparisons of exact and calculated values will be made in a later paper, in which the formulæ will be used to survey the dependence of lateral stability roots upon the minor parameters, over a wide range of representative conditions.

6. ACCURACY OF LATERAL STABILITY ROOTS IN A TYPICAL CASE

Table V also indicates, for the case considered, the extent to which the calculated roots of the secular equation would be altered by changes in the individual parameters. If we regard these changes as the probable errors of estimated values, then the average probable error in any root may be taken as equal to the square root of the sum of the squares of the probable errors due to the separate uncertainties. Since these differ considerably in order of magnitude, the overall error will not be very different from the largest individual error.

Clearly, then, the uncertainty in n_r is the most important source of inaccuracy, affecting particularly the dampings of the important spiral and oscillatory modes. Next to it in order of importance comes n_v, affecting spiral damping and oscillatory frequency: note, however, that the assumed change in n_v is larger than the probable error of this derivative, which is commonly determined in a model test. An important source of error in oscillation damping is uncertainty in y_v, which could be much reduced if this derivative were more commonly measured in the wind tunnel.

If these large sources of error could be removed, the stability characteristics in this typical case would become much more definite. The assumed changes in the other derivatives are larger than the probable errors of estimation, and cause no serious errors. In fact, if we could cut down the probable error of y_v to 0.03, and those of n_v and n_r to 0.006, it would be possible to specify the roots, with their probable errors, as

$$\left.\begin{aligned} q_s &= 0.011 \pm 0.006, \quad q_r = 4.3 \pm 0.6 \\ r &= 0.22 \pm 0.02, \quad\quad s = 1.42 \pm 0.12 \end{aligned}\right\} \quad . \quad . \quad . \quad (6.1)$$

instead of with errors about four times as great. We may note, also, that the usual

neglect of y_p and y_r is amply justified, unless these derivatives are much larger than the assumed changes: on the other hand, i_B may have a significant influence on oscillation damping.

APPENDIX A

Formulæ for longitudinal stability

The coefficients of the longitudinal stability quartic are

$$\left.\begin{aligned}
A &= 1 \\
B &= -x_u - z_w - \frac{m_q}{i_B} - \left(1+\frac{z_q}{\mu_1}\right)\frac{\mu_1 m_{dw/dt}}{i_B} \\
C &= x_u z_w - x_w z_u + \frac{m_q}{i_B}(x_u + z_w) - \left(1+\frac{z_q}{\mu_1}\right)\frac{\mu_1 m_w}{i_B} + \\
&\quad + \left\{x_u\left(1+\frac{z_q}{\mu_1}\right) - z_u\frac{x_q}{\mu_1} + k\tan\gamma_e\right\}\frac{\mu_1 m_{dw/dt}}{i_B} - \frac{x_q}{\mu_1}\frac{\mu_1 m_u}{i_B} \\
D &= -\frac{m_q}{i_B}(x_u z_w - x_w z_u) + \left\{x_u\left(1+\frac{z_q}{\mu_1}\right) - z_u\frac{x_q}{\mu_1} + k\tan\gamma_e\right\}\frac{\mu_1 m_w}{i_B} - \\
&\quad - \left\{x_w\left(1+\frac{z_q}{\mu_1}\right) - z_w\frac{x_q}{\mu_1} - k\right\}\frac{\mu_1 m_u}{i_B} + k(-x_u\tan\gamma_e + z_u)\frac{\mu_1 m_{dw/dt}}{i_B} \\
E &= k(z_u - x_u\tan\gamma_e)\frac{\mu_1 m_w}{i_B} - k(z_w - x_w\tan\gamma_e)\frac{\mu_1 m_u}{i_B}
\end{aligned}\right\} \quad \text{(A.1)}$$

The notation is that of Ref. 7, modified as in the text. We also use the portmanteau symbols due to Neumark[6], slightly modified:

$$\left.\begin{aligned}
N_1 &= -x_u - z_w \\
P_1 &= x_u z_w - x_w z_u \\
Q_1 &= -\left(1+\frac{z_q}{\mu_1}\right)x_u + \frac{x_q}{\mu_1}z_u - k\tan\gamma_e \\
R_1 &= -k(z_u - x_u\tan\gamma_e) \\
S_1 &= k - x_w\left(1+\frac{z_q}{\mu_1}\right) + z_w\frac{x_q}{\mu_1} \\
T_1 &= -k(z_w - x_w\tan\gamma_e)
\end{aligned}\right\} \quad \text{(A.2)}$$

and

$$\left.\begin{aligned} \omega &= -\mu_1 m_w / i_B \\ v &= -m_q / i_B \\ \chi &= -\mu_1 m_{dw/dt} / i_B \\ \mathscr{H} &= -\mu_1 m_u / i_B \end{aligned}\right\} \quad . \quad . \quad . \quad . \quad (A.3)$$

The rates of change of the coefficients with respect to the parameters are given in Table VI.

APPENDIX B

Notation

The following symbols have the meanings usual in stability theory, as defined in Bryant and Gates R. & M. 1801 on Nomenclature for Stability Coefficients.

i_A, i_B, i_C

μ_1, μ_2

S, ρ, b, m, E, k, θ_o

l_v, l_p, l_r, n_v, n_p, n_r, y_v

x_u, x_w, x_q, z_u, z_w, z_q, m_u, m_w, m_q,

$m_{dw/dt}$ has been used instead of $m_{\dot{w}}$

In addition the symbol i_E ($=4E/mb^2$) is used, *see* equation (3.1.2).

Additional symbols used are as follows:—

A, B, C, D, E — coefficients in stability period equation.

A_o, B_o, C_o, D_o, E_o — standard values of A, B, C, D, E, respectively.

$f(p)$ — stability period equation.

K_{qA}, etc. — rates of change of roots with respect to coefficients, the first suffix specifying the root, the second the coefficient. Defined in equation (2.1.4), formulæ for calculating and checking in Sections 2.2 to 2.5.

l_1 — $-l_p/i_A$, equation (3.1.4).

l_3 — l_r/i_A, *ibid.*

$\mathscr{L}$ — $-\mu_2 l_v/i_A$, *ibid.*

TABLE VI

Values of the quantities $(1/A_0)\,d\kappa'/d\kappa$, $\partial A/\partial\kappa'$, etc., needed in calculating changes in coefficients and stability roots. $\partial A/\partial\kappa'=0$ for all κ'. Exact coefficient change $\Delta A = A_0\left(\frac{1}{A_0}\frac{d\kappa'}{d\kappa}\right)\frac{\partial A}{\partial\kappa'}\Delta\kappa$, etc. Approximate root change $\Delta q = \frac{1}{A_0}\frac{d\kappa'}{d\kappa}\left(K_{q\Delta}\frac{\partial A}{\partial\kappa'}+\dots\right)\Delta\kappa$.

κ	$(1/A_0)\partial\kappa'/\partial\kappa$	$\partial B/\partial\kappa'$	$\partial C/\partial\kappa'$	$\partial D/\partial\kappa'$	$\partial E/\partial\kappa'$
x_u	-1	1	$B+x_u$	$-z_w\nu+\omega\,(1+z_q/\mu_1)-k\tan\gamma_e$	$-\omega k\tan\gamma_e$
x_w	1	0	$-z_u$	$-z_u\nu+\mathscr{H}\,(1+z_q/\mu_1)$	$-\mathscr{H}k\tan\gamma_e$
x_q	$-1/\mu_1$	0	$-z_u\chi-\mathscr{H}$	$-\omega z_u+\mathscr{H}z_w$	0
z_u	-1	0	$x_w-\chi x_q/\mu_1$	$x_u\nu-\omega x_q/\mu_1+\chi$	ωk
z_w	-1	1	$\nu-x_u$	$-\nu x_u+\mathscr{H}x_q/\mu_1$	$-\mathscr{H}k$
z_q	$1/\mu_1$	χ	$\omega-\chi x_u$	$-\omega x_u+\mathscr{H}x_w$	0
m_u	μ_1/i_B	0	$-x_q/\mu_1$	S_1	T_1
$\mathscr{H}$	-1				
m_w	$-\mu_1/i_B$	0	$1+z_q/\mu_1$	Q_1	R_1
ω	1				
$m_{dw/dt}$	$-\mu_1/i_B$	$1+z_q/\mu_1$	Q_1	R_1	0
χ	1				
m_q	$-1/i_B$	1	N_1	P_1	0
ν	1				
$1/i_B$	i_B	$B-N_1$	$C-P_1$	D	E
μ_1	$1/\mu_1$	$-\chi z_q/\mu_1$	$\omega-\chi\,(z_qx_q/\mu_1-x_uz_q/\mu_1)$	$\mathscr{H}(x_w-k)-\omega(x_u+k\tan\gamma_e)$	E
$\tan\gamma_e$	$-\frac{1}{2}C_L$	0	χ	$\omega-\chi x_u$	$-\omega x_u+\mathscr{H}x_w$

n_1 $-n_p/i_C$, equation (3.1.4).

n_3 $-n_r/i_C$, *ibid.*

$\mathcal{N}$ $\mu_2 n_r/i_C$, *ibid.*

$N_1, P_1, Q_1, R_1, S_1, T_1$ portmanteau symbols, equation (A.2).

p variable in stability equation.

p_0 standard value of p.

q, q_l damping factors of roots.

q_s, q_r damping factors of spiral and rolling modes of lateral motion.

U_0 steady forward speed of aeroplane.

y_2 $-y_v$, equation (3.1.4).

y_p, y_r dimensionless forms of Y_p, Y_r, equation (3.1.3).

Y_p, Y_r side force (lb.) due to unit rate of roll and yaw, respectively, (rad./sec.).

γ_0 angle of climb.

Γ_1, Γ_2 portmanteau symbols, equation (3.1.5).

ϵ_A, ϵ_C $-i_E/i_A$, $-i_E/i_C$, equation (3.1.4).

κ typical parameter in stability equation.

κ_0 standard value of κ.

κ' intermediate parameter.

$\Pi_1, \Pi_2, \Pi_3, \Pi_4$ portmanteau symbols, equation (3.1.5).

ω, ν, χ, $\mathcal{H}$ modified longitudinal stability derivatives, equation (A.3).

σ_n portmanteau symbol, Section 2.5.

REFERENCES

1. BRYANT, L. W., and HOPWOOD, M. L. (1942). Calculation of the Damping of the Lateral Oscillation of an Aeroplane. R. & M. 1956, 1942.

2. GANDY, R. W. (1943). The Response of an Aeroplane to the Application of Ailerons and Rudders. Part I—Response in Roll. R. & M. 1915, 1943.

3. MITCHELL, K., THORPE, A. W., and FRAYN, E. M. (1945). The Theoretical Response of a High-Speed Aeroplane to a Side Gust. Part of R. & M. 2294, 1945.

4. COWLEY, W. L., and SKAN, S. W. (1930). A Study of Polynomial Equations. R. & M. 1325, 1930.

5. MITCHELL, K., THORPE, A. W., and FRAYN, E. M. (1945). The Theoretical Response of a High-Speed Aeroplane to the Application of Ailerons and Rudder. Part of R. & M. 2294, 1945.

6. NEUMARK, S. (1943). The Disturbed Longitudinal Motion of an Uncontrolled Aeroplane and of an Aeroplane with Automatic Control. R. & M. 2078, 1943.

7. BRYANT, L. W., and GATES, S. B. (1937). Nomenclature for Stability Coefficients. R. & M. 1801, 1937.

8. MITCHELL, K. (1943). A Supplementary Notation for Theoretical Lateral Stability Investigations. R.A.E. Tech. Note No. Aero. 1183, 1943.

9. BUXTON, D. H. L., and MINHINNICK, I. T. (1945). Expressions for the Rates of Change of Critical Flutter Speeds and Frequencies with Inertial Aerodynamic and Elastic Coefficients. R. & M. 2444, 1945.

FLUTTER OF SYSTEMS WITH MANY FREEDOMS

by

W. J. DUNCAN, D.Sc., F.R.S., F.R.Ae.S.

(Professor of Aerodynamics, College of Aeronautics, Cranfield)

SUMMARY

Experience has shown that it is often necessary to retain many degrees of freedom in order to calculate critical flutter speeds reliably, but this entails much labour. Part I discusses the choice of a minimum set of freedoms and suggests that this should be based on the equation of energy and the use of the Lagrangian dynamical equation corresponding to any proposed additional freedom. The methods for conducting flutter calculations so as to minimise labour are treated in Part II.

1. INTRODUCTION

The aim of this paper is to discuss methods for calculating the critical flutter speeds and the nature of the motion at these speeds for systems with a large number of degrees of freedom. This problem is becoming increasingly important since it is now recognised that reliable estimates of critical speeds can, in many instances, only be made when many independent kinds of motion of the structure are admitted. However, the labour in the calculations increases exceedingly rapidly as the number of degrees of freedom is increased. Hence two principal problems arise:—

(*a*) The choice of a minimum set of dynamical co-ordinates or degrees of freedom which leads to calculated results of adequate accuracy.

(*b*) The choice of the method of conducting the calculations after the dynamical co-ordinates have been chosen.

These problems are considered separately in Parts I and II of the paper.

It is concluded that a particular freedom F must be retained when the balance of energy at a critical flutter speed is sensitive to its inclusion, unless it can be shown that the amplitude of F is very small. This amplitude will be very small when one or both of the following conditions is satisfied:—

(*a*) The coupling terms in the Lagrangian dynamical equation corresponding to F are all very small.

(*b*) The direct impedance for F at the critical flutter speed and for the flutter frequency is very large.

Paper received October 1948.

[The Aeronautical Quarterly, Vol. 1, May 1949]

The equation of energy for any number of freedoms is reduced to a convenient form showing explicitly the influence of the phase relations of the motions. It is shown that large skew-symmetric components in the aerodynamic stiffnesses will result in a large intake of energy when the phase relations of the motions are favourable for this. Hence dynamical co-ordinates giving rise to such aerodynamic stiffnesses must be scrutinised with special care.

Some simple illustrative applications given in Section 8 support the validity of the proposed method of selecting co-ordinates, but its general usefulness can only be judged on the results of extended trials. In any event, it is hoped that the analysis of the flutter problem given here will contribute towards a better understanding of the physics of flutter.

Attention is drawn to the usefulness of comparing the various aerodynamic couplings with the corresponding inertial couplings, since this may suffice to show that the former are small (*see* Sections 5 and 6).

Inverse methods appear to be the most advantageous for the calculation of critical flutter speeds when there are many freedoms.

There are a few known special cases where "exact" calculations of critical flutter speeds can be made for elastic continuous systems having infinitely many degrees of freedom. Such systems throw much light on the general problem of the choice of freedoms and they are considered briefly in the following Section.

2. SOME EXACTLY SOLUBLE PROBLEMS OF THE FLUTTER OF ELASTIC WINGS

Exact solutions of two problems on the flutter of continuous elastic cantilever wings have already been published and the details are as follows:—

(*a*) Uniform rectangular wing supported by a pair of uniform parallel spars. The covering has no proper torsional stiffness and both the flexural and torsional stiffnesses are provided by the uniform spars. The inertial and aerodynamic coefficients are independent of spanwise position.[1, 3, 4]

(*b*) Uniform rectangular wing as for case (*a*) but now the torsional stiffness is provided by the uniform covering or by a torque tube and the flexural stiffness is assumed to be negligible* (*see* the Appendix to Ref. 7).

Both wings have the following special dynamical characteristics. The modes of oscillation *in vacuo* or in an air stream occur in pairs which, in general, have both flexural and torsional components. The displacements in both flexure and torsion for the r^{th} pair are proportional to the displacements in the r^{th} mode† of the purely

* This is an artificial case but it is not without interest since the flexural stiffness does not greatly influence the flutter.

† Or $(r-1)^{th}$ overtone.

flexural oscillation of a uniform cantilever beam for case (*a*) and to the displacements in the r^{th} mode of the purely torsional oscillations of a uniform cantilever for case (*b*). When the wings are exposed to an air current the two modes of the r^{th} pair become coupled together aerodynamically, but remain uncoupled to all other modes. The flutters which occur are therefore effectively binary and the earliest flutter occurs in the modal pair corresponding to the fundamental free mode.

These results are not, in fact, isolated and it is hoped to discuss other similar cases in a separate paper. At present we wish to emphasise the remarkable simplicity of the solutions, which were obtained in an orthodox way by solving the differential equations of the problems. An independent explanation of the results is given in Section 6 by means of an analysis of the various couplings between the modes.

PART I

CHOICE OF THE DEGREES OF FREEDOM*

3. TYPES OF GENERALISED CO-ORDINATES

The generalised co-ordinates should be chosen so as to secure some advantage of simplicity or convenience, There appear to be two particularly advantageous types:—

(*a*) Those for which the specification of the displacements is specially simple.

Examples. The purely flexural and purely torsional co-ordinates of the classical theory of wing flutter.

(*b*) Those which secure the greatest simplification of the dynamical equations, as by the vanishing of certain coefficients.

Examples. Normal co-ordinates for which the inertial and elastic coupling coefficients vanish.

In the further discussion we shall adopt normal co-ordinates for the main structural deformations. These correspond, strictly, to the free modes of oscillation of the structure *in vacuo*, but differ little from the modes of oscillation in still air. They must be supplemented by certain general rigid body freedoms, for the resultant force and moment on the system are not, in general, zero when the oscillations occur in an air stream. Lastly, there will be one co-ordinate for the angular movement of each control surface which is concerned in the flutter. The main problem is to decide which of the normal modes and general freedoms must be retained in the calculations.

* The ideas of Part I are to some extent based on Ref. 5.

For a conventional aircraft, having a fore-and-aft plane of symmetry, and in straight symmetric flight, the small oscillations of symmetric and anti-symmetric types will be independent. For each type of flutter only the corresponding normal modes, general freedoms and control movements must be retained. For example, in symmetric flutter a single symmetrically placed rudder takes no part and the body freedoms are pitching, normal displacement and fore-and-aft displacement; the latter will usually be negligible.

In order to determine what normal co-ordinates are to be retained the influence of an added co-ordinate on the energy balance must be examined. We accordingly pass next to the equation of energy.

4. THE EQUATION OF ENERGY

For the sake of conciseness and perspicuity we shall use the matrix notation. Thus the whole set of the equations of free motion will be written

$$A\ddot{q}+B\dot{q}+Cq=0 \quad . \quad . \quad . \quad . \quad . \quad . \quad . \quad (1)$$

where A, B, C are the square matrices of the inertias, damping coefficients and stiffnesses, respectively, and q is the column matrix of the generalised co-ordinates. A, B and C are independent of the generalised co-ordinates and of time. The equation of energy is obtained by pre-multiplying the last by $\dot{q}'$, *i.e.* by the row matrix* whose elements are the generalised velocities, and it is accordingly

$$\dot{q}'A\ddot{q}+\dot{q}'B\dot{q}+\dot{q}'Cq=0. \quad . \quad . \quad . \quad . \quad . \quad . \quad (2)$$

Now A is always symmetric and the kinetic energy of the system is

$$\mathbf{T}=\tfrac{1}{2}\dot{q}'A\dot{q}, \quad . \quad . \quad . \quad . \quad . \quad . \quad (3)$$

a quadratic form in the generalised velocities. Therefore

$$\frac{d\mathbf{T}}{dt}=\tfrac{1}{2}\dot{q}'A\ddot{q}+\tfrac{1}{2}\ddot{q}'A\dot{q}$$

since A is independent of time. But

$$\ddot{q}'A\dot{q}=\dot{q}'A\ddot{q}$$

by transposition, since $A'=A$, and we obtain

$$\frac{d\mathbf{T}}{dt}=\dot{q}'A\ddot{q}. \quad . \quad . \quad . \quad . \quad . \quad (4)$$

* An accent appended to the symbol for a matrix indicates that its *transposed* is to be taken.

For a system subject to aerodynamic actions neither B nor C is, in general, symmetric. We may always put

$$B=B_1+B_2, \quad . \quad . \quad . \quad . \quad . \quad . \quad . \quad (5)$$

$$C=C_1+C_2, \quad . \quad . \quad . \quad . \quad . \quad . \quad . \quad (6)$$

where the suffixes 1, 2 are applied to symmetric and skew-symmetric matrices respectively. Then

$$B_1=\tfrac{1}{2}(B+B'), \quad . \quad . \quad . \quad . \quad . \quad . \quad (5a)$$

$$B_2=\tfrac{1}{2}(B-B'), \quad . \quad . \quad . \quad . \quad . \quad . \quad (5b)$$

and there are similar expressions for C_1 and C_2. Let the dissipation function be

$$\mathbf{F}=\tfrac{1}{2}\dot{q}'B\dot{q}=\tfrac{1}{2}\dot{q}'B_1\dot{q}, \quad . \quad . \quad . \quad . \quad . \quad (7)$$

since

$$x'Yx=0 \quad . \quad . \quad . \quad . \quad . \quad . \quad . \quad (8)$$

when Y is skew-symmetric and x is an arbitrary column matrix. Also let the "potential" be

$$\mathbf{V}=\tfrac{1}{2}q'C_1q, \quad . \quad . \quad . \quad . \quad . \quad (9)$$

so that

$$\frac{d\mathbf{V}}{dt}=\dot{q}'C_1q. \quad . \quad . \quad . \quad . \quad . \quad . \quad (10)$$

The equation of energy (2) can now be written

$$\frac{d}{dt}(\mathbf{T}+\mathbf{V})+2\mathbf{F}+\dot{q}'C_2q=0. \quad . \quad . \quad . \quad . \quad (11)$$

The final term in the last equation is of great importance and must be discussed in detail.

The equation of energy is valid for any free motion of the system, but particularly illuminating deductions can be drawn when the motion consists of a single constituent, corresponding either to a single real root or to a conjugate complex pair of roots of the determinantal equation.

Case (a). Real exponential motion (Divergence or subsidence)

Here we have

$$q=q_0e^{\lambda t} \quad . \quad . \quad . \quad . \quad . \quad . \quad . \quad (12)$$

with λ real and q_o a column of real constants. Then

$$\dot{q}=\lambda q$$

and
$$\dot{q}'\,C_2 q=\lambda q'\,C_2 q=0 \quad . \quad . \quad . \quad . \quad . \quad (13)$$

by equation (8). Therefore the equation of energy (11) becomes

$$\frac{d}{dt}(\mathbf{T}+\mathbf{V})+2\mathbf{F}=0. \quad . \quad . \quad . \quad . \quad . \quad (14)$$

If **F** is negative, obviously the motion can grow. But suppose now that **F** is positive during the motion.* Then we get

$$\frac{d}{dt}(\mathbf{T}+\mathbf{V})<0$$

at all instants. So long as **V** is essentially positive this implies decay of the motion. However, **V** is not wholly of elastic origin and at higher values of the relative wind speed it may cease to be essentially positive. Then **T** may increase, *i.e.* the motion may grow, through $d\mathbf{V}/dt$ being negative. At a critical speed for divergence λ, **F** and **T** are zero and the equation of energy becomes

$$\mathbf{V}=\text{constant}, \quad . \quad . \quad . \quad . \quad . \quad . \quad (15)$$

but the displacements need not be zero as they can be supposed to grow exceedingly slowly to finite values. This equation can be made the basis for calculating the critical divergence speeds, but we shall not pursue this question here.

Case (b). Exponential oscillatory motion (Damped, steady or growing oscillation)

The motion corresponds to the complex pair of roots $\mu \pm i\omega$ of the determinantal equation and the displacements can be expressed in the real form

$$q=e^{\mu t}(q_o \cos \omega t+q_1 \sin \omega t). \quad . \quad . \quad . \quad . \quad . \quad . \quad (16)$$

Hence
$$\dot{q}=\mu q+\omega e^{\mu t}(-q_o \sin \omega t+q_1 \cos \omega t)$$

and
$$\dot{q}'\,C_2 q=\omega e^{2\mu t}(-q_o' \sin \omega t+q_1' \cos \omega t)C_2\,(q_o \cos \omega t+q_1 \sin \omega t)$$

$$=\omega e^{2\mu t}(\cos^2 \omega t\; q_1' C_2 q_o-\sin^2 \omega t\; q_o' C_2 q_1)$$

$$=\omega e^{2\mu t} q_1' C_2 q_1, \quad . \quad . \quad . \quad . \quad . \quad . \quad . \quad . \quad (17)$$

* When the values of the aerodynamic damping coefficients for divergent motion as given by two-dimensional vortex sheet theory are used, the condition that the dissipation function shall be essentially positive is *not* satisfied for any value of the non-dimensional divergence parameter $\lambda\bar{c}/V$. The dissipation function will be essentially positive when there is enough structural damping.

for $x'Py=-y'Px$ when P is skew-symmetric, while x and y are column matrices, since $P'=-P$. Hence the equation of energy (11) becomes

$$\frac{d}{dt}(\mathbf{T}+\mathbf{V})=\omega e^{2\mu t}q_0'C_2q_1-2\mathbf{F}. \quad . \quad . \quad . \quad . \quad (18)$$

The special case of this for 3 degrees of freedom is equivalent to equation (42) of R. and M. 1155.[2] We add the explicit expression

$$C_2=\tfrac{1}{2}(C-C'). \quad . \quad . \quad . \quad . \quad . \quad (19)$$

Exactly at a critical speed for flutter μ is zero and we get by integration of (18) over a complete period T

$$\pi q_0'C_2q_1=\int_0^T \mathbf{F}dt. \quad . \quad . \quad . \quad . \quad . \quad (20)$$

This is the equation of energy balance at the critical speed.

5. GENERAL DISCUSSION OF COUPLINGS

The couplings between the various generalised co-ordinates can be classified broadly as follows:—

(*a*) *Inertial couplings or "products of inertia"*

It follows from Lagrange's dynamical equations that the contribution of the structure to A_{rs}, the coefficient of $\dot{q}_s$ in the equation corresponding to q_r, is

$$\Sigma\left(\frac{\partial x}{\partial q_r}\frac{\partial x}{\partial q_s}+\frac{\partial y}{\partial q_r}\frac{\partial y}{\partial q_s}+\frac{\partial z}{\partial q_r}\frac{\partial z}{\partial q_s}\right)\delta m \quad . \quad . \quad . \quad (21)$$

where x, y, z are the rectangular Cartesian co-ordinates of the element of mass δm, and the summation covers all the elements of mass for which the expression in the bracket does not vanish. The complete coefficient A_{rs} contains, in addition, the corresponding virtual inertia or reversed acceleration derivative.

When q_r and q_s are normal co-ordinates the coefficient $A_{rs}=A_{sr}$ vanishes.* The same is true when q_r is a normal co-ordinate and q_s is one of the general rigid body freedoms. This follows from the fact that motion in any normal mode can persist independently of any other motion.

For a cantilever wing with rigid support at the root we may usually neglect the chordwise and spanwise displacements in the flutter. Then the structural contribution to A_{rs} is

$${}_sA_{rs}=\Sigma\frac{\partial z}{\partial q_r}\frac{\partial z}{\partial q_s}\delta m. \quad . \quad . \quad . \quad . \quad . \quad (22)$$

* If we assume that the virtual inertias are the same for a finite air speed as for still air then q_r and q_s should be normal co-ordinates for oscillations in still air.

Further, when the wing is straight and not swept back or forward and it is assumed that each fore-and-aft strip moves as a rigid body,* this expression can be reduced to the form (*see* the list of symbols)

$$\frac{{}_sA_{rs}}{\sigma c_r^4 l} = \int \mathscr{A}_{rs}(\eta)\, d\eta, \qquad (23)$$

where

$$\mathscr{A}_{rs}(\eta) = m\frac{d\zeta}{dq_r}\frac{d\zeta}{dq_s}\left(\frac{\bar{c}}{c_r}\right)^2 + p\left(\frac{d\zeta}{dq_r}\frac{d\vartheta}{dq_s} + \frac{d\zeta}{dq_s}\frac{d\vartheta}{dq_r}\right)\left(\frac{\bar{c}}{c_r}\right)^3 + j\frac{d\vartheta}{dq_r}\frac{d\vartheta}{dq_s}\left(\frac{\bar{c}}{c_r}\right)^4. \qquad (24)$$

(*b*) *Cross or compound damping coefficients*

These are mainly or wholly of aerodynamic origin and the array of the coefficients is, in general, not symmetric, *i.e.* $B_{rs} \neq B_{sr}$ in general. We may, if we please, analyse these coupling coefficients into symmetric and skew-symmetric parts (*see* equations (5*a*), (5*b*)) and we may call these pure dampings and gyrostatic terms respectively. This analysis, however, does not appear to be particularly helpful.

For the type *C* wing the general formula for an aerodynamic damping coefficient is

$$\frac{B_{rs}}{\rho V c_r^3 l} = \int \mathscr{B}_{rs}(\eta)\, d\eta, \qquad (25)$$

where

$$\mathscr{B}_{rs}(\eta) = l_w\frac{d\zeta}{dq_r}\frac{d\zeta}{dq_s}\left(\frac{\bar{c}}{c_r}\right) + \left(l_{d\alpha/dt}\frac{d\zeta}{dq_r}\frac{d\vartheta}{dq_s} - m_w\frac{d\zeta}{dq_s}\frac{d\vartheta}{dq_r}\right)\left(\frac{\bar{c}}{c_r}\right)^2 - m_{d\alpha/dt}\frac{d\vartheta}{dq_r}\frac{d\vartheta}{dq_s}\left(\frac{\bar{c}}{c_r}\right)^3 \qquad (26)$$

This expression is equivalent to that given in Appendix 3 of R. and M. 1904.[6]

(*c*) *Cross or compound stiffness coefficients*

When normal co-ordinates are used these coefficients are entirely of aerodynamic origin and their array is, in general, not symmetric. For a type *C* wing

$$\frac{C_{rs}}{\rho V^2 c_r^2 l} = \int \mathscr{C}_{rs}(\eta)\, d\eta, \qquad (27)$$

where, in accordance with R. and M. 1904,[6]

$$\mathscr{C}_{rs} = l_\alpha\frac{d\zeta}{dq_r}\frac{d\vartheta}{dq_s}\left(\frac{\bar{c}}{c_r}\right) - m_\alpha\frac{d\vartheta}{dq_r}\frac{d\vartheta}{dq_s}\left(\frac{\bar{c}}{c_r}\right)^2. \qquad (28)$$

* To avoid circumlocution we shall henceforward call this a type *C* wing.

6. COMPARISON OF INERTIAL AND AERODYNAMIC COUPLINGS

When normal co-ordinates are used the inertial couplings are zero and in certain instances a comparison of the expressions for the inertial and aerodynamic couplings shows that the latter also vanish. More generally, the comparison may enable us to show that certain aerodynamic couplings are small.

The special uniform wings mentioned in Section 2 provide examples of what has been said. Here $\bar{c}/c_r$ is unity, the various coefficients are constants, and

$$\frac{d\zeta}{dq_r} = k_r \frac{d\vartheta}{dq_r} \quad . \quad . \quad . \quad . \quad . \quad . \quad (29)$$

where k_r is constant for each r; this expresses the similarity of the normal and torsional displacements in every natural mode. Hence

$$\frac{{}_sA_{rs}}{\sigma c_r^4 l} = \{ mk_rk_s + p(k_r + k_s) + j \} \int \frac{d\vartheta}{dq_r} \frac{d\vartheta}{dq_s} d\eta, \quad . \quad . \quad (30)$$

$$\frac{B_{rs}}{\rho V c_r^3 l} = \{ l_w k_r k_s + l_{d\alpha/dt} k_r - m_w k_s - m_{d\alpha/dt} \} \int \frac{d\vartheta}{dq_r} \frac{d\vartheta}{dq_s} d\eta, \quad . \quad (31)$$

$$\frac{C_{rs}}{\rho V^2 c_r^2 l} = (l_\alpha k_r - m_\alpha) \int \frac{d\vartheta}{dq_r} \frac{d\vartheta}{dq_s} d\eta, \quad . \quad . \quad . \quad . \quad . \quad (32)$$

and all three coefficients vanish when

$$\int \frac{d\vartheta}{dq_r} \frac{d\vartheta}{dq_s} d\eta = 0. \quad . \quad . \quad . \quad . \quad . \quad (33)$$

7. PRINCIPLES GOVERNING THE CHOICE OF FREEDOMS

Suppose that a critical flutter speed V_c has been calculated on the assumption that a particular set of freedoms is effective and let it be enquired whether some other freedom, F say, should be included in the calculation. The complete answer to the question is given by repeating the whole calculation with the new freedom F introduced and by comparison of the new and original critical speeds and modes of displacement. This method is usually extremely laborious and it is most desirable to find an easier basis of judgment. It is suggested here that judgment may be based on a consideration of the possible influence of F upon the energy balance at the critical speed V_c. If it can be shown that the introduction of F can neither add nor subtract more than a relatively very small amount of energy then F may safely be neglected.

The influence of F upon the energy balance will certainly be small when the amplitude of F is very small. We may estimate the amplitude of F by forming the

additional Lagrangian equation of motion *corresponding to* F and then assume that the other generalised co-ordinates have the values already calculated at the critical speed; this approximation will be justified if the amplitude of F is in fact small. The amplitude of F will then be given by

(Sum of coupling terms reversed)/(Direct impedance in F at the flutter frequency).

Clearly the sum of the coupling terms will certainly be small when all the coupling coefficients are small and it may be possible to see that this is so without calculating these coefficients. The impedance will be large when the flutter frequency (in the absence of freedom F) differs widely from the natural frequency for F alone, calculated at the wind speed V_c (since the direct stiffness coefficient for F may depend on V). We conclude that it will not usually be safe to neglect F when its proper frequency is near that of the flutter. On the other hand, when the proper frequency of F is much higher than that of the flutter the impedance will be very large and the amplitude of F will be very small; hence F can be neglected.

When the amplitude of F is neither large nor very small the decision to retain or reject should be based on a consideration of the sensitiveness of the energy balance to F. If some of the stiffness couplings between F and the other degrees of freedom show large skew-symmetric components (*see* Section 4) then F should be retained.

8. ILLUSTRATIVE EXAMPLES ON THE CHOICE OF FREEDOMS

A few simple examples are added here to illustrate the principles put forward in Section 7.

(*a*) *In what circumstances can the aileron co-ordinate* ξ *be neglected in wing flutter*?

The stiffness coupling derivatives L_ξ and H_ϕ (zero) are widely different[2]; likewise M_ξ and H_θ are widely different.[2] Hence the equation of energy shows that movement of the aileron may feed in much energy to the system, as is otherwise obvious. Consequently the aileron co-ordinates ξ must be retained unless it can be shown that the amplitude in ξ is very small. This will be true when either or both of the following conditions are satisfied:—

(*i*) The aileron impedance is very high. This can only be attained by providing the aileron with a very stiff elastic constraint (irreversible control).

(*ii*) All the coupling coefficients affecting the aileron hinge moment are extremely small. These are the two aileron products of inertia, and the aerodynamic derivatives $H_{d\phi/dt}$, $H_{d\theta/dt}$, H_θ. The latter will all be small for a certain location of the aileron hinge and the products of inertia can be made very small by suitable disposition of masses.

(*b*) *Must we bring in overtone modes in considering the flexural-torsional flutter of a cantilever wing not carrying large concentrated masses?*

We have seen in Section 2 that for a uniform cantilever wing with a certain special, but quite reasonable, elastic specification, the two gravest modes* are strictly uncoupled to the higher modes. For other straight cantilever wings of normal proportions the couplings will be small, although not zero. Also, the impedances in the overtone modes at the flutter frequency will be large on account of the great disparity in frequency. We conclude that the amplitudes in the overtone modes will be very small and that only minor errors in the critical flutter speed will result from neglect of such modes.

(*c*) *Flexural-torsional flutter of a cantilever wing carrying a large concentrated mass*

If we take one of the two gravest modes, the inertial coupling coefficient with any higher overtone mode is zero. In the expression for this "product of inertia" the displacements at the large mass are clearly heavily "weighted," but these displacements are *not* heavily weighted in the expressions for the aerodynamic couplings. Thus we have evidently no right to assume that the aerodynamic couplings of the modes are small just because the inertial couplings are zero. Hence the higher overtone modes can only be neglected when their impedances at the flutter frequency are very large, *i.e.* when the disparity of frequency is large. Hence we must expect to find it necessary to retain some of the lower overtone modes beyond the first.

PART II

METHODS FOR PREDICTING FLUTTER CHARACTERISTICS

9. NON-DIMENSIONAL FORM OF THE EQUATIONS OF MOTION

It is convenient to reduce the equations of motion to a standard non-dimensional form. When all the displacements are proportional to $\exp(\lambda t)$ the complete set of dynamical equations in the selected degrees of freedom can be written in the matrix notation

$$(A\lambda^2 + BV\lambda + DV^2 + E)\,q = 0 \quad . \quad . \quad . \quad . \quad (34)$$

where A is the inertia matrix

BV is the damping matrix

E is the matrix of the elastic stiffnesses

DV^2 is the matrix of the aerodynamic stiffnesses.

* In general both involving both flexure and torsion; the first mainly flexural and the second mainly torsional.

We shall now suppose that the m dynamical co-ordinates q are all non-dimensional (*e.g.* angles). Then, if ρ and σ are air and material densities and l is a typical linear dimension, we may define a set of non-dimensional matrices of coefficients by the equations

$$A = \sigma l^3 a \quad . \quad . \quad . \quad . \quad . \quad (35)$$

$$B = \rho l^4 b \quad . \quad . \quad . \quad . \quad . \quad (36)$$

$$D = \rho l^3 d \quad . \quad . \quad . \quad . \quad . \quad (37)$$

$$E = \sigma l^3 U^2 e \quad . \quad . \quad . \quad . \quad . \quad (38)$$

where U is one of the velocities of propagation of elastic waves in a typical material of construction. Next, introduce the auxiliary non-dimensional variables

$$\eta = \sqrt{(\rho/\sigma)} \quad . \quad . \quad . \quad . \quad . \quad (39)$$

$$\xi = (U/\eta V)^2 \quad . \quad . \quad . \quad . \quad . \quad (40)$$

$$\kappa = (l\lambda/\eta V) \quad . \quad . \quad . \quad . \quad . \quad (41)$$

The equation (34) can now be rewritten in the non-dimensional form

$$(a\kappa^2 + \eta b\kappa + d + \xi e)\, q = 0. \quad . \quad . \quad . \quad . \quad . \quad (42)$$

At a critical flutter speed and for the flutter component we can put

$$\kappa = \pm i\omega \quad . \quad . \quad . \quad . \quad . \quad . \quad (43)$$

and the equation to be satisfied is

$$(-a\omega^2 \pm i\eta b\omega + d + \xi e)\, q = 0. \quad . \quad . \quad . \quad . \quad (44)$$

The problem consists in finding ξ and ω so that the set of linear scalar equations represented by the foregoing matrix equation shall be compatible. Methods for doing this are described below.

10. THE ORTHODOX METHOD OF SOLUTION[2]

We regard η and the matrices a, b, d and e as known constants. If frequency-dependent derivatives are used this implies that some estimate of the flutter frequency parameter has already been made.

The condition for compatibility of the scalar equations represented by (42) is the "determinantal equation"

$$\Delta(\kappa, \xi)=0, \quad . \quad . \quad . \quad . \quad . \quad . \quad (45)$$

where the expression on the left is a polynomial in κ, in general of degree $2m$, whose coefficients are functions of ξ. At a critical value of ξ this equation is satisfied by the pair of equal and opposite roots $\pm i\omega$. Accordingly the parts of Δ containing even and odd powers of ω vanish separately and we derive a pair of equations which we may write

$$\Delta_1(\omega^2, \xi)=0 \quad . \quad . \quad . \quad . \quad . \quad . \quad (46)$$

$$\Delta_2(\omega^2, \xi)=0. \quad . \quad . \quad . \quad . \quad . \quad . \quad (47)$$

The result of eliminating ω from these is

$$T_{n-1}(\xi)=0 \quad . \quad . \quad . \quad . \quad . \quad . \quad (48)$$

where T_{n-1} is the penultimate Routhian test function and n is the degree in κ of the determinantal equation. Equation (48) is a polynomial equation for ξ and when its roots have been found the critical flutter speeds can be obtained from (40). Finally, the flutter frequency and the complex modal ratios can be calculated.

It is worthy of remark that the test function always vanishes when the relative density parameter η is zero. Thus T_{n-1} contains a power of η as a factor and when this is removed we are left with a polynomial in η whose "constant" term is the asymptotic form of the test function for low relative air density. Since the critical values of ξ are then independent of η, equation (40) shows that the "equivalent" or indicated critical flutter speeds are independent of the densities. It appears that modern heavily loaded aircraft are in or near this asymptotic condition.

The orthodox method is systematic and yields all the desired information. Its drawback is that it becomes unworkably laborious when the number of freedoms is greater than three.

11. THE METHOD OF R. A. FRAZER[8]

Frazer writes the equations (46) and (47) as*

$$f(x, y)=0 \quad . \quad . \quad . \quad . \quad . \quad . \quad (49)$$

* Frazer does not use the special reduction to the non-dimensional form adopted here, but his method is essentially as stated.

$$g(x, y)=0 \quad . \quad . \quad . \quad . \quad . \quad . \quad (50)$$

where $$x=-\omega^2 \quad . \quad . \quad . \quad . \quad . \quad (51)$$

and $$y=\xi. \quad . \quad . \quad . \quad . \quad . \quad . \quad (52)$$

Since x and y are both real they could be found from the real intersections of the curves (49) and (50). Frazer shows that the full expressions for the functions f and g can be calculated from expressions in partial fraction form containing the values of $\Delta(\kappa, \xi)$ corresponding to a special set of points (x, y). These are the intersections of a standard set of straight lines satisfying the conditions

(*a*) No two are parallel

(*b*) No three are concurrent.

Much labour can be saved by use of this method when the number of freedoms is large. It is to be regarded as a special development of the classical method, designed to minimise labour. A new lattice has been proposed by Williams[12] which is thought to reduce the labour still further.

Frazer and Bratt have proposed mechanical and electrical methods for the description of the curves (49) and (50).

12. METHODS BASED ON THE USE OF MATRICES

The determination of the roots κ for a given ξ can be made to depend on the problem of finding the latent roots of a certain matrix (Duncan and Collar[9, 10]). An iterative method for finding the latent roots without expanding the characteristic determinant is given by Duncan and Collar and other treatments are described by Hermann and Dörr.[11] It is not considered that these methods have yet been developed to the stage where they would be advantageous from the aspect of labour saving in flutter problems.

13. THE METHOD OF DUNCAN, COLLAR AND LYON[7]

This method is based on the fact that the mechanical impedance of the system is zero at the critical flutter speed and for simple harmonic applied forces having the frequency of the flutter. The method consists, in effect, in calculating the impedance for a number of assumed air speeds and frequencies and in determination of the condition of zero impedance by interpolation. Since the impedance is found merely by solving a set of simultaneous linear equations with known coefficients, the calculations are relatively simple. The method has the further advantage that the modes of oscillation in the flutter are obtained incidentally from the calculations.

It is convenient to make the calculations in the following manner. Arbitrarily assign the amplitude of one dynamical co-ordinate (say, put $q_r = 1$) and use the dynamical equations corresponding to *free motion* in the *other* co-ordinates to calculate the amplitudes of these for the assumed air speed and frequency; this requires only the solution of a set of simultaneous linear equations whose coefficients are, in general, complex, on acount of the presence of the damping terms. The amplitudes of all the dynamical co-ordinates are now known and when these are inserted in the equation for the co-ordinate q_r the expression on the left hand side is equal to the amplitude of the generalised force Q_r which must be applied in order to maintain the assumed motion. This is the impedance, in general complex, since q_r is unity. The vanishing of the complex impedance implies *two* conditions and it thus becomes possible to find both the critical flutter speed and frequency by interpolation when the impedance has been calculated for a few pairs of values.

The quick success of this method evidently depends on making a good preliminary guess or estimate of the critical flutter speed and frequency.

14. ANOTHER INVERSE METHOD

We may proceed exactly as in the last method until we reach the final dynamical equation corresponding to the assigned co-ordinate q_r. However, the expression on the left hand side of the equation is equated to zero (free motion) while ξ in this is regarded as unknown. We shall thus derive a value ξ' for ξ, in general complex; the condition to be satisfied is

$$\xi' - \xi = 0$$

which is equivalent to a pair of real equations. The critical values of ξ and ω are to be obtained by trial and interpolation, as in the previously described method.

LIST OF PRINCIPAL SYMBOLS USED

The symbols are in alphabetical order and the Greek letters follow the Roman.
An accent indicates the transposed of a matrix.
A dot above a symbol indicates its time rate of change.
The numbered references are to equations.

A	matrix of inertial coefficients.
A_{rs}	general inertial coefficient. *See* (21).
$\mathscr{A}_{rs}$	*see* (24).
a	non-dimensional form of A. *See* (35).

B	matrix of damping coefficients or, in equations (34) and (36), the same divided by V.
B_1	symmetric part of B. *See* (5*a*).
B_2	skew-symmetric part of B. *See* (5*b*).
B_{rs}	general damping coefficient. *See* (25).
$\mathscr{B}_{rs}$	*see* (26).
b	non-dimensional form of B. *See* (36).
C	matrix of stiffness coefficients.
C_1	symmetric part of C.
C_2	skew-symmetric part of C.
C_{rs}	general stiffness coefficient. *See* (27).
$\mathscr{C}_{rs}$	*see* (28).
$\bar{c}$	chord of wing.
c_r	chord at wing root.
D	matrix of aerodynamic stiffnesses, divided by V^2. *See* (34).
d	non-dimensional form of D. *See* (37).
E	matrix of elastic stiffnesses.
e	non-dimensional form of E. *See* (38).
$\mathbf{F}$	dissipation function. *See* (7).
H_ϕ	rate of change of hinge moment with flexural co-ordinate ϕ.
$H_{d\phi/dt}$	rate of change of hinge moment with rate of change of ϕ.
H_θ	rate of change of hinge moment with torsional co-ordinate θ.
$H_{d\theta/dt}$	rate of change of hinge moment with rate of change of θ.
h	distance of local flexural centre aft of leading edge as fraction of local chord.
j	local value of moment of inertia about leading edge, per unit span, divided by $\sigma\bar{c}^4$.
k_r	*see* (29).
l	distance from wing root to reference section or other typical linear dimension ($\eta = y/l$).
L_ξ	rate of change of aerodynamic flexural moment with aileron angle ξ.
M_ξ	rate of change of torsional moment with aileron angle ξ.

l_w non-dimensional derivative coefficient giving local rate of change of lift with normal velocity w.

l_α non-dimensional derivative coefficient giving local rate of change of lift with angle of incidence α.

$l_{d\alpha/dt}$ non-dimensional derivative coefficient giving local rate of change of lift with rate of change of α.

m_w non-dimensional derivative coefficient giving local rate of change of moment about leading edge with normal velocity w.

m_α non-dimensional derivative coefficient giving local rate of change of moment about leading edge with angle of incidence α.

$m_{d\alpha/dt}$ non-dimensional derivative coefficient giving local rate of change of moment about leading edge with rate of change of α.

m number of dynamical co-ordinates, in Sections 9 and 10.

m local value of mass per unit span, divided by $\sigma\bar{c}^2$, in Section 5.

p local value of mass moment about leading edge, per unit span, divided by $\sigma\bar{c}^3$.

q column matrix of dynamical co-ordinates, which are taken to be non-dimensional.

q_0, q_1 *see* (16).

q_r r^{th} dynamical co-ordinate or its amplitude.

$\mathbf{T}$ kinetic energy of system.

T periodic time of flutter.

T_{n-1} penultimate test function in Routh's sequence.

t time.

U a velocity of propagation of elastic waves in a typical material of construction

$\mathbf{V}$ "potential" of system. *See* (9).

V true air speed.

y lateral distance from plane of symmetry or wing root.

z normal displacement.

η y/l in (23), (25) and (27).

η $\sqrt{(\rho/\sigma)}$, in Sections 9 and 10.

ϑ local twisting or pitching displacement.

ζ downward normal displacement of leading edge, divided by c_r.

ξ aileron angle in Section 8.

ξ	non-dimensional speed coefficient elsewhere. *See* (40).
κ	a non-dimensional frequency parameter. *See* (41).
λ	coefficient of t in $\exp(\lambda t)$.
μ	real part of λ.
ρ	air density.
σ	density of typical material of wing.
ω	coefficient of imaginary unit in λ or κ. *See* (16),-(43).

REFERENCES

1. GATES, S. B. (1928). The Torsion-Flexure Oscillations of Two Connected Beams. *Phil. Mag.*, Jan. 1928.
2. FRAZER, R. A. and DUNCAN, W. J. (1928). The Flutter of Aeroplane Wings. (A.R.C. Monograph). R. & M. 1155, Aug. 1928.
3. FRAZER, R. A. and DUNCAN, W. J. (1928). Conditions for the Prevention of Flexural-Torsional Flutter of an Elastic Wing. R. & M. 1217, Dec. 1928.
4. FRAZER, R. A. and DUNCAN, W. J. (1931). The Flutter of Monoplanes, Biplanes and Tail Units (A.R.C. Monograph). R. & M. 1255, Jan. 1931.
5. DUNCAN, W. J. (1944). Note on the Flutter of Complicated Systems. A.R.C. 7630 (Unpublished), April 1944.
6. DUNCAN, W. J. (1943). The Representation of Aircraft Wings, Tails and Fuselages by Semi-Rigid Structures in Dynamic and Static Problems. R. & M. 1904, Feb. 1943.
7. DUNCAN, W. J., COLLAR, A. R. and LYON, H. M. (1936). Oscillations of Elastic Blades and Wings in an Airstream. R. & M. 1716, Jan. 1936.
8. FRAZER, R. A. (1946). Bi-variate Partial Fractions and their Applications to Flutter and Stability Problems. *Proc. Roy. Soc.*, A., Vol. 185, p. 465, 1946.
9. DUNCAN, W. J. and COLLAR, A. R. (1935). Matrices Applied to the Motions of Damped Systems. *Phil. Mag.*, Ser. 7, Vol. 19, p. 197, Feb. 1935.
10. FRAZER, R. A., DUNCAN, W. J. and COLLAR, A. R. (1938). *Elementary Matrices.* Cambridge University Press, 1938.
11. HERRMAN, A. and DÖRR, J. Forschungsbericht, No. 1769, Feb. 1943. Translation by Miss S. W. Skan. Methods of Investigating Flutter Behaviour when there are a Number of Degrees of Freedom. A.R.C. 10,439, March 1947.
12. WILLIAMS, J. (1948). A New Framework of Lines for the Bi-variate Expansion Method of Solving Flutter Problems. A.R.C. 11,757, Sept. 1948.

NOTE ON PROPELLER-TURBINE REDUCTION METHODS

by

E. C. PIKE, M.A., A.F.R.Ae.S.

(*Member of the Technical Staff of the Royal Aeronautical Society*)

1. INTRODUCTION

It has been shown[1] that since the performance of a turbo-jet engine can be expressed theoretically as a function of the two variables $N/\sqrt{\theta}$ and $V/\sqrt{\theta}$, the performance of a turbo-jet aircraft can also be expressed as a function of two variables, $N/\sqrt{\theta}$ and $W/\tilde{\omega}$. Two methods can then be used for the reduction of the performance to standard conditions. In the "non-dimensional" graphical method, flight test measurements of, for instance, $V/\sqrt{\theta}$ are plotted against $N/\sqrt{\theta}$ and $W/\tilde{\omega}$, and the standard value of $V/\sqrt{\theta}$ is read from these curves at the standard values of $N/\sqrt{\theta}$ and $W/\tilde{\omega}$. In this way, the relation between the parameters is established during the tests. The alternative method is an analytical one in which corrections are applied to, for example, the level speed for differences from standard in the independent variables. For this method the effect on the performance of changes in these variables must be predetermined.

The case of the propeller-turbine aircraft is more difficult than for turbo-jets for two reasons:—

(*i*) A third variable is introduced into the engine performance equations, which makes a "non-dimensional" graphical method awkward from the flight-testing viewpoint.

(*ii*) There is little information on the variation of engine performance with the independent variables, because little test flying has been done, and there is no variable altitude test plant in this country.

For propeller-turbine aircraft there are three possible ways of reducing the performance to standard conditions:—

(*a*) By a "non-dimensional" graphical method (with an extra variable), in which the relations between the variables are established during the test, as for turbo-jets.

(*b*) By a derivative method, in which the variation, for instance of $F/\tilde{\omega}$ with $V/\sqrt{\theta}$, is established previously by test.

(*c*) By a derivative method, in which the variation, for instance of $F/\tilde{\omega}$ with $V/\sqrt{\theta}$, is assumed from firms' estimates.

The possibilities of establishing such methods are discussed.

Paper received June 1948
[The Aeronautical Quarterly, Vol. 1, May 1949]

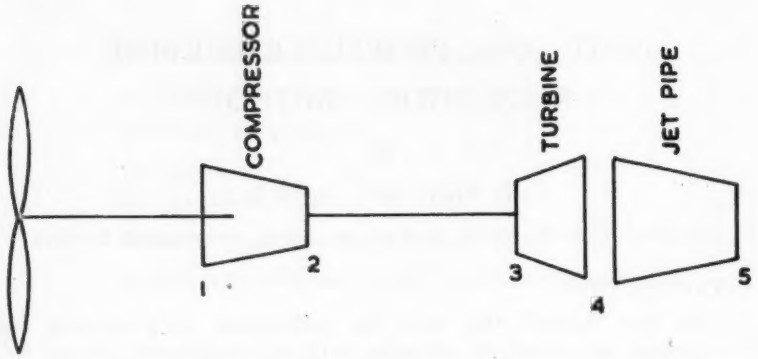

Fig. 1.
Single shaft engine.

2. NOTATION

Temperature and pressure symbols without suffix denote atmospheric conditions Other suffixes to temperature and pressure symbols refer to the positions indicated in Figs. 1 and 2.

B	$\dfrac{V/\sqrt{\theta}}{f_6}\dfrac{\partial f_6}{\partial (V/\sqrt{\theta})}$.
BHP	brake horsepower supplied to propellers (h.p.).
C	$\dfrac{\psi}{f_6}\dfrac{\partial f_6}{\partial \psi}$.
C_P	propeller power coefficient.
D	aircraft total drag (lb.).
E	$\dfrac{N/\sqrt{\theta}}{f_6}\dfrac{\partial f_6}{\partial (N/\sqrt{\theta})}$.
F	net jet thrust (lb.).
f_6	total propulsive thrust power (ft. lb./sec.).
G	$\dfrac{V/\sqrt{\theta}}{BHP/\tilde{\omega}\sqrt{\theta}}\dfrac{\partial (BHP/\tilde{\omega}\sqrt{\theta})}{\partial (V/\sqrt{\theta})}$.
H	$\dfrac{V/\sqrt{\theta}}{F/\tilde{\omega}}\dfrac{\partial (F/\tilde{\omega})}{\partial (V/\sqrt{\theta})}$.
J	propeller advance ratio.
K	$\dfrac{V/\sqrt{\theta}}{\eta}\dfrac{\partial \eta}{\partial (V/\sqrt{\theta})}$.
M	mass flow (lb./sec.).

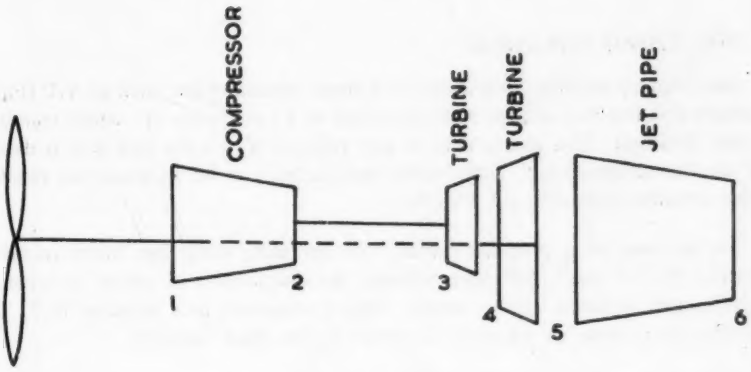

Fig. 2.
Free turbine engine.

N	engine speed (r.p.m.).	
N_C	compressor rotational speed (r.p.m.)	free turbine engines.
N_P	propeller shaft rotational speed (r.p.m.)	
p	air pressure (lb./in.^{2}).	
Q	fuel flow (lb./sec.).	
T	absolute temperature ($^\circ K$).	
THP	total thrust horsepower.	
V	forward speed (knots).	
V_i	equivalent air speed $= V\sqrt{\sigma}$ (knots).	
$V_{i_{md}}$	equivalent air speed for minimum drag (knots).	
W	aircraft weight (lb.).	
Z	$\frac{V_i}{D}\frac{\partial D}{\partial V_i} = 2\frac{\lambda_v^4 - 1}{\lambda_v^4 + 1}$ (as in Ref. 1).	
$\Delta'(W/\tilde{\omega})$	*correction* to $W/\tilde{\omega} = (W/\tilde{\omega})_s - (W/\tilde{\omega})_s$	and similarly for
$\Delta(W/\tilde{\omega})$	$(W/\tilde{\omega})_s - (W/\tilde{\omega})_s$	ΔV, $\Delta' V$ etc.
η	propeller efficiency.	
θ	relative temperature $= T/288$.	
λ_v	$V_i/V_{i_{md}}$.	
$\tilde{\omega}$	relative pressure $= p/14.7$.	
σ	relative density.	
ψ	the "third variable" (*see* Section 3).	

3. THE THIRD VARIABLE

An ordinary turbo-jet unit works on a single operating line such as AA' (Fig. 3). (Actually this line fans out for different values of $V/\sqrt{\theta}$ below A', where conditions are not choking.) This means that for any value of $N/\sqrt{\theta}$ the fuel flow is defined, and the "non-dimensional" performance parameters can be expressed as functions of two variables only, $(N/\sqrt{\theta}, V/\sqrt{\theta})$.

In the case of a propeller-turbine the operating point can move round the "constant $N/\sqrt{\theta}$ line" (BB' say), because the distribution of power between the propeller and jet thrust can be varied. This corresponds to a variation in T_3/T or propeller pitch angle, or whatever is chosen as the third variable.

Broadly speaking, propeller-turbines can be divided into two classes, "single shaft" engines with the propeller geared to the compressor-turbine shaft, and free turbine engines in which a separate power turbine drives the propeller. S. J. Moyes of The National Gas Turbine Establishment, in an unpublished note has shown that, for constant exit area, in the first case,

$F/\tilde{\omega}$, $BHP/(\tilde{\omega}\sqrt{\theta})$ and $Q/(\tilde{\omega}\sqrt{\theta})$ are all functions of $N/\sqrt{\theta}$, $V/\sqrt{\theta}$ and T_3/T

and in the second case

$F/\tilde{\omega}$, $BHP/(\tilde{\omega}\sqrt{\theta})$ and $Q/(\tilde{\omega}\sqrt{\theta})$ are all functions of $N_C/\sqrt{\theta}$, $V/\sqrt{\theta}$ and $N_P/\sqrt{\theta}$.

In either case the third variable could equally well be pitch angle or T_4/T, but it should be noted that in the second case (free-turbines), $N_P/\sqrt{\theta}$ has replaced T_3/T because it is possible to have a variation in $N_P/\sqrt{\theta}$ at constant $N_C/\sqrt{\theta}$ and T_3/T.

It has been found that firms prefer to use jet pipe temperature T_4 instead of turbine inlet temperature T_3 in the third variable, because it is easier to measure.

If the exit area is not fixed, a fourth variable is introduced, unless the area can be expressed as a *dimensionally correct* function of the existing variables. For example, it might be arranged that the exit area was a function of Mach number (*i.e.* of $V/\sqrt{\theta}$). The case of a fourth independent variable will not be considered here, as it does not occur among current engines.

In some cases the three fundamental variables may be reduced to two by a suitable control arrangement which must be *dimensionally correct*. For example, in the case of a single shaft engine if T_3/T or pitch angle is related to $N/\sqrt{\theta}$ and $V/\sqrt{\theta}$, there are only two independent variables, but if, say T_3 is kept constant, there will still be three variables. Again, in the case of the Bristol Theseus, N_C/N_P is kept constant (but not by a direct gearing), so there are only two independent

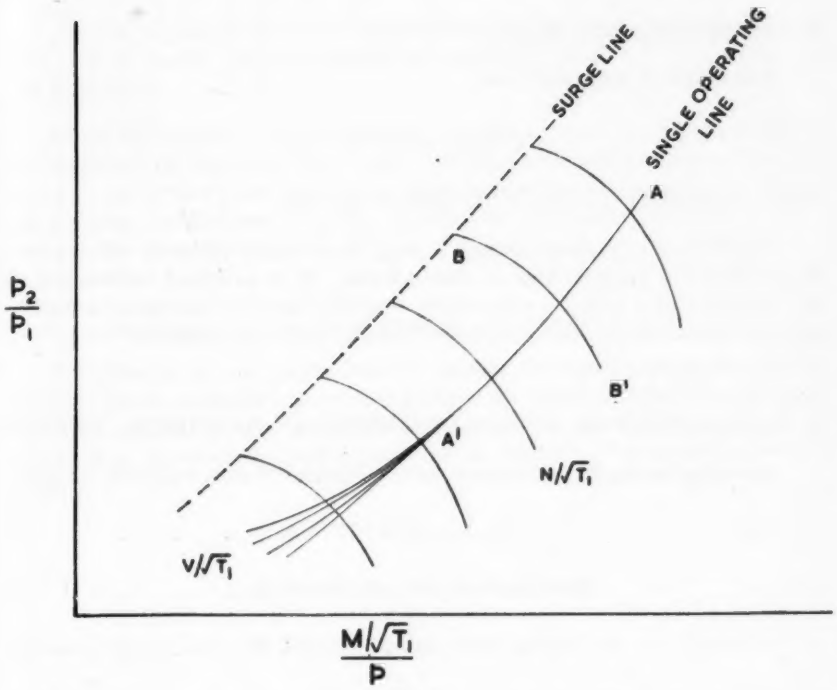

Fig. 3.
Compressor characteristics.

variables (for constant exit area). For a free turbine engine, a simplification arises for fuel consumption when the power turbine is choking. In this case

$$Q/(\tilde{\omega}\sqrt{\theta}) = f(N_C/\sqrt{\theta}, V/\sqrt{\theta})$$

irrespective of any relation between N_P and N_C.

The third variable might be eliminated under certain conditions—for instance the propeller pitch angle might be constant in the cruising range—but the possibility is remote.

4. OTHER VARIABLES

Combustion efficiency may vary with pressure; calorific value of the fuel may alter; and there may be viscosity effects on the engine performance. None of these variables is included in current turbo-jet reduction methods, but it has been suggested that viscosity effects may be important.

5. PROPELLER EFFICIENCY

It is shown in Appendix I that

$$\eta = f_4(N/\sqrt{\theta},\ V/\sqrt{\theta},\ \psi).$$

where ψ is the third variable, (T_3/T, T_4/T, or $N_P/\sqrt{\theta}$).

Therefore, if a graphical method is used, the propeller efficiency will not enter the problem as a separate item, as shown below. If an analytical method is used, the variations of η with the independent variables must be determined separately and will depend on the variations of $BHP/(\tilde{\omega}\sqrt{\theta})$ with these variables.

6. POSSIBILITIES OF A "NON-DIMENSIONAL" GRAPHICAL METHOD

Assuming the engine performance to be a function of three variables, we have:

$$F/\tilde{\omega} = f_1(N/\sqrt{\theta},\ V/\sqrt{\theta},\ \psi) \quad . \quad . \quad . \quad . \quad (1)$$

$$BHP/(\tilde{\omega}\sqrt{\theta}) = f_2(N/\sqrt{\theta},\ V/\sqrt{\theta},\ \psi) \quad . \quad . \quad . \quad . \quad (2)$$

$$Q/(\tilde{\omega}\sqrt{\theta}) = f_3(N/\sqrt{\theta},\ V/\sqrt{\theta},\ \psi) \quad . \quad . \quad . \quad . \quad (3)$$

(where ψ is the "third variable"), and it is possible to use a graphical method, although owing to the presence of the third variable, the flight test programme required is considerable.

For example for level speed: —

$$THP = DV/326$$

$$\frac{THP}{\tilde{\omega}\sqrt{\theta}} = \frac{DV}{326} \times \frac{1}{(\tilde{\omega}\sqrt{\theta})}$$

i.e.

$$\frac{BHP}{\tilde{\omega}\sqrt{\theta}} \times \eta + \frac{FV}{326} \times \frac{1}{\tilde{\omega}\sqrt{\theta}} = \frac{DV}{326} \times \frac{1}{\tilde{\omega}\sqrt{\theta}}$$

or

$$326\, f_4 \times f_2 + (V/\sqrt{\theta})\, f_1 = f_5(V/\sqrt{\theta},\ W/\tilde{\omega}) \times (V/\sqrt{\theta}) \quad . \quad . \quad . \quad (4)$$

since $D/\tilde{\omega} = f_5(V/\sqrt{\theta},\ W/\tilde{\omega})$ as for turbo-jets. Therefore in level flight

$$V/\sqrt{\theta} = f_6(N/\sqrt{\theta},\ \psi,\ W/\tilde{\omega}).$$

Therefore if curves of $V/\sqrt{\theta}$ against $N/\sqrt{\theta}$ are plotted for several values of $W/\tilde{\omega}$ and ψ under ambient conditions, standard values of $V/\sqrt{\theta}$ can be read from them.

Climb (assuming a relation between $V/\sqrt{\theta}$ and $W/\tilde{\omega}$ as for turbo-jets[2]) and range can be dealt with in a similar way and are functions of three variables, except in the special cases where the engine performance is a function of $V/\sqrt{\theta}$ and one other variable only, when the method is the same as for turbo-jets.

7. POSSIBILITIES OF AN ANALYTICAL METHOD

The difficulty here is that the relations between the engine performance and the variables are not established, and that in addition the variation of propeller efficiency must be included. Assuming that these relations can be established, there are several bases on which the performance can be reduced. For example, for level speed:—

$$THP = DV/326$$

$$326\ THP/(\tilde{\omega}\sqrt{\theta}) = (D/\tilde{\omega})(V/\sqrt{\theta})$$

and as in (4), the left hand side is a function of $(N/\sqrt{\theta}, V\sqrt{\theta}, \psi)$. Therefore

$$(V/\sqrt{\theta})(D/\tilde{\omega}) = f_6(N/\sqrt{\theta}, V\sqrt{\theta}, \psi) \quad . \quad . \quad . \quad (5)$$

where f_6 represents the total "non-dimensional" thrust horse power, *i.e.*

$$f_6 = 326\eta \frac{BHP}{\tilde{\omega}\sqrt{\theta}} + \frac{V}{\sqrt{\theta}} \cdot \frac{F}{\tilde{\omega}} \quad . \quad . \quad . \quad . \quad (6)$$

It is now assumed that

$$D = aV_i^2 + \frac{bW^2}{V_i^2}$$

and therefore, as shown in Appendix II

$$\frac{V/\sqrt{\theta}}{D/\tilde{\omega}} \cdot \frac{\partial(D/\tilde{\omega})}{\partial(V/\sqrt{\theta})} = Z$$

$$\frac{W/\tilde{\omega}}{D/\tilde{\omega}} \frac{\partial(D/\tilde{\omega})}{\partial(W/\tilde{\omega})} = 1 - \frac{Z}{2}$$

7.1. Differentiating equation (5) at constant $N/\sqrt{\theta}$

$$\left[D/\tilde{\omega}+(V/\sqrt{\theta})\frac{\partial(D/\tilde{\omega})}{\partial(V/\sqrt{\theta})}\right]d(V/\sqrt{\theta})+(V/\sqrt{\theta})\frac{\partial(D/\tilde{\omega})}{\partial(W/\tilde{\omega})}d(W/\tilde{\omega})$$

$$=\frac{\partial f_6}{\partial(V/\sqrt{\theta})}d(V/\sqrt{\theta})+\frac{\partial f_6}{\partial\psi}d\psi$$

$$\frac{D}{\tilde{\omega}}(1+Z)\,d(V/\sqrt{\theta})+(V/\sqrt{\theta})\left(\frac{D/\tilde{\omega}}{W/\tilde{\omega}}\right)\left(1-\frac{Z}{2}\right)d(W/\tilde{\omega})$$

$$=\frac{f_6}{V/\sqrt{\theta}}\,.\,B\,.\,d(V/\sqrt{\theta})+\frac{f_6}{\psi}\,.\,C\,.\,d\psi\,.$$

where $B=\dfrac{V/\sqrt{\theta}}{f_6}\cdot\dfrac{\partial f_6}{\partial(V/\sqrt{\theta})}$

$C=\dfrac{\psi}{f_6}\dfrac{\partial f_6}{\partial\psi}$

i.e. the percentage change in *thrust* horsepower for one per cent. change in $V/\sqrt{\theta}$ or in ψ.

Using the fact that $(V/\sqrt{\theta})\,(D/\tilde{\omega})=f_6$ and dividing through by f_6,

$$(1+Z)\frac{d(V/\sqrt{\theta})}{V/\sqrt{\theta}}+\left(1-\frac{Z}{2}\right)\frac{d(W/\tilde{\omega})}{W/\tilde{\omega}}=B\frac{d(V/\sqrt{\theta})}{V/\sqrt{\theta}}+C\frac{d\psi}{\psi}$$

Rearranging, and writing as a *correction*

$$\frac{\Delta'(V/\sqrt{\theta})}{V/\sqrt{\theta}}=\left[\left(1-\frac{Z}{2}\right)\frac{\Delta(W/\tilde{\omega})}{W/\tilde{\omega}}-C\frac{\Delta\psi}{\psi}\right]\Big/(1+Z-B)$$

Therefore it would be possible to correct the results at constant $N/\sqrt{\theta}$ which is the most convenient method for turbo-jets, but the difficulty arises in the determination of B and C. (It should be noted that reduction at constant $N/\sqrt{\theta}$ neglects change in drag due to Mach number.)

To find the form of B and C:—

Differentiating equation (6) partially with respect to $V/\sqrt{\theta}$

$$\frac{\partial f_6}{\partial(V/\sqrt{\theta})}=326\left(\frac{BHP}{\tilde{\omega}\sqrt{\theta}}\right)\frac{\partial\eta}{\partial(V/\sqrt{\theta})}+326\eta\frac{\partial\left(\frac{BHP}{\tilde{\omega}\sqrt{\theta}}\right)}{\partial(V/\sqrt{\theta})}+\frac{F}{\tilde{\omega}}+\left(\frac{V}{\sqrt{\theta}}\right)\frac{\partial(F/\tilde{\omega})}{\partial(V/\sqrt{\theta})}$$

$$B=\frac{V\sqrt{\theta}}{f_6}\frac{\partial f_6}{\partial(V/\sqrt{\theta})}=\frac{1}{f_5}\left[326\eta\frac{BHP}{\tilde{\omega}\sqrt{\theta}}\,.\,K+326\eta\frac{BHP}{\tilde{\omega}\sqrt{\theta}}\,.\,G+\frac{F}{\tilde{\omega}}\,.\,\frac{V}{\sqrt{\theta}}+\frac{F}{\tilde{\omega}}\,.\,H\,.\,\frac{V}{\sqrt{\theta}}\right]$$

where $K = \dfrac{V/\sqrt{\theta}}{\eta}\dfrac{\partial\eta}{\partial(V/\sqrt{\theta})}$

$G = \dfrac{V/\sqrt{\theta}}{BHP/\tilde{\omega}\sqrt{\theta}} \cdot \dfrac{\partial(BHP/\tilde{\omega}\sqrt{\theta})}{\partial(V/\sqrt{\theta})}$

$H = \dfrac{V/\sqrt{\theta}}{F/\tilde{\omega}}\dfrac{\partial(F/\tilde{\omega})}{\partial(V/\sqrt{\theta})}$

i.e. the percentage change in η, BHP or thrust ("non-dimensional") for one per cent. change in $V/\sqrt{\theta}$.

Simplifying,

$$B = K + G + (1 + H - G - K) \times (F/\tilde{\omega})(V/\sqrt{\theta})/f_e$$

C can be expressed in a similar way in terms of the variation of η, $BHP/(\tilde{\omega}\sqrt{\theta})$ and $(F/\tilde{\omega})$ with ψ.

7.2. *At constant* $V/\sqrt{\theta}$

$$\frac{\Delta'(W/\tilde{\omega})}{W/\tilde{\omega}} = \frac{E\dfrac{\Delta(N/\sqrt{\theta})}{N/\sqrt{\theta}} + C\dfrac{\Delta\psi}{\psi}}{Z/2 - 1}$$

$$\text{where } E = \frac{N/\sqrt{\theta}}{f_e}\frac{\partial f_e}{\partial(N/\sqrt{\theta})}$$

and is about as complicated as B.

The advantage here would be that change of drag due to Mach number is avoided in using constant $V/\sqrt{\theta}$.

7.3. *At constant temperature*

$$\frac{\Delta' V}{V} = \frac{1}{1 + Z - B}\left\{\left(1 - \frac{Z}{2}\right)\left(\frac{\Delta W}{W} - \frac{\Delta\tilde{\omega}}{\tilde{\omega}}\right) - C\frac{\Delta\psi}{\psi} - E\frac{\Delta N}{N}\right\}$$

A similar expression can be derived at constant pressure.

8. DATA REQUIRED TO USE AN ANALYTICAL METHOD

It is obvious from the foregoing that in order to apply an analytical method, it is necessary to know the percentage change in

$$\eta,\ BHP/(\tilde{\omega}\sqrt{\theta}),\ F/\tilde{\omega} \text{ and } Q/(\tilde{\omega}\sqrt{\theta})$$

due to one per cent. change in any two of the three variables.

$$N/\sqrt{\theta},\ V/\sqrt{\theta},\ \psi.$$

The change in η with the other variables could possibly be determined in a general way from available data on propellers, and it would probably be necessary to use different values for cruising, top speed and climb conditions.

The changes in the other parameters could be left for the individual operator to fit in the values applying to the particular aircraft-engine combination (*e.g.* $X = \frac{N/\sqrt{\theta}}{F} \frac{\partial F}{\partial (N/\sqrt{\theta})}$ for turbo-jets[1]). It would be more satisfactory if representative values could be determined either from flight tests, or from firms' estimates, but it seems unlikely that this is possible.

9. CONCLUSIONS

A graphical method of reduction is much simpler than an analytical method, provided enough flying can be carried out to cover three variables. In special cases where there are only two variables the graphical method is always easier.

An analytical method is feasible, but hampered by lack of generalised information on the variation of η, $BHP/(\tilde{\omega}\sqrt{\theta})$, $F/\tilde{\omega}$ and $Q/(\tilde{\omega}\sqrt{\theta})$ with the variables $N/\sqrt{\theta}$, $V/\sqrt{\theta}$, ψ. Reduction at constant $N/\sqrt{\theta}$ or constant $V/\sqrt{\theta}$ seems simpler than at constant temperature or pressure.

ACKNOWLEDGMENTS

The author would like to acknowledge advice and assistance from the National Gas Turbine Establishment and the Aircraft and Armament Experimental Establishment, and from Armstrong Siddeley Motors Ltd., the Bristol Aeroplane Co. Ltd., D. Napier and Son Ltd. and Rolls-Royce Ltd. and the Royal Aeronautical Society's Performance Panel.

APPENDIX 1

$$\eta = f(C_P, J, \text{Mach number}).$$

But C_P varies as $\frac{BHP}{\sigma N^3}$ for constant diameter

$$= \frac{BHP}{\tilde{\omega}\sqrt{\theta}} \cdot \frac{1}{(N/\sqrt{\theta})^3} \quad \text{since } \tilde{\omega} = \sigma\theta$$

J varies as $\frac{V/\sqrt{\theta}}{N/\sqrt{\theta}}$ for constant diameter

Mach number varies as $V/\sqrt{\theta}$

and therefore, since $\frac{BHP}{\tilde{\omega}\sqrt{\theta}} = f_2(N/\sqrt{\theta}, V/\sqrt{\theta}, \psi)$

$$\eta = f_4(N/\sqrt{\theta}, V/\sqrt{\theta}, \psi).$$

APPENDIX II

$D = aV_i^2 + \frac{bW^2}{V_i^2}$ where a, b are constants.

Therefore

$$\frac{D}{\tilde{\omega}} = a(V_i/\sqrt{\tilde{\omega}})^2 + b\frac{W^2}{\tilde{\omega}^2} \Big/ \left(\frac{V_i}{\sqrt{\tilde{\omega}}}\right)^2$$

$$= a(V/\sqrt{\theta})^2 + b\frac{W^2}{\tilde{\omega}^2} \Big/ (V/\sqrt{\theta})^2.$$

Differentiating partially with respect to $V/\sqrt{\theta}$

$$\frac{\partial(D/\tilde{\omega})}{\partial(V/\sqrt{\theta})} = 2aV/\sqrt{\theta} - 2b\frac{W^2}{\tilde{\omega}^2} \Big/ (V/\sqrt{\theta})^3$$

$$\frac{V/\sqrt{\theta}}{D/\tilde{\omega}} \frac{\partial(D/\tilde{\omega})}{\partial(V/\sqrt{\theta})} = \left\{2a(V/\sqrt{\theta})^2 - 2b\frac{W^2}{\tilde{\omega}^2}\Big/(V/\sqrt{\theta})^2\right\} \Big/ \left\{a(V/\sqrt{\theta})^2 + b\frac{W^2}{\tilde{\omega}^2}\Big/(V/\sqrt{\theta})^2\right\}$$

$$= 2\frac{aV_i^2 - bW^2/V_i^2}{aV_i^2 + bW^2/V_i^2}$$

$$= 2\frac{\lambda_v^4 - 1}{\lambda_v^4 + 1}$$

$$= Z$$

Differentiating partially with respect to $W/\tilde{\omega}$

$$\frac{\partial (D/\tilde{\omega})}{\partial (W/\tilde{\omega})} = 2b \frac{W}{\tilde{\omega}} \Big/ (V/\sqrt{\theta})^2$$

$$\frac{W/\tilde{\omega}}{D/\tilde{\omega}} \frac{\partial (D/\tilde{\omega})}{\partial (W/\tilde{\omega})} = \left\{ 2b \frac{W^2}{\tilde{\omega}^2} \Big/ (V/\sqrt{\theta})^2 \right\} \Big/ \left\{ a (V/\sqrt{\theta})^2 + b \frac{W^2}{\tilde{\omega}^2} \Big/ (V/\sqrt{\theta})^2 \right\}$$

$$= \frac{2bW^2/V_i^2}{aV_i^2 + bW^2/V_i^2}$$

$$= 1 - \frac{Z}{2}$$

REFERENCES

1. SMITH, F. (1943). Note on Various Methods of Performance Reduction for Jet-propelled Aircraft (and Addendum). R.A.E. Tech. Note No. Aero 1348 and 1348a, 1943.

2. ROYAL AERONAUTICAL SOCIETY Performance Data Sheets (in the press).

DETERMINATION OF DRAG OF JET-PROPELLED AIRCRAFT IN FLIGHT

by

G. W. TREVELYAN, M.A.,

and

D. R. BLUNDELL, Grad.R.Ae.S.

(*Aerodynamics Department, de Havilland Aircraft Co. Ltd.*)

1. INTRODUCTION

In order to obtain full knowledge of the performance of an aircraft, one of the important quantities to be determined is the drag. The usual procedure is to measure the level speed of the aeroplane and to calculate the drag under these conditions from the engine thrust, as obtained from the engine makers' specification. To do this, accurate thrust data are essential and in certain cases these may not be readily available.

In order to eliminate the possibility of systematic errors in the determination of engine thrust, a method has been developed whereby the drag at low Mach number can be measured directly under such conditions that accurate knowledge of the engine performance is of minor importance. This method is satisfactory only on jet-propelled aircraft, since on conventional aircraft there are the added complications of propellers, slipstream, radiators and so on.

The method has been used to determine the drag of the de Havilland D.H. 100 Vampire and has given good results. The drag determined from earlier tests by the usual procedure is found to be in good agreement with that given by the new method.

2. THE METHOD

The motion of an aeroplane in straight flight is defined by the following equation based on Newton's Second Law (*see* Notation):—

$$F = C_D Sq + \frac{k}{\pi} \cdot \frac{W^2}{b^2} \cdot \frac{1}{q} + W \sin\theta + \frac{W}{g} \cdot \frac{dV_E}{dt} \quad . \quad . \quad . \quad (1)$$

When the aircraft is flying with insufficient thrust for sustained steady level speed,

Paper received October 1948.

[The Aeronautical Quarterly, Vol. 1, May 1949]

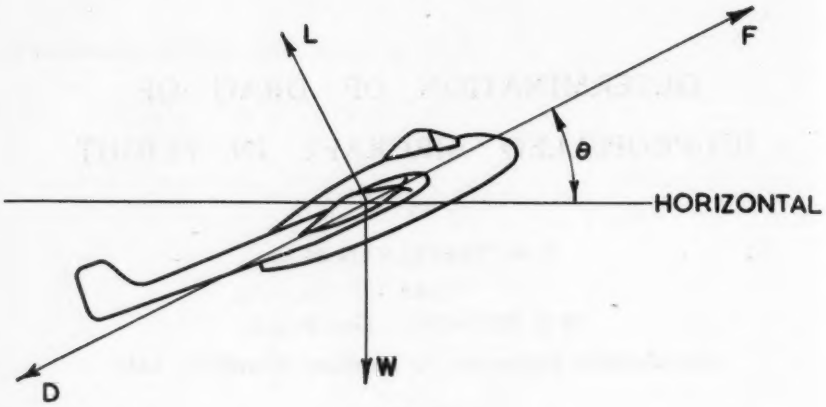

Fig. 1.
Force diagram.

straight flight can be maintained either by decelerating at constant height or by gliding (at constant or varying forward speed).

The method consists of either decelerating or gliding at minimum r.p.m. and determining the deceleration or angle of glide. By this procedure, the thrust term is a relatively unimportant factor in equation (1), and the drag deduced is not dependent on accurate knowledge of the engine performance.

In deceleration at constant height, $\sin\theta$ is zero, and the important quantity to be measured is the deceleration, $-dV_E/dt$. It is assumed that, over the distance covered, the wind velocity is constant, so that

$$\frac{dV_E}{dt} = \frac{dV_T}{dt} \quad . \quad . \quad . \quad . \quad . \quad . \quad . \quad (2)$$

Modifying equation (1) and including equation (2), the following expression is obtained for extra-to-induced drag at 100 ft./sec. at sea level: –

$$D_{100} = \frac{q_{100}}{q}\left(F - \frac{k}{\pi} \cdot \frac{W^2}{b^2} \cdot \frac{1}{q} - \frac{W}{g} \cdot \frac{dV_T}{dt}\right) \quad . \quad . \quad . \quad (3)$$

In a glide, on the other hand, the true speed is ideally kept constant, the deceleration therefore is zero, and $\sin\theta$, which is obtained from the rate of descent and forward speed, becomes the important quantity. In practice it is easier to maintain constant indicated speed, and consequently the analysis becomes more complicated. For this reason, and others to be discussed later, more emphasis has been placed on the deceleration method.

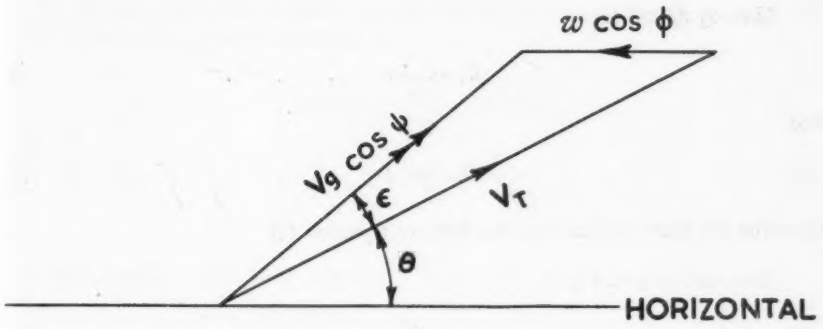

Fig. 2.
Triangle of velocities.

2.1. *Theory*

Figure 1 shows diagrammatically the external forces on an aeroplane in straight flight in a vertical plane. It is assumed that the thrust line is parallel to the relative air flow.

Figure 2 shows the corresponding triangle of velocities, taking into account the wind velocity.

The diagrams show the aeroplane in climbing attitude to facilitate the use of the usual sign convention.

The derivation of equation (1), showing the approximations made therein, is given below:—

Resolving parallel to the relative air flow, by Newton's Second Law,

$$F - D - W \sin\theta = \frac{W}{g} \cdot \frac{d}{dt}(V_g \cos\psi \cos\epsilon) \quad . \quad . \quad . \quad (4)$$

It is now assumed that the cosines of the angles θ, ψ and ϵ are unity: so

$$V_g = V_T - w\cos\phi \quad . \quad . \quad . \quad . \quad . \quad . \quad (5)$$

and

$$L = W = C_L S q \quad . \quad . \quad . \quad . \quad . \quad . \quad (6)$$

Using equation (6), the induced drag is then given by:—

$$D_i = \frac{k}{\pi} \cdot \frac{W^2}{b^2} \cdot \frac{1}{q} \quad . \quad . \quad . \quad . \quad (7)$$

Also, by definition,

$$D_t = C_D S q \quad . \quad . \quad . \quad . \quad . \quad . \quad . \quad (8)$$

and

$$D = D_t + D_i \quad . \quad . \quad . \quad . \quad . \quad . \quad . \quad (9)$$

Equation (4) then resolves into the form of equation (1).

Now, referring to Fig. 2,

$$\sin\theta = \frac{dh}{dt} \cdot \frac{1}{V_T} \quad . \quad . \quad . \quad . \quad . \quad . \quad . \quad (10)$$

The equation of calibration of the altimeter, based on hydrostatic laws, is as follows:—

$$\delta p = -\rho_0 g \sigma_s \delta h_1 \quad . \quad . \quad . \quad . \quad . \quad . \quad (11)$$

where δh_1 is the change in altimeter reading for a change of pressure, δp.

The change, δh, in true or "tape line" height for a change of pressure δp is, however, given by:—

$$\delta p = -\rho_0 g \sigma_a \delta h. \quad . \quad . \quad . \quad . \quad . \quad . \quad (12)$$

From equations (11) and (12),

$$\frac{dh}{dt} = \frac{\sigma_s}{\sigma_a} \cdot \frac{dh_1}{dt}$$

$$= \frac{\sigma_s}{\sigma_a} \cdot R_p$$

$$= \frac{T_a}{T_s} \cdot R_p \quad . \quad . \quad . \quad . \quad . \quad . \quad . \quad (13)$$

Substituting for dh/dt in equation (10),

$$\sin\theta = \frac{R_p}{V_T} \cdot \frac{T_a}{T_s} \quad . \quad . \quad . \quad . \quad . \quad . \quad . \quad (14)$$

In the decelerations, $\theta = \epsilon = 0$. This method therefore is potentially more accurate, since half the approximations of the generalised theory are eliminated.

If, for some reason or another, constant altitude is not maintained, a correction of the following form can be applied:—

$$\Delta D_{100} = -\frac{q_{100}}{q} \cdot W \sin\theta$$

$$= -\frac{q_{100}}{q} \cdot W \frac{R_p}{V_T} \cdot \frac{T_s}{T_a} \quad . \quad . \quad . \quad . \quad (15)$$

3. DESCRIPTION OF THE TESTS

Tests were made on a D.H.100 Vampire, fitted with a Goblin 2 engine. The aircraft was in standard service condition, except that the gun ports were faired over. No special cleaning or polishing was done.

The aircraft was fitted with an automatic observer containing altimeter, air speed indicator, ambient air thermometer, time base, engine r.p.m. indicator, jet-pipe total-head gauge and jet-pipe temperature gauge. These were photographed by a camera operated as required by the pilot from a button on the control column. Ambient air temperature was also obtained from the Meteorological Office, Dunstable, as confirmation of that from the electrical impact type thermometer transmitting to the automatic observer. Wind data were also obtained from the Meteorological Office.

As stated before, greater emphasis was placed on the level flight decelerations than on the glides because of the easier flight programme for the pilot, the simpler reduction and greater accuracy of the results and also, the wider speed range that could be covered.

For the decelerations, the aircraft was flown level at 10,000 ft. at approximately the Mach number at which the compressibility drag rise sets in. The throttle was closed rapidly, reducing the r.p.m. to the minimum, and the aircraft held in straight and level flight until the speed had dropped to 140-150 m.p.h. I.A.S., camera shots being taken at frequent intervals.

Allowance was made in the flight programme for the effect of position error on the altimeter, and the accuracy of the piloting was such that the true pressure altitude was maintained in each case within ± 80 ft. from a mean value.

The glides were made at minimum engine r.p.m. at constant I.A.S. from 10,000 ft. to 1,000 ft.

Four decelerations and two glides were done, the whole of the tests consisting of two flights of half an hour each.

Tests were also made on other aircraft with equally satisfactory results.

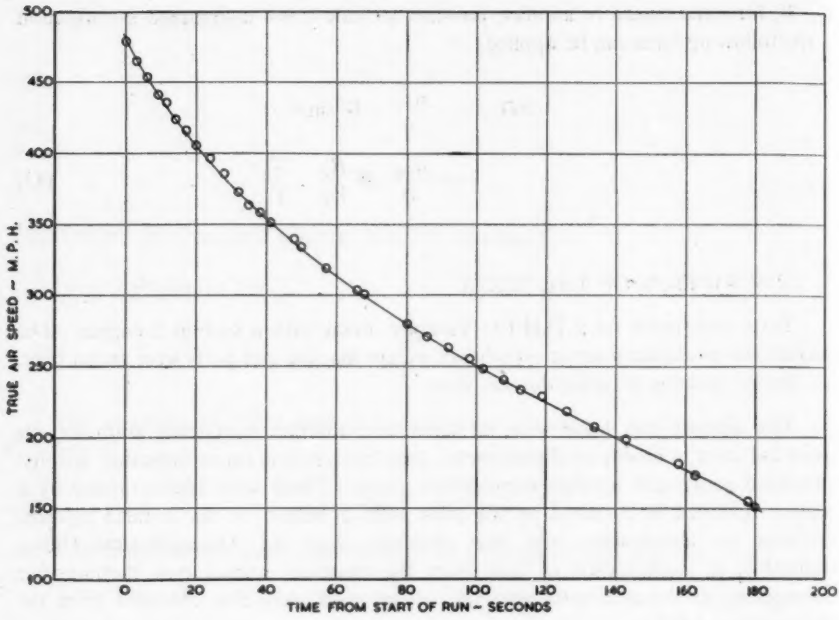

Fig. 3.
True air speed and time from deceleration No. 4.

4. ANALYSIS OF THE TEST RESULTS

The deceleration tests were analysed as follows:—

The weight at any time during the tests was determined by estimates of fuel used and flying time and was checked by fuel gauge readings and by the total fuel used during the flight.

From each shot of the automatic observer film records, the true air speed was determined, and these values were plotted against time throughout the test. Fig. 3 gives an example (Deceleration No. 4) of the True Air Speed—Time curve obtained, showing the mean line used in the analysis.

The deceleration, $-dV_T/dt$, and hence the inertia term, $-(W/g)(dV_T/dt)$, were obtained by graphical differentiation of this mean curve. Although graphical methods are not in general fully satisfactory, they do appear to be the best available for this purpose. Since the curve at the extreme beginning and end of the deceleration cannot be determined accurately, two or three shots at either end have been omitted in each case.

The net engine thrust (including intake drag) was obtained, as usual, by determination of engine mass flow and jet velocity from the readings of jet-pipe total head and temperature.

The induced drag, D_i, was evaluated on the assumption that the factor, k, was 1.15 (*see* equation (7) and Section 5).

Knowing these quantities, D_{100}, the extra-to-induced drag at 100 ft./sec. at sea level, was obtained from equation (3).

Table I shows the main figures of the calculation for three representative shots from the same test as Fig. 3 (Deceleration No. 4).

TABLE I

Time from start	t	*sec.*	17	68	143
True pressure altitude		ft.	10,060	10,040	10,000
Ambient air temperature		°C.	+7	+7	+7
True air speed		m.p.h.	416	300	198
Dynamic pressure	q	lb./sq. ft.	312	163	71
Weight	W	lb.	7,770	7,770	7,770
Deceleration	$-\frac{dV_T}{dt}$	ft./sec.^{2}	4.49	2.48	1.79
Inertia term	$-\frac{W}{g}\cdot\frac{dV_T}{dt}$	lb.	1,082	598	431
Thrust	F	lb.	46	35	31
Induced drag	$\frac{k}{\pi}\cdot\frac{W^2}{b^2}\cdot\frac{1}{q}$	lb.	44	85	195
Extra-to-induced drag	C_DSq	lb.	1,084	548	267
Extra-to-induced drag at 100 ft./sec. at sea level	D_{100}	lb.	41.4	40.0	44.8
Reynolds number ·	R		18.7×10^6	13.5×10^6	8.9×10^6

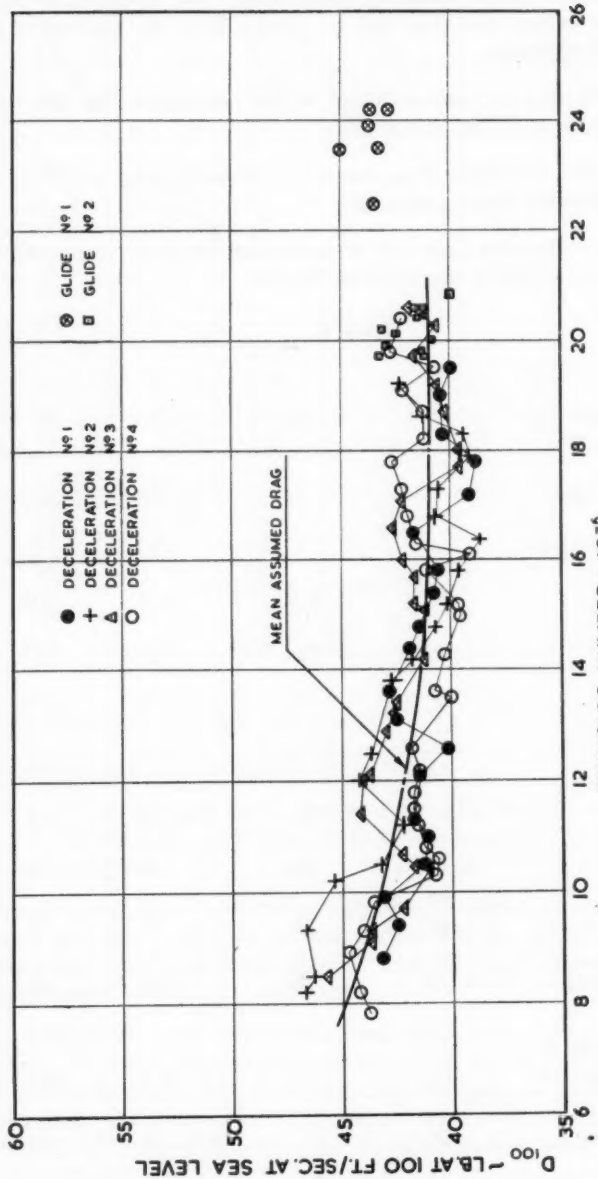

Fig. 4.
Extra-to-induced drag and Reynolds number.

The drag from the glides was obtained in substantially the same way, except that, in addition, graphical differentiation of the True Pressure Altitude—Time curve was necessary to give R_p and hence $W \sin \theta$ (*see* equation (14)). Also in order to take account of any variation of wind speed with height,

$$-\frac{d}{dt}(V_T - w \cos \phi)$$

was substituted for $-dV_T/dt$ in equation (3).

The values of D_{100} deduced from all the decelerations and glides are plotted against Reynolds number in Fig. 4.

Below a Reynolds number of about 16×10^6, D_{100} shows the expected behaviour, increasing with decreasing R. Previous tests on the Vampire (*see* Section 6) have indicated that D_{100} remains sensibly constant over a wide Reynolds number range from 12×10^6 to 27×10^6. From these deceleration tests, the value of this constant drag is about 41 lb.

It would appear, therefore, that the glides (particularly Glide No. 1 at $R = 24 \times 10^6$) do not give as satisfactory results as the decelerations, and the latter method is therefore recommended as the better and more accurate.

5. ACCURACY OF THE METHOD

The aim of this method is the determination of the drag (at low Mach number) directly from flight tests under conditions when any systematic errors in engine performance have only a small effect on the result.

It will be seen from Table I that this aim has been achieved, since an error of ± 10 per cent. in the thrust causes not more than about $\pm$ one per cent. alteration to the drag. With the usual procedure of level speed tests, this error in the thrust would cause slightly more than 10 per cent. change in the drag.

The deceleration, $-dV_T/dt$, as determined by graphical differentiation, is considered to be accurate within ± 5 per cent. A test was made using a sensitive accelerometer (by the method developed at the Royal Aircraft Establishment for high Mach number dives), but it was found that, due to the large change of incidence during the run, the corrections for the attitude of the instrument were excessive and the results unsatisfactory.

Allowance cannot be made in this analysis for the effect of horizontal and vertical air currents, since it is impracticable to collect all the requisite meteorological data. An up-current of 2 ft./sec. would cause a decrease in the deduced drag of about 2 per cent. at the highest speed and about 20 per cent. at the lowest. The

tests were, however, all done on calm, fine days, and each pair of decelerations was made over a different district, covering in each direction about 15 miles in about three minutes. By taking these precautions, it is thought that the effects of any gusts encountered were eliminated.

Examination of Fig. 4 shows a scatter of about ± 6 per cent. in the test points. However, if a statistical analysis is made of the results available from the decelerations (97 test points) taking into account all the random errors in deceleration, weight, speed and so on, it appears that the accuracy of the mean line is about ± 1.5 per cent. (95 per cent. probability).

Beyond these random errors, there may be a systematic error due to the use of an incorrect value of the induced drag factor, k. However, from analysis of these and other tests on the Vampire, the true value might be expected to lie within ± 5 per cent. of the assumed value, $k = 1.15$. This error would have negligible effect on the deduced drag at the higher Reynolds numbers, but would cause an alteration of about ∓ 4 per cent. at the lower speeds.

6. COMPARISON WITH OTHER TESTS

In level speed tests on a number of other Vampires, the thrusts in flight were determined from the readings of jet-pipe total head and temperature and, using these, the drag was deduced in the usual way. Over the Reynolds number range of these tests (11×10^6 to 28×10^6), it appeared that D_{100} for the Vampire was constant at about 42 lb., showing good agreement with the results from the decelerations.

Level speed tests were also made with and without transition wires at 4 per cent. chord on both surfaces. These tests showed that the wires caused a loss of speed of 23 m.p.h. at $R = 12 \times 10^6$, decreasing to five m.p.h. at $R = 27 \times 10^6$. This indicates that the effective transition point moved forward from about 20 per cent. chord at the lower Reynolds number to the leading edge at the higher. This change in the effective length of laminar flow is sufficient to explain the fact that D_{100} remains constant over this Reynolds number range.

7. CONCLUSIONS

The drag (at low Mach numbers) has been determined directly from flight tests under conditions when the engine thrust is an unimportant factor.

Results from a Vampire show, in the Reynolds number range from 21×10^6 to 16×10^6, that D_{100} is constant at about 41 lb. at 100 ft./sec. at sea level. Below this range the drag increases to about 45 lb. at $R = 8 \times 10^6$. Although there is some scatter in the test results, the accuracy of the mean curve is considered to be ± 1.5 per cent.

It appears that the deceleration method is better and more accurate than the glide method.

Tests have been made on other aircraft, with equally satisfactory results.

The drag obtained by this method is with small mass flow through the engine. With greater mass flow there may be differences in the external flow over the intakes, and allowances may have to be made in applying these results to conditions of high thrust.

ACKNOWLEDGMENTS

The authors would like to acknowledge the excellent flying technique of Mr. J. Cunningham and Mr. G. H. Pike, which contributed considerably to the success of the tests.

NOTATION

F	total propulsive thrust.
L	total lift.
W	instantaneous aircraft weight.
D	total aircraft drag, $=D_i+D_t$.
D_i	induced drag $=\frac{k}{\pi}\cdot\frac{W^2}{b^2}\cdot\frac{1}{q}$.
D_t	total extra-to-induced drag $=C_D Sq$.
D_{100}	extra-to-induced drag at 100 ft./sec. at sea level.
k	induced drag factor.
b	wing span.
S	gross wing area.
C_L	coefficient of lift, based on gross wing area.
C_D	coefficient of extra-to-induced drag, based on gross wing area.
θ	angle between relative air flow and horizontal (positive for climb).
ψ	angle of drift in horizontal plane (usual definition).
ϵ	angle of drift in vertical plane, as defined by Fig. 2.
ϕ	angle between wind direction and aircraft headings (=wind direction − true course).
V_g	velocity relative to ground.
V_T	true air speed.
V_i	equivalent air speed.

I.A.S.	indicated air speed.
w	horizontal wind speed.
h	true altitude.
h_1	pressure altitude.
$\frac{dh}{dt}$	true or "tape-line" rate of climb.
R_p	$\frac{dh_1}{dt}$ = rate of change of pressure altitude (positive for climb).
R	Reynolds number.
t	time.
q	dynamic pressure $= \frac{1}{2}\rho_0 V_1^2$ (suffix $_{100}$ refers to 100 ft./sec. at sea level).

Atmospheric quantities

ρ	atmospheric density.
σ	relative atmospheric density.
p	atmospheric pressure.
T	atmospheric absolute temperature.

Suffix $_0$ refers to sea level conditions.

Suffix $_a$ refers to ambient conditions at pressure altitude.

Suffix $_s$ refers to I.C.A.N. conditions at pressure altitude.

NOTES ON THE LINEAR THEORY OF INCOMPRESSIBLE FLOW ROUND SYMMETRICAL SWEPT-BACK WINGS AT ZERO LIFT

by

F. URSELL

(Department of Mathematics, The University, Manchester)

SUMMARY

In much of the recent work on the flow of an incompressible fluid past a swept-back symmetrical wing of small thickness at zero incidence it has been assumed that the disturbance introduced by the wing can be represented by means of a distribution of sources and sinks over the centre plane of the wing, the source strength being determined from the equation of the wing profile. It was found by Neumark[1] that on the wing itself this procedure was liable to lead to serious errors. Neumark and Küchemann[2] studied certain special types of wings for which they were able to find the correct value of the pressure at the surface by evaluation of the pressure at points off the wing and continuity considerations. This process is rather cumbersome; it may therefore be convenient to regard the problem from a rather different point of view.

In this paper a derivation is first given of the linearised equations of motion. Green's theorem on potential functions then leads at once from these equations to the method of sources, whereby the pressure is expressed as a surface integral extended over the wing. For points on the wing, the principal value in some sense of the surface integral must be taken. To this must be added a line integral depending on the definition of the principal value. When the swept-back wing consists of two equal cylindrical surfaces joined at an angle, an integral equation can be derived giving the pressure distribution along the centre section in terms of the profile, agreeing with that given by Neumark and Küchemann.

Paper received July 1948.

[The Aeronautical Quarterly, Vol. I, May 1949]

It is next shown that this equation can be solved explicitly[4] without making use of the numerical process devised by Küchemann. The solution is applied to the simple pressure distribution studied by the latter, and it is confirmed that the profile corresponding to this distribution crosses itself. A closer examination of the solution shows that this difficulty can be avoided, if the pressure distribution is slightly modified near the edges, where, on the linear theory here considered, it becomes infinite. (It is known that the linear theory is incorrect near the edges, so these infinities are not disturbing.)

When two cylindrical surfaces are joined at an angle to form a swept-back wing, the wing plan, consisting of straight lines, has a discontinuity in gradient near the nose. Suppose that the wing plan is slightly changed so as to have a small but finite radius of curvature at the nose, the section remaining unchanged. It is shown that the change in the pressure distribution along the centre section tends to zero as the radius of curvature decreases to zero, so that the discontinuity in the gradient of the wing plan has no pronounced effect on the pressure distribution.

It is next shown that it is not possible to design wings with kinked isobars in the centre, unless suction slots or similar devices are used. Finally, it is proved that there may be no wing or one wing with a given plan form and pressure distribution, but that there cannot be more than one.

1. DERIVATION OF LINEAR THEORY

Consider the flow past a wing possessing a central plane of symmetry, which is taken as the plane $y=0$ (Fig. 1); the plane $z=0$ is taken perpendicularly to $y=0$ through the chord of the centre section; the plane $x=0$ is taken bisecting the chord of the centre section, the nose being at $x=+1$.

Suppose that the wing is symmetrical about $z=0$ and at zero incidence to the stream. Then no trailing vortex sheets are formed in the fluid and a velocity potential Φ exists, such that the velocity vector grad Φ is continuous in any region excluding the wing.

Write

$$\Phi = -V_\infty x + \phi \quad . \quad . \quad . \quad . \quad . \quad . \quad (1)$$

where V_∞ is the velocity of the main stream; ϕ satisfies

$$\frac{\partial^2\phi}{\partial x^2} + \frac{\partial^2\phi}{\partial y^2} + \frac{\partial^2\phi}{\partial z^2} = 0, \quad . \quad . \quad . \quad . \quad . \quad (2)$$

and grad $\phi \to 0$ as the distance from the wing tends to infinity. . . . (3)

The whole motion is symmetrical about $z=0$; it is therefore sufficient to consider only the region $z \geqslant 0$ in this paper.

Take as the equation of the wing

$$z = \zeta(x, y) \geqslant 0; \quad . \quad . \quad . \quad . \quad . \quad . \quad (4)$$

The region of the plane $z=0$ where $\zeta(x, y)>0$ is called the wing plan A. Outside A, ϕ satisfies $\partial\phi/\partial z=0$ on $z=0$. There is no velocity component normal to the wing, *i.e.*

$$\left(V_\infty - \frac{\partial\phi}{\partial x}\right)\frac{\partial\zeta}{\partial x} - \frac{\partial\phi}{\partial y}\cdot\frac{\partial\zeta}{\partial y} + \frac{\partial\phi}{\partial z} = 0 \text{ when } z=\zeta(x, y)>0.$$

It is assumed that if $\zeta(x, y)$, is of the form $\epsilon Z(x, y)$, where ϵ is a small parameter, ϕ may be expanded in powers of ϵ. A linear theory is obtained by ignoring powers of ϵ higher than the first.

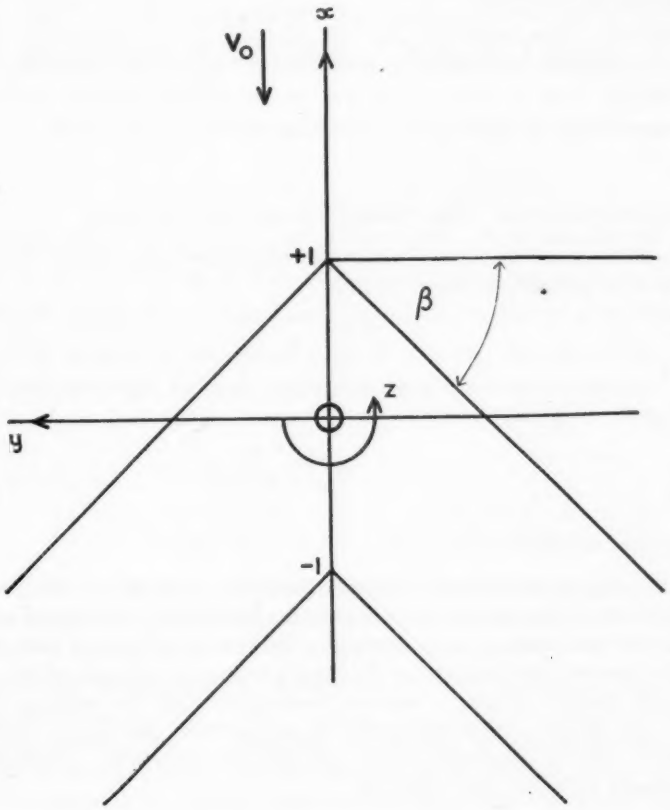

Fig. 1.
Co-ordinate system.

The linear potential satisfies

$$V_\circ \frac{\partial \zeta}{\partial x} + \frac{\partial \phi}{\partial z} = 0 \text{ when } z=0 \text{ and } (x, y) \text{ is on } A. \quad . \quad . \quad (5)$$

$\partial\phi/\partial z$ is thus prescribed on the whole plane $z=0$ when $\zeta(x, y)$ is given. Also ζ vanishes at the leading and trailing edges, whence

$$\int_{\text{T.E.}}^{\text{L.E.}} \frac{\partial \phi}{\partial z} dx = -V_\circ \int_{\text{T.E.}}^{\text{L.E.}} \frac{\partial \zeta}{\partial x} = 0 \text{ when } z=0 \text{ and } y \text{ has any constant value.} \quad (6)$$

The pressure on the wing is

$$\text{constant} - \tfrac{1}{2}\rho \mid \text{grad } \Phi \mid^2 = \text{constant} + \rho V_\circ \frac{\partial \phi}{\partial x} \text{ to the first order.} \quad . \quad (7)$$

The components of the vector grad ϕ will be denoted by (u, v, w).

2. CALCULATION OF THE PRESSURE ON THE PROFILE

The linear equations (1) to (7) form the basis of the linear theory. It has been seen that ϕ is symmetrical about $z=0$, *i.e.*

$$\frac{\partial \phi}{\partial z} = 0 \quad . \quad . \quad . \quad . \quad . \quad . \quad . \quad (8)$$

except on the wing plan A where

$$\frac{\partial \phi}{\partial z} = -V_\circ \frac{\partial \zeta}{\partial x} \quad . \quad . \quad . \quad . \quad . \quad (9)$$

and is a given function.

If the wing is finite, grad ϕ vanishes for large values of $x^2+y^2+z^2$, and the normal derivative is given on $z=0$. With these conditions ϕ is uniquely defined in $z>0$ as the potential due to a continuous distribution of sources over the wing plan; the pressure is proportional to the corresponding x-component of the velocity. The double integral defining ϕ becomes meaningless when z is put equal to zero, and near the plane $z=0$ the convergence is non-uniform. This was overlooked by Ludwieg[3], whose calculation was corrected by Neumark. Neumark used the continuity of $\partial\phi/\partial x$ with respect to z:

$$\left(\frac{\partial \phi}{\partial x}\right)_{x,\, y,\, 0.} = \lim_{z \to +0} \left(\frac{\partial \phi}{\partial x}\right)_{x,\, y,\, z} \quad . \quad . \quad . \quad . \quad (10)$$

The latter quantity is uniquely defined and can be evaluated for the class of cylindrical wings considered by Neumark.

It will now be shown from Green's formula that the definition of u as a double integral still holds on A, provided that a line integral depending on the definition of the surface integral is added.

2.1. *Application of Green's Theorem*

It is thus required to determine $u(X, Y)$ in terms of $w(X, Y)$ on the wing. Denote by $\mathbf{R}$ the position vector of $(X, Y, 0)$, and by $\mathbf{r}$ the position vector of (x, y, z). Let the point $P(X, Y)$ on the wing plan be enclosed in a small surface symmetrical about $z=0$, the upper half of which will be called S_P, and which intersects the plane $z=0$ along a closed curve C_P. Define a closed surface S consisting of S_P, the part of the plane $z=0$ outside C_P and a large hemisphere, centre $P(X, Y)$, in the upper half space $z>0$. If dS denotes an element of the surface area of S, then Green's theorem applied to the functions u and $|\mathbf{r}-\mathbf{R}|^{-1}$ harmonic and regular in S, gives

$$\iint_S \left[u \frac{\partial}{\partial n}\left(\frac{1}{|\mathbf{r}-\mathbf{R}|}\right) - \frac{1}{|\mathbf{r}-\mathbf{R}|}\frac{\partial u}{\partial n}\right] dS = 0,$$

$\frac{\partial}{\partial n}$ denoting differentiation along the normal to dS. (It is necessary to exclude the point $P(X, Y)$ from the domain of integration by means of S_P as $|\mathbf{r}-\mathbf{R}|^{-1}$ is not regular there.) The contribution to the surface integral from the large hemisphere tends to zero as the radius tends to infinity. By use of the relation $\frac{\partial u}{\partial z} = \frac{\partial w}{\partial x}$ and integration by parts, the surface integral is transformed into

$$\iint_{S_P}\left[u \frac{\partial}{\partial n}\left(\frac{1}{|\mathbf{r}-\mathbf{R}|}\right) - \frac{1}{|\mathbf{r}-\mathbf{R}|}\frac{\partial u}{\partial n}\right] dS - \\ - \iint \frac{w(x, y)(x-X)\,dxdy}{[(x-X)^2+(y-Y)^2]^{3/2}} + \oint_{C_P} \frac{w(x, y)\sin\theta\, dl}{[(x-X)^2+(y-Y)^2]^{1/2}} = 0 \quad . \qquad (11)$$

The second integral is taken over the part of the wing plan outside C_P; in the last integral θ is the angle between the x-axis and the tangent to C_P, dl is an element of arc of C_P, and the integration is in the positive direction round $P(X, Y)$.

The second integral may be evaluated on $Y=0$ by choosing as the curve C_P segments of the lines $x - X + |y| \tan\beta = \pm\epsilon$; $x - X - |y| \cot\beta = -2a \operatorname{cosec} 2\beta$, where a is a small number (Fig. 2). The surface S_P consists of sections of right circular cylinders. If $\epsilon \to 0$ and then $a \to 0$ the integral over S_P tends to $-2\pi u(X, 0)$, the integral over the wing to Ludwieg's value, and the line integral omitted by Ludwieg to

$$2w(X, 0)\cos\beta \log\frac{1+\sin\beta}{1-\sin\beta}.$$

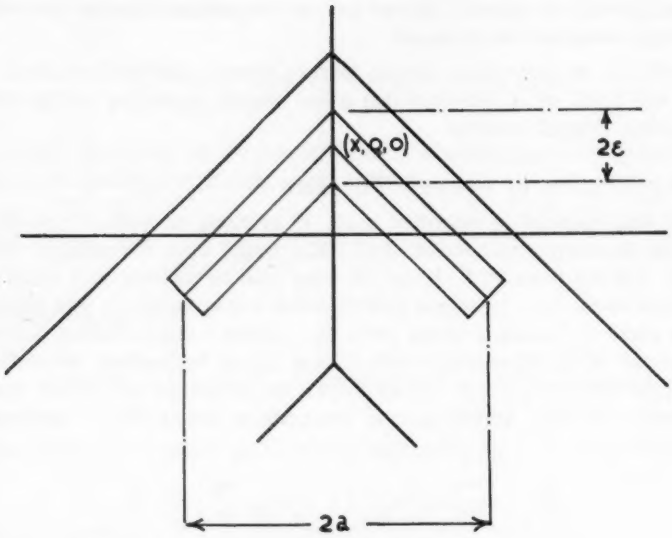

Fig. 2.
The operation P_L.

Hence

$$2\pi u(X, 0) = -P_L \iint \frac{w(x, y)(x-X)\,dxdy}{[(x-X)^2+y^2]^{3/2}} + 2w(X, 0)\cos\beta \log \frac{1+\sin\beta}{1-\sin\beta}. \quad (12)$$

Here P_L denotes the operation of evaluating the integral by Ludwieg's method, $\lim_{a\to 0} \lim_{\epsilon\to 0}$.

Alternatively the curve C_P may consist of segments of $x-X=\pm\epsilon$, $y=\pm a$ (Fig. 3). In the limit the line integral tends to zero, whence

$$2\pi u(X, 0) = -P_X \iint \frac{w(x, y)(x-X)\,dxdy}{[(x-X)^2+y^2]^{3/2}} \quad . \quad . \quad . \quad (12a)$$

where P_X denotes the operation $\lim_{a\to 0} \lim_{\epsilon\to 0}$.

For the sake of comparison, consider the case when (X, Y, Z) is not on the wing, $Z > 0$. Then P may be surrounded by a small sphere of radius ϵ. When $\epsilon\to 0$ Green's theorem gives in the limit

$$2\pi u(X, Y, Z) = -\iint \frac{w(x, y)(x-X)\,dxdy}{[(x-X)^2+(y-Y)^2+Z^2]^{3/2}}.$$

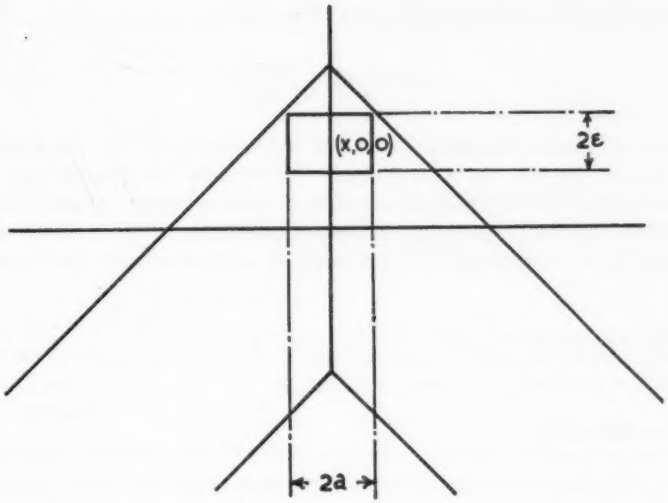

Fig. 3.
The operation P_x.

Comparison with (12*a*) shows that when the definition of the surface integral makes the line integral $\neq 0$, the convergence is non-uniform;

$$\lim_{Z\to 0} u(X, Y, Z) = u(X, Y, 0), \quad . \quad . \quad . \quad . \quad (13)$$

but

$$\lim_{Z\to 0} \iint \frac{w(x, y)(x-X)\,dxdy}{[(x-X)^2+(y-Y)^2+Z^2]^{3/2}} \neq P_L \iint \frac{w(x, y)(x-X)\,dxdy}{[(x-X)^2+(y-Y)^2]^{3/2}} . \quad (14)$$

3. KINKED DOUBLY-CYLINDRICAL WINGS

Ludwieg has considered the case

$$w(x, y) = w(x+|y|\tan\beta) \quad \text{for } -1 < x+|y|\tan\beta < 1$$
$$= 0 \text{ outside}$$

where β is the angle of sweepback. Here the operation P_L is appropriate for points on the centre line:

$$u(x) = -\frac{\cos\beta}{\pi} \int_{-1}^{1} \frac{w(\tau)\,d\tau}{\tau - x} + \cos\beta\, f(\beta)\, w(x), \quad -1 < x < 1 \quad . \quad (15)$$

where the integral is Cauchy's principal value and

$$f(\beta)=\frac{1}{\pi}\log\frac{1+\sin\beta}{1-\sin\beta}.$$

This relation is due to Neumark, IV.17, and Küchemann, eqn. 15. (In Küchemann's report the integral has the wrong sign.) Küchemann has pointed out that the equation may be used to obtain the function $w(x)$ from a given pressure distribution $u(x)$, and has indicated a numerical method of calculating w. However, the equation, considered as an integral equation for w has an explicit solution (*see* Appendix)

$$w(x)=\sec\beta\sin\pi\alpha\cos\pi\alpha\left[u(x)+\frac{\tan\pi\alpha}{\pi}(1-x)^{\alpha-1}(1+x)^{-\alpha}\int_{-1}^{1}\frac{(1+\tau)^{\alpha}(1-\tau)^{1-\alpha}u(\tau)\,d\tau}{\tau-x}\right] \quad . \quad . \quad . \quad . \quad . \quad (16)$$

where α is defined by

$$\cot\pi\alpha=f(\beta)>0, \quad 0<\alpha\leqslant\tfrac{1}{2}$$

and the condition (*see* equation (6))

$$\int_{-1}^{1}w(x)\,dx=0$$

has been used to ensure uniqueness.

The limiting case $\alpha=\frac{1}{2}$ corresponds to a wing with no sweepback, and $\alpha=0$ would correspond to the unrealisable case of a sweepback of 90 degrees. When $\alpha=\frac{1}{2}$, the integral equation (15) and its solution (16) reduce to the well-known equations of two-dimensional theory.

As an example of the use of (16) suppose that

$$u(x)=-\frac{4\delta}{\pi V_0}\cos\beta\left\{1+\frac{x}{2}\log\frac{1-x}{1+x}\right\} \quad . \quad . \quad . \quad (17)$$

which gives the pressure distribution at infinity on a wing whose equation is

$$\zeta(x,\,y)=\delta\,[1-(x+|\,y\,|\tan\beta)^2\,].$$

This is the example discussed by Küchemann in his paper. The integrals arising from the substitution of the value of $u(x)$ in the solution may be obtained by contour integration, whence

$$-V_\infty \frac{\partial \zeta}{\partial x} = w(x) = 2\delta V_\infty x - 2\delta V_\infty (1-x)^{\alpha-1}(1+x)^{-\alpha}\cos \pi\alpha\,(2\alpha - 2\alpha^2 - 2x\alpha + x - x^2).$$

Near $x = +1$

$$\frac{\partial \zeta}{\partial x} \sim -2^{2-\alpha}\delta (1-x)^{\alpha-1}\cos \pi\alpha \,.\, \alpha^2 < 0.$$

Near $x = -1$

$$\frac{\partial \zeta}{\partial x} \sim -2^{\alpha+1}\delta (1+x)^{-\alpha}\cos \pi\alpha \,.\, (1-\alpha)^2 < 0.$$

But $\dfrac{\partial \zeta}{\partial x} > 0$ at $x = -1$

is a necessary geometrical condition. Thus the wing contour obtained in this way crosses itself and has no physical reality. (The wing contour is shown crossing itself in Küchemann's Fig. 16.)

Küchemann suggests that the design of wings should proceed by successive approximation. The wing being supposed to have infinite aspect ratio, the pressure distribution at infinity is easily found from an assumed wing contour at infinity. The integral equation (15) is then used to find the equation of a wing surface of the form $z = \zeta(x, y) = \zeta(x + |y| \tan \beta)$ which will have the same pressure distribution along its centre line $y = z = 0$. If a wing is now designed having the given contour at infinity, the calculated contour at the centre section, and a smooth transition between them, it may be expected that the pressure distribution will be the same over every section. The foregoing example shows that this procedure may lead to meaningless results when $u(x)$ becomes logarithmically infinite at the edges of the wing.

Suppose now that $u(x) = \dfrac{4\delta}{\pi V_\infty} \cos \beta (1+x)^{-p}(1-x)^{-q}$, $1 > p > 0$, $1 > q > 0$.

It will be shown that p and q can be chosen in such a way that at infinity and at the centre section

$$\frac{\partial \zeta}{\partial x} > 0, \quad x = -1,$$

$$\frac{\partial \zeta}{\partial x} < 0, \quad x = +1,$$

i.e.

$$w(x) < 0, \quad x = -1,$$

$$w(x) > 0, \quad x = +1.$$

The value at infinity may be deduced from the solution of the integral equation for $\alpha = \frac{1}{2}$:

$$w(x) = \frac{\sec \beta}{\pi}(1-x^2)^{-\frac{1}{2}} \int_{-1}^{1} \frac{(1-\tau^2)^{\frac{1}{2}} u(\tau)\, d\tau}{\tau - x}$$

$$= \frac{4\delta}{\pi^2 V_0} \int_{-1}^{1} \frac{(1-\tau^2)^{\frac{1}{2}} (1+\tau)^{-p} (1-\tau)^{-q}}{\tau - x} \, d\tau.$$

If $p > \frac{1}{2}$, $q > \frac{1}{2}$, the asymptotic expressions for $w(x)$ near the wing edges are easily deduced from

$$\int_0^\infty \frac{x^{a-1}}{y-x} \, dx = \pi y^{a-1} \cot \pi a, \quad 0 < a < 1.$$

Near $x = -1$

$$w(x) \sim -\frac{4\delta}{\pi^2 V_0} 2^{-q} \pi \cot \pi (p - \tfrac{1}{2}) \, . \, (1+x)^{-p} < 0.$$

Near $x = +1$

$$w(x) \sim \frac{4\delta}{\pi^2 V_0} 2^{-p} \pi \cot \pi (q - \tfrac{1}{2}) \, . \, (1-x)^{-q} > 0.$$

The value on the centre line is

$$w(x) = \frac{4\delta}{\pi V_0} \sin \pi\alpha \cos \pi\alpha \left[(1+x)^{-p} (1-x)^{-q} + \right.$$
$$\left. + \frac{\tan \pi\alpha}{\pi} (1-x)^{\alpha-1} (1+x)^{-\alpha} \int_{-1}^{1} \frac{(1+\tau)^{\alpha-p} (1-\tau)^{1-\alpha-q} \, d\tau}{\tau - x} \right]$$

where it is now supposed that $q \geqslant 1 - \alpha > \frac{1}{2}$.

Asymptotic expressions are:

$$w(x) \sim \frac{4\delta}{\pi V_0} \sin \pi\alpha \cos \pi\alpha \, . \, 2^{-q} [(1+x)^{-p} - \tan \pi\alpha \cot \pi (p - \alpha) \, . \, (1+x)^{-p}] < 0$$

near $x = -1$ if $\cot \pi (p - \alpha) \tan \pi\alpha > 1$, *i.e.* $\alpha \leqslant p < 2\alpha$,

and

$$w(x) \sim \frac{4\delta}{\pi V_0} \sin \pi\alpha \cos \pi\alpha \, . \, 2^{-p} [(1-x)^{-q} + \tan \pi\alpha \cot \pi (\alpha + q - 1) \, . \, (1-x)^{-q}] > 0$$

near $x = +1$ if $\cot \pi (\alpha + q - 1) \tan \pi\alpha > -1$, *i.e.* $1 - \alpha \leqslant q < 2(1 - \alpha)$.

The inequalities are satisfied if

$$1 > q \geqslant 1 - \alpha, \quad 2\alpha > p > \tfrac{1}{2}. \qquad . \quad . \quad . \quad . \quad (18)$$

The last equation requires that $2\alpha > \frac{1}{2}$, $\beta < 66.5$ degrees. With these restrictions p and q must both be less than 1; $\partial\zeta/\partial x$ will then be integrable over $(-1, 1)$.

This example shows that under suitable conditions the behaviour of the profile near the edges is dominated by the behaviour of the pressure near the edges. Too much weight should not, therefore, be attached to the occurrence of profiles twisted near an edge as it is known from two-dimensional theory that the linear approximation is unsatisfactory there. In the above examples the pressure at the stagnation point will be finite and large, and not infinite as predicted by linear theory.

4. EFFECT OF A DISCONTINUITY IN $\partial\zeta/\partial y$ ALONG THE CENTRE LINE

The wing plans considered by Neumark and Küchemann have discontinuities in $\partial\zeta/\partial y$ across the centre line $y=z=0$. The effect of rounding off the discontinuity will be considered in this section. For the sake of simplicity each half of the wing is taken as cylindrical and of constant chord, its equation being

$$z=\zeta(x, y, l)=\zeta\left[x+|y|\tan\beta+l\,.\,g\left(\left|\frac{y}{l}\right|\right)\right] \quad . \quad . \quad . \quad (19)$$

where $g(1)=0$, $g'(1)=0$, $g'(0)=-\tan\beta$, $g(x)=0$ for $x>1$. l is a small parameter. $\partial\zeta/\partial y$ is now equal to zero along the centre line, except when $l=0$ (Fig. 4).

The difference between the velocities u of $\zeta(x, y, l)$ and $\zeta(x, y, 0)$ at a point on the centre line, taken to be the origin, is given by Δu, where

$$-2\pi\Delta u=\iint\left\{w\left[x+|y|\tan\beta+l\,.\,g\left(\left|\frac{y}{l}\right|\right)\right]-w\left[x+|y|\tan\beta\right]\right\}\frac{x\,dx\,dy}{(x^2+y^2)^{3/2}}$$

plus the limit of a line integral depending on the method of evaluation of the surface integral.

The integrand of the double integral vanishes except in $|y|<l$. Also, it is easy to see that the contribution from the region $|x|\geqslant a$ is $O(l^2)$.

Now by Taylor's theorem

$$w\left[x+|y|\tan\beta+l\,.\,g\left(\left|\frac{y}{l}\right|\right)\right]-w\left[x+|y|\tan\beta\right]$$

$$=l\,.\,g\left(\left|\frac{y}{l}\right|\right)\left[\frac{\partial w}{\partial x_0}+x\frac{\partial^2 w}{\partial x^2}\left\{|y|\tan\beta+\theta l\,.\,g\left(\left|\frac{y}{l}\right|\right)\right\}+O(x^2)\right],\quad 0<\theta<1,$$

whence the integral over $|x|<a$, $|y|<l$ is

$$4\int_0^l dy\int_0^a dx\,\frac{x^2 l\,.\,g(|y/l|)}{(x^2+y^2)^{3/2}}\,\frac{\partial^2 w}{\partial x^2}\left\{y\tan\beta+\theta l\,.\,g\left(\left|\frac{y}{l}\right|\right)\right\}+O(l^2)$$

$$\sim 4\,\frac{\partial^2 w}{\partial x_0^2}\int_0^l dy\int_0^a dx\,\frac{x^2 l\,.\,g(|y/l|)}{(x^2+y^2)^{3/2}}\,.$$

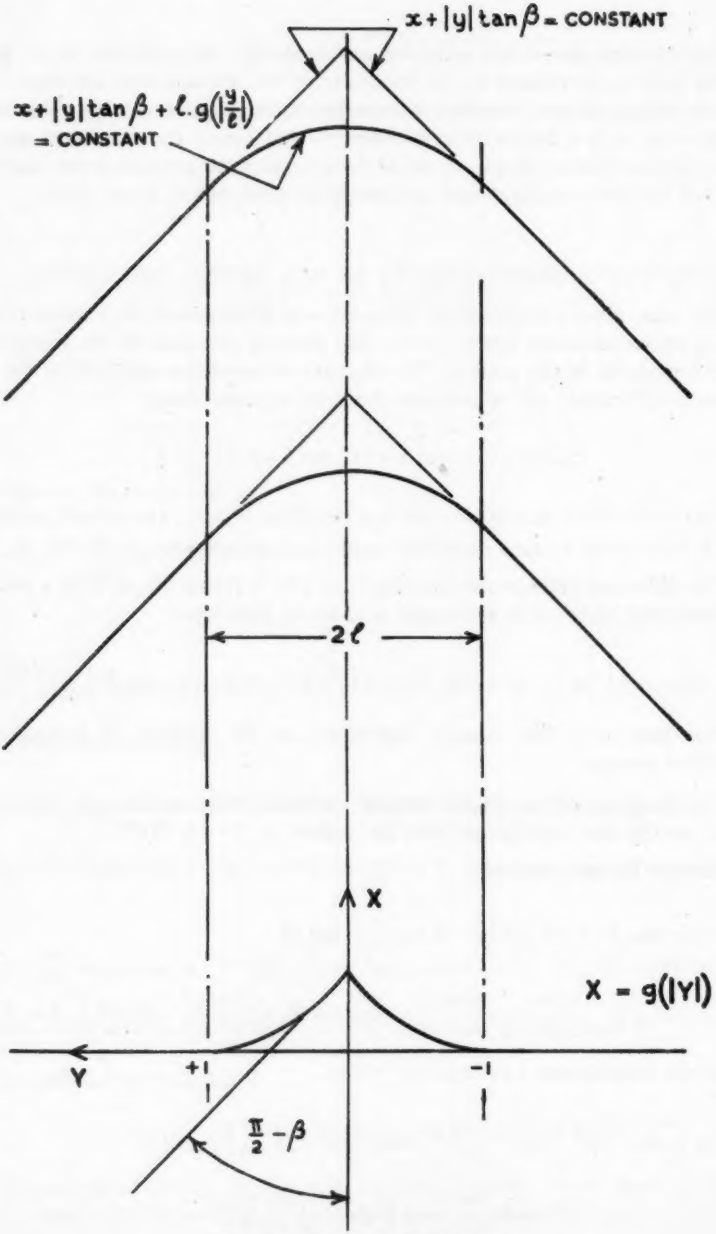

Fig. 4. Rounding off the nose.

In this last expression the integration with respect to x can be carried out explicitly. The corresponding line integral vanishes. Hence

$$-2\pi\Delta u = 4l^2 \frac{\partial^2 w}{\partial x_0^2} \int_0^1 dt\, g(t) \left[\log \frac{1}{l} + \log \frac{1}{t} + \log (a + \sqrt{a^2 + l^2 t^2}) - \frac{a}{\sqrt{(a^2 + l^2 t^2)}} \right]$$

$$\sim 4l^2 \frac{\partial^2 w}{\partial x_0^2} \log \frac{a}{l} \int_0^1 dt\, g(t) \longrightarrow 0 \quad . \quad . \quad . \quad (20)$$

as l tends to zero.

There is thus a smooth transition from a finite large curvature to a discontinuous gradient.

5. WINGS WITH KINKED ISOBARS

The computations of Neumark and Küchemann have shown that in the centre section the isobars are in general at right angles to the main stream. It may be asked whether it is possible to design a wing in such a way that the isobars are always inclined at an angle to the main stream and have a kink in the middle. It will be shown that unless the surface has a steep ridge over the centre section this is not possible without the introduction of special devices, such as suction slots.

Let Θ be the angle of sweepback of the isobars, Θ being a function of x not zero everywhere. Along each isobar $\partial\phi/\partial x$ is constant, so that by differentiation along the curve

$$\frac{\partial^2 \phi}{\partial x^2} + \frac{\partial^2 \phi}{\partial y \partial x} \frac{dy}{dx} = 0.$$

But $\dfrac{dy}{dx} = -\cot \Theta$, so

$$\frac{\partial^2 \phi}{\partial y \partial x} = \tan \Theta \frac{\partial^2 \phi}{\partial x^2}.$$

Hence, by integration in the x-direction,

$$\left(\frac{\partial \phi}{\partial y}\right)_{x=A} - \left(\frac{\partial \phi}{\partial y}\right)_{x=B} = \int_B^A \tan \Theta \frac{\partial^2 \phi}{\partial x^2} dx \quad . \quad . \quad . \quad (21)$$

$\partial^2\phi/\partial x^2$ has only a finite number of zeros. (A and B denote here the limits of integration.) Let A, B be chosen in such a way that $\partial^2\phi/\partial x^2 \neq 0$ and $\Theta(x) \neq 0$ in $B < x < A$. A and B may clearly be arbitrarily near each other.

Put $A-B=h$ and consider the potential function

$$\phi(x+h, y, z)-\phi(x, y, z)=\phi_1(x, y, z) \quad . \quad . \quad . \quad (22)$$

Then at $x=B$,

$$\frac{\partial\phi_1}{\partial y}=\int_B^A \tan\Theta\,\frac{\partial^2\phi}{\partial x^2}\,dx$$

is not zero; by continuity there is an interval including B where $\partial\phi_1/\partial y\neq 0$. It follows that there is a cross-flow component on the centre line. It must now be examined whether the existence of such a component is compatible with linear theory.

Take the point B as the origin and consider the component $v_1=\partial\phi_1/\partial y$ of the velocity. It must have a discontinuity across $y=0$, since $v_1(X, Y)$ is an odd function of Y. Now

$$2\pi v_1(0, Y)=-P_Y\iint\frac{w_1(x, y)(y-Y)\,dxdy}{[x^2+(y-Y)^2]^{3/2}} \quad . \quad . \quad . \quad (23)$$

where the operator P_Y implies that the first integration is with respect to x and the second with respect to y, and $w_1=\partial\phi_1/\partial z$. To determine the discontinuity in $v_1(0, Y)$ it is sufficient to take as the domain of integration the rectangle $|y|<\epsilon$, $|x|<\delta$, and to suppose that $0<|Y|<\epsilon$. The contribution from outside the rectangle is clearly a continuous function of Y. Choose δ, ϵ so small that in the rectangle

$$|w_1(x, y)-w_1(0, y)|<G(y)|x|,$$

where $G(y)$ is a bounded function of y.

Then

$$\left|2\pi v_1(0, Y)+\iint\frac{w_1(0, Y)(y-Y)\,dxdy}{[x^2+(y-Y)^2]^{3/2}}\right|<\iint\frac{|x|G(y)|y-Y|\,dxdy}{[x^2+(y-Y)^2]^{3/2}}$$

$$<2\int_{-\epsilon}^{\epsilon}G(y)\,dy$$

and

$$\iint\frac{w_1(0, y)(y-Y)\,dxdy}{[x^2+(y-Y)^2]^{3/2}}=2P\int_{-\epsilon}^{\epsilon}\frac{w_1(0, y)\,dy}{y-Y}-$$

$$-2\int_{-\epsilon}^{\epsilon}\frac{w_1(0, y)(y-Y)\,dy}{|y-Y|^2}\left[1-\frac{\delta}{\{\delta^2+(y-Y)^2\}^{\frac{1}{2}}}\right].$$

Hence

$$\left|2\pi v_1(0, Y)+2P\int_{-a}^{a}\frac{w_1(0, y)\,dy}{y-Y}\right|<2\int_{-a}^{a}G(y)\,dy+\frac{1}{\delta^2}\int_{-\epsilon}^{\epsilon}\left|w_1(0, y)\right|dy\,|y-Y|$$

$$<2\int_{-a}^{a}G(y)\,dy+\frac{2\epsilon}{\delta^2}\int_{-\epsilon}^{\epsilon}\left|w_1(0, y)\right|dy.$$

As Y passes through zero, $v_1(0, Y)$ has a discontinuity D_1, while the discontinuity D_2 in

$$P\int_{-a}^{a}\frac{w_1(0, y)\,dy}{y-Y}$$

is easily seen to be independent of ϵ. Thus

$$|2\pi D_1+2D_2|<4\int_{-a}^{a}G(y)\,dy+\frac{4\epsilon}{\delta^2}\int_{-\epsilon}^{\epsilon}|w_1(0, y)|\,dy \quad . \quad . \quad (24)$$

The left side of the inequality is independent of ϵ, while the right side can be made arbitrarily small by choice of ϵ. The left side is therefore zero, *i.e.* a discontinuity D_1 in v_1 implies a discontinuity $-\pi D_1$ in

$$P\int_{-a}^{a}\frac{w_1(0, y)\,dy}{y-Y}$$

and conversely.

It will now be shown that the latter integral is continuous at $Y=0$. $w_1(0, y)$ is an even function of y; the difference between the integrals at Y and $-Y$ is

$$4|Y|\int_0^a\frac{w_1(0, y)\,dy}{y^2-Y^2}.$$

It may be reasonably assumed that $w_1(0, Y)$ satisfies a condition

$$|w_1(0, y)-w_1(0, Y)|<M|y-Y|^{\lambda}, \quad y, Y>0, \quad 0<\lambda<1.$$

Then

$$4|Y|\left|\int_0^a\frac{w_1(0, y)\,dy}{y^2-Y^2}\right|<4|Y|\int_0^a\frac{M|y-Y|^{\lambda}dy}{|y^2-Y^2|}+$$

$$+2|w_1(0, Y)|\log\frac{a+|Y|}{a-|Y|}$$

but $|Y|\int_0^a\left|\frac{|y-Y|^{\lambda-1}}{y+Y}\right|dy<|Y|^{\lambda}\int_0^{\infty}\frac{|1-u|^{\lambda-1}}{1+u}\,du=O(1)$ as $Y\longrightarrow 0$

and $w_1(0, Y) \log \dfrac{a+Y}{a-Y}$ is clearly $O(1)$ since $w_1(0, Y)$ is bounded.

It follows that the integral

$$P\int_{-a}^{a} \frac{w_1(0, y)\, dy}{y-Y}$$

is continuous at $Y=0$, whence it follows that $v_1(0, Y)$ is also continuous. But it has been seen that there must be a discontinuity in v_1 if the isobars cross the centre line at an angle other than $\pi/2$. This contradiction shows that the isobars must cross the centre line at right angles.

6. UNIQUENESS

It has just been seen that to a prescribed wing plan A and a given distribution of u (*e.g.* one with kinked isobars) there does not always correspond a profile $\zeta(x, y)$. But it is easy to prove that there is either one profile or none.

Suppose that two profiles exist; let $\zeta(x, y)$ denote their difference and let ϕ denote the difference between the corresponding potentials.

Then

$$\int_{\text{T.E.}}^{\text{L.E.}} \frac{\partial \phi}{\partial z}\, dx = 0, \quad z=0, \; y \text{ constant} \qquad . \quad . \quad . \quad (25)$$

$$\frac{\partial \phi}{\partial x} = 0 \text{ on } A \qquad . \quad . \quad . \quad . \quad . \quad (26)$$

ϕ is continuous across the edge of the wing, and $|\operatorname{grad} \phi| = O(R^{-\mu})$, $0 < \mu < 1$, where R denotes the distance from the edge. For the sake of simplicity it is assumed that A is finite.

Let S be the closed surface consisting of a large hemisphere in the upper half-plane and the plane $z=0$; the edges of the wing are excluded by small surfaces. By one of Green's formulæ

$$\iiint |\operatorname{grad} \phi|^2 d\tau = -\iint \phi \frac{\partial \phi}{\partial n}\, dS \qquad . \quad . \quad . \quad . \quad (27)$$

where the volume integral is taken through the interior of S, and $\dfrac{\partial}{\partial n}$ denotes differentiation into S. It is easy to see that the contribution to the surface integral from the large hemisphere tends to zero as its radius tends to infinity, since

$\partial\phi/\partial r = O(r^{-3})$. The contribution from the small surfaces used to exclude the edges also tends to zero as the surface area tends to zero. In the limit, therefore,

$$\iiint_{z>0} |\operatorname{grad}\phi|^2 d\tau = -\iint_A \phi \frac{\partial\phi}{\partial z}\, dxdy. \qquad (28)$$

But on A, $\frac{\partial\phi}{\partial x} = 0$, so $\phi = F(y)$, and also $\int \frac{\partial\phi}{\partial z}\, dx = 0$, whence

$$\iiint |\operatorname{grad}\phi|^2 d\tau = 0. \qquad (29)$$

This implies

$$\operatorname{grad}\phi \equiv 0, \qquad (30)$$

and the result follows.

APPENDIX

An Integral Equation

The equation connecting the velocity components $u(x)$ and $w(x)$ on the centre line is of the form

$$g(x) - \frac{\tan \pi\alpha}{\pi} \int_{-1}^{1} \frac{g(u)\, du}{u - x} = f(x), \quad -1 < x < 1, \qquad (31)$$

where $\int_{-1}^{1} g(x)\, dx = 0$.

This equation may be treated by the methods of the theory of functions of a complex variable, as was first done by Carleman.[4]

$$G(z) = \int_{-1}^{1} \frac{g(u)\, du}{u - z}$$

defines an analytic function one-valued in the plane cut from -1 to $+1$.

$$\left.\begin{aligned} G(x \pm 0i) &= P\int_{-1}^{1} \frac{g(u)\, du}{u - x} \pm i\pi g(x) \quad , |x| < 1, \\ &= \int_{-1}^{1} \frac{g(u)\, du}{u - x} \qquad\qquad\quad , |x| > 1, \end{aligned}\right\}$$

At infinity

$$|G(z)| = O(|z|^{-2}), \text{ since } \int_{-1}^{1} g(u)\, du = 0.$$

It is convenient to consider the function

$$H(z)=(z+1)^{\alpha}(z-1)^{1-\alpha}G(z)$$

on the real axis $y=+0$.

When $|x|>1$, $H(z)$ is clearly real, *i.e.* $\mathscr{I}H(z)=0$.

When $|x|<1$, $H(z)=-(1+x)^{\alpha}(1-x)^{1-\alpha}(\cos\pi\alpha-i\sin\pi\alpha)\left(\int_{-1}^{1}\frac{g(u)\,du}{u-x}+i\pi g(x)\right)$

of which the imaginary part is

$$(1+x)^{\alpha}(1-x)^{1-\alpha}\left[\sin\pi\alpha\int_{-1}^{1}\frac{g(u)\,du}{u-x}-\pi\cos\pi\alpha\,g(x)\right]$$
$$=-\pi\cos\pi\alpha\,(1+x)^{\alpha}(1-x)^{1-\alpha}f(x)$$

from the integral equation. The imaginary part of $H(z)$ is therefore given everywhere on the real axis, and

$$|H(z)|=O(|z|^{-1})$$

at infinity.

$H(z)$ is then given everywhere in the upper half-plane by Poisson's integral

$$H(z)=\frac{1}{\pi}\int_{-1}^{1}\frac{\mathscr{I}H(u)\,du}{u-z}\,.$$

In particular, on the real axis

$$\mathscr{R}H(z)=\frac{1}{\pi}P\int_{-1}^{1}\frac{\mathscr{I}H(u)\,du}{u-x}\,.$$
$$=-\cos\pi\alpha\int_{-1}^{1}\frac{(1+u)^{\alpha}(1-u)^{1-\alpha}f(u)\,du}{u-x}$$

But $G(z)=(1-z)^{\alpha-1}(1+z)^{-\alpha}H(z)$

$$=-(1-x)^{\alpha-1}(1+x)^{-\alpha}(\cos\pi\alpha+i\sin\pi\alpha)(\mathscr{R}H(z)+i\,\mathscr{I}H(z))$$

of which the imaginary part is $\pi\,g(x)$, *i.e.*

$$g(x)=\cos^2\pi\alpha\left[f(x)+\frac{\tan\pi\alpha}{\pi}(1-x)^{\alpha-1}(1+x)^{-\alpha}\int_{-1}^{1}\frac{(1+u)^{\alpha}(1-u)^{1-\alpha}\,f(u)\,du}{u-x}\right]$$

Uniqueness

From the construction it is clear that the formula gives one solution. To show that it is the only one the following assumption is sufficient:

The integrable solution $g(x)$ has a differential coefficient in the open interval satisfying

$$g'(x)=o\left(\frac{1}{(1-x^2)^2}\right), \quad x^2\longrightarrow 1.$$

This is satisfied for all functions $f(x)$ occurring in practice. It follows immediately that

$$g(x)=o\left(\frac{1}{(1-x^2)}\right), \quad x^2\longrightarrow 1.$$

Lemma

$$G(z)=O\left[\frac{\log(1-z^2)}{(1-z^2)^2}\right] \text{ near } z=\pm 1$$

It is sufficient to consider the neighbourhood of $z=1$.

$$(1-z)^2 G(z)=\int_{-1}^{1}\frac{(1-u+u-z)^2 g(u)\,du}{u-z}$$
$$=\int_{-1}^{1}\frac{(1-u)^2 g(u)\,du}{u-z}+O(1)$$

Write $g_1(x)=(1-x)^2 g(x) \qquad |x|<1,$
$=0 \qquad |x|>1.$

$g_1(x)$ has by hypothesis a continuous differential coefficient near $x=1$. Let $Z=X+iY$ be any point in the neighbourhood of unity.

$$(1-Z)^2 G(Z)=\int_{-1}^{1}\frac{g_1(u)\,du}{u-Z}+O(1)$$
$$=\int_{-1}^{1}\frac{g_1(u)-g_1(X)}{u-X}\,du\,\frac{u-X}{u-Z}+$$
$$+g_1(X)\int_{-1}^{1}\frac{du}{u-Z}+O(1).$$

$$|(1-Z)^2 G(Z)|<\int_{-1}^{1}\left|\frac{g_1(u)-g_1(X)}{u-X}\right|\left|\frac{u-X}{u-Z}\right|du+|g_1(X)|\,|\log(1-Z)|+O(1).$$

The integrand is bounded and $|g_1(X)|<M$, so

$$(1-Z)^2 G(Z)=O\{\log(1-Z)\}$$

which proves the lemma.

Suppose now that $g(x)$ is the difference between two solutions of the integral equation, so that

$$g(x)=\frac{\tan \pi\alpha}{\pi}\int_{-1}^{1}\frac{g(u)\,du}{u-x}$$

and $g(x)$ is integrable and $O\left(\frac{1}{(1-x^2)^{\frac{1}{2}}}\right)$

Consider the function

$$H(x)=(z+1)^{\alpha}(z-1)^{1-\alpha}G(z).$$

The imaginary part of $H(z)$ vanishes everywhere on the real axis. Define $H(z)=\overline{H(\bar{z})}$ in the lower half-plane. By Schwarz's reflection principle, $H(z)$ is an analytic function defined in the whole plane, whose only singularities are poles or isolated essential singularities at ± 1.

But at $Z=1$

$$H(z)=O\{(z-1)^{-\alpha-1}\log(1-z)\},\ 0<\alpha<1,$$

so the singularity at $z=1$ is a pole of order unity at most and

$$H(z)=\frac{a}{z-1}+\text{a regular function.}$$

Here a is real since $H(z)$ is real on the real axis. Now as z tends to $1+0$ along the real axis,

$$\left|(x-1)\int_{-1}^{1}\frac{g(u)\,du}{u-z}\right|<\int_{-1}^{1}|g(u)|\,du$$

and is bounded, *i.e.* $|(z-1)^{\alpha}H(z)|$ is bounded along this path. Hence a is zero; $H(z)$ is regular at $+1$; similarly it is regular at -1, and therefore in the whole plane. Also at infinity $H(z)=O(|z|^{-1})$. By Liouville's theorem $H(z)$ is therefore zero in the whole plane. Hence $g(x)\equiv 0$ on the real axis, and the solution of the integral equation is unique.

If the condition $\int_{-1}^{1}g(u)\,du=0$ is dropped, the argument shows that

$$g(x)=\frac{\tan \pi\alpha}{\pi}\int_{-1}^{1}\frac{g(u)\,du}{u-x}$$

has the unique eigenfunction $(1+x)^{-\alpha}(1-x)^{\alpha-1}$. As α goes from 0 to 1, $(\tan \pi\alpha)/\pi$ takes all values from $-\infty$ to $+\infty$. Thus the integral equation has a continuous spectrum consisting of all points on the real axis except 0, for which value the equation becomes trivial.

Addendum

For reference some functions occurring in the calculation are given here:

$$-\frac{\sin \pi\alpha}{\pi}\int_{-1}^{1}\frac{(1+u)^{\alpha}(1-u)^{1-\alpha}u^{n}du}{u-x}-\cos\pi\alpha\,(1+x)^{\alpha}(1-x)^{1-\alpha}x^{n}$$

$$=x-1+2\alpha \qquad n=0$$

$$=x^{2}-x+2\alpha\,(x-1)+2\alpha^{2} \qquad n=1$$

$$=x^{3}-x^{2}+2\alpha\,(x^{2}-x)+2\alpha^{2}\,(x-1)+\frac{3}{4}\alpha^{3}+\frac{2}{3}\alpha \qquad n=2$$

NOTATION

a	a small parameter.
A	wing plan.
C_P	curve of intersection of A and S_P.
dl	element of arc of C_P.
l	in Section 4, a small parameter.
M	a fixed number.
P_X, P_Y, P_L	operations of determining principal values of integrals, *see* Figs. 2 and 3.
p, q	numbers satisfying equation (18).
$\mathbf{r}$, $\mathbf{R}$	position vectors.
dS	element of surface area.
S_P	surface defined in Section 2.1.
V_0	velocity of the main stream.
u, v, w	components of velocity due to the presence of the wing.
u_1, v_1, w_1	components of velocity derived from potential ϕ_1.
x, y, z	components of position vector $\mathbf{r}$.
X, Y, Z	components of position vector $\mathbf{R}$.
α	defined by $\pi\cot\pi\alpha=\log\dfrac{1+\sin\beta}{1-\sin\beta}$.
β	angle of sweepback, *see* Fig. 1.
δ, ϵ	arbitrarily small constants.
$z=\zeta(x, y)=cZ(x, y)$	equation of wing surface.
Θ	angle of sweepback of isobars.
ρ	density.
$\Phi=-V_0x+\phi$	velocity potential.
ϕ_1	defined by equation (22).
$\mathscr{R}H(z)$, $\mathscr{I}H(z)$	real and imaginary parts of the complex function $H(z)$.

REFERENCES

1. NEUMARK, S. (1947). Velocity Distribution on Straight and Swept-Back Wings of Small Thickness and Infinite Aspect Ratio at Zero Incidence. R.A.E. Report No. Aero 2200. A.R.C. 10907, May 1947.

2. KÜCHEMANN, D. (1947). Wing Junction, Fuselage and Nacelles for Swept-Back Wings. R.A.E. Report No. Aero 2219. A.R.C. 11035, August 1947.

3. LUDWIEG, H. (1946). Improvement on the Critical Mach Number of Aerofoils by Sweep-Back. M.A.P. Völkenrode. Reports and Translations. No. 84. A.R.C. 9826, July 1946.

4. CARLEMAN, T. (1922). Sur la Résolution de Certaines Equations Intégrales. Arkiv. för Mat. Astron. och Fysik, 16, Nr. 26, 1922.